Journal of Statistical Physics, Vol. 51, Nos. 3/4, 1988

Exact Partition Functions and Correlation Functions of Multiple Hamiltonian Walks on the Manhattan Lattice

Bertrand Duplantier[1] **and François David**[1]

Received December 7, 1987

This is a general and exact study of multiple Hamiltonian walks (HAW) filling the two-dimensional (2D) Manhattan lattice. We generalize the original exact solution for a single HAW by Kasteleyn to a system of *multiple* closed walks, aimed at modeling a polymer melt. In 2D, two basic nonequivalent topological situations are distinguished. (1) the Hamiltonian loops are all *rooted* and *contractible* to a point: *adjacent* one to another, and, on a torus, *homotopic to zero*. (2) the loops can *encircle* one another and, on a torus, can *wind* around it. For *case 1*, the grand canonical partition function and multiple correlation functions are calculated exactly as those of multiple rooted spanning *trees* or of a massive 2D *free field*, *critical* at zero mass (zero fugacity). The conformally invariant continuum limit on a Manhattan *torus* is studied in detail. The melt entropy is calculated exactly. We also consider the relevant effect of free boundary conditions. The number of single HAWs on Manhattan lattices with other perimeter shapes (rectangular, Kagomé, triangular, and arbitrary) is studied and related to the spectral theory of the Dirichlet Laplacian. This allows the calculation of exact shape-dependent configuration exponents γ. An exact surface critical exponent is obtained. For *case 2*, nested and winding Hamiltonian circuits are allowed. An exact equivalence to the *critical* Q-state Potts model exists, where $Q^{1/2}$ is the walk fugacity. The Hamiltonian system is then always critical (for $Q \leqslant 4$). The exact critical exponents, in infinite numbers, are universal and identical to those of the $O(n = Q^{1/2})$ model in its low-temperature phase, i.e. are those of dense polymers. The exact critical partition functions on the torus are given from conformal invariance theory. These models 1 and 2 yield the two first exactly solved models of polymer melts.

KEY WORDS: Manhattan torus; two dimensions; multiple Hamiltonian walks; partition functions; correlations; free field; conformal invariance; polymer melt; entropy; free boundary conditions; Potts and $O(n)$ models; critical exponents; Coulomb gas.

[1] Service de Physique Théorique, Institut de Recherche Fondamentale, CEA, CEN-Saclay, 91191 Gif-sur-Yvette, France.

0022-4715/88/0500-0327$06.00/0

0. INTRODUCTION

Like the Hamiltonian in mechanics, Hamiltonian circuits take their name from William Hamilton, who solved the first "Hamiltonian" problem, namely the "tour around the world" problem on a dodecahedron.[2] A Hamiltonian circuit is a closed path that visits once and only once all the sites of a given graph, following the edges of the graph.[2] A Hamiltonian walk (HAW) is a similar open path. Note that the usual meaning of HAW understands that there is only a single walk filling the lattice. As we shall see, it is, however, natural to generalize to multiple HAWs, filling the lattice. There is no general solution for listing HAWs on any graph.[2] A related problem is that of Eulerian circuits,[2,3] first solved by Euler for the well-known problem of Königsberg's seven bridges.[3] An Eulerian circuit must visit once and only once all edges of a given graph or lattice.

In 1963, Kasteleyn[4,5] gave a solution for counting single HAWs on any oriented lattice graph $\mathcal{G}^c$, which is the "covering" graph[2,4] of a closed oriented graph[2,4] $\mathcal{G}$. Single HAWs on $\mathcal{G}^c$ are related to Euler walks on $\mathcal{G}$ and to spanning trees[4,6] of $\mathcal{G}$ (a spanning tree is a subgraph of $\mathcal{G}$ without loops that covers all the sites of $\mathcal{G}$). Enumerating spanning trees on an (oriented) graph $\mathcal{G}$ is made by a determinant formula.[7,8] Applying this to the $\mathbf{M} \times \mathbf{N}$ periodic *Manhattan lattice* $\mathcal{M}$, which is a 2D square lattice with

[2] Hamilton[1] found the closed paths visiting all 20 towns only once and following the edges of a dodecahedron; see ref. 2, p. 179.

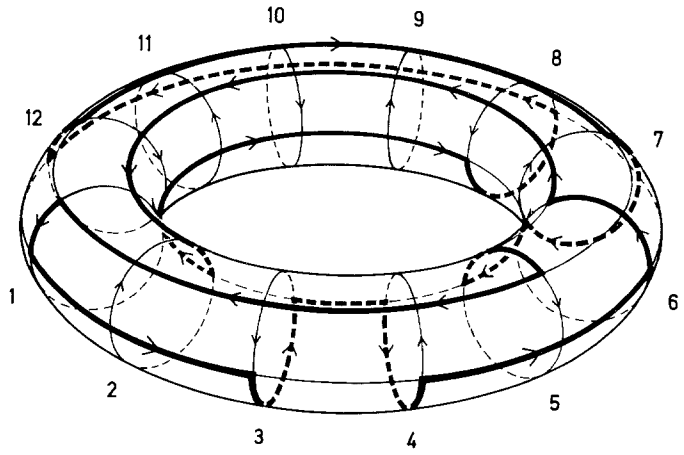

Fig. 1. A torus with a 4×12 Manhattan oriented lattice drawn on it, and a single Hamiltonian circuit. This circuit is necessarily contractible to a point.

horizontal and vertical alternating orientations (Fig. 1) and is a covering graph, Kasteleyn[4] gave the number of single HAWs:

$$N_{\mathrm{H},1} = 2^{\mathbf{MN}/2+1} \prod_{k=1}^{\mathbf{M}/2} \prod_{l=1}^{\mathbf{N}/2} \left(\sin^2 \frac{2\pi k}{\mathbf{M}} + \sin^2 \frac{2\pi l}{\mathbf{N}} \right)$$

$$(k, l) \neq \left(\frac{\mathbf{M}}{2}, \frac{\mathbf{N}}{2} \right) \tag{0.1}$$

Note that this product (0.1) is also identically, in a compact notation,

$$N_{\mathrm{H},1} = 8 \det'(-\Delta) \tag{0.2}$$

where Δ is the (discrete) Laplacian in a periodic box $\mathbf{M}/2 \times \mathbf{N}/2$, the prime eliminating the zero mode. Kasteleyn actually gave a direct explanation of (0.2), which counts spanning trees on another *unoriented* square lattice whose mesh is twice that of $\mathcal{M}$. The asymptotic expression of (0.1) is[4,9]

$$N_{\mathrm{H},1} \sim e^{G\mathbf{MN}/\pi} \tag{0.3}$$

giving the exact entropy per site G/π, where G is Catalan's constant

$$G = 1 - \frac{1}{3^2} + \frac{1}{5^2} + \cdots \tag{0.4}$$

This exact entropy has played an important role in condensed polymer physics[10-19] and in the theory of mixing, where very few reliable results are available. Concerning exact results on the HAW on $\mathcal{M}$, one should note that Barber[9] performed a more complete asymptotic analysis of (0.1), and that Malakis[10] considered successive coverings of $\mathcal{M}$ and calculated their entropy.

The purpose of this paper is to give a thorough and somewhat pedagogical description of the statistical mechanics of HAWs on the 2D Manhattan lattice, including numerous exact results: partition functions, multiple correlation functions, entropy, and discussion of the effect of the topology and of boundary conditions. Before describing the progress made, let us first make precise the relation of (Manhattan) HAWs to polymer physics. HAWs are an extreme case of *dense polymers*,[20-22] which are self-avoiding walks (SAW) filling a finite fraction of the lattice. Dense polymers form a new *critical* phase, different from the usual dilute one. In 2D, the infinite set of their exact exponents is now known[20-22] from the Coulomb gas method.[23,24] On the *Manhattan* lattice the HAWs respect two stringent constraints: they fill all the sites and follow oriented arrays of lattice atoms, hence the question arose[25] of their universality. The critical

exponents of two-dimensional Manhattan HAWs were addressed in ref. 25 and shown to be those of the critical 2D Q-state Potts model in the $Q \to 0$ limit, or, equivalently, of the $O(n)$ model for $n \to 0$ in its critical low-temperature phase. The latter model describes precisely *dense* polymers,[20–22] and this shows[25] that the Hamiltonian and Manhattan constraints are both *irrelevant* in the infrared critical limit. This indicates that studies of HAWs on the Manhattan lattice can give access to much more *universal* properties of *polymer melts* than previously imagined.

In summary, the exact results known for HAWs on the Manhattan lattice are the exact number of single HAWs on a torus[4,9,10] and, quite recently, the infinite set of exact critical exponents.[25]

We now describe the approach used in this work and summarize the content of this paper:

We work first with periodic boundary conditions, i.e., on the 2D Manhattan *torus* $\mathcal{M}$ (Fig. 1). Later, we consider free boundary conditions and the effect of the shape of the domain which is *relevant* for a dense system. The essential idea is to consider not only a single HAW, but a set of *multiple* HAWs filling $\mathcal{M}$. They are described here by a grand ensemble with a fugacity associated with the number of walks. This provides a model of a *polymer melt*. On $\mathcal{M}$, a single HAW is nearly closed,[4] so we actually consider multiple Hamiltonian circuits. Then two nonequivalent topological situations are studied:

A. The loops are *rooted*, *adjacent* to one another and, on the torus, *contractible* to *a point*. They simulate a close packing of polymer loops.

B. The (now unrooted) loops can encircle one another by being *nested* in one another, and on the torus they can *wind* around the latter. Hence, loops noncontractible to a point are allowed.

The reasons for distinguishing A and B are rather mathematical and we use different methods to solve the two cases.

The "adjacent" case A is exactly transformed in 2D into a *multiple* (*rooted*) *spanning tree* problem (generalizing the second method by Kasteleyn[4]). Then we show that the generating functions of multiple spanning trees are exactly calculable as massive *free-field* partition functions.

The generating function for multiple HAWs

$$\mathcal{Z}_{\mathrm{H}} = \sum_{K \geqslant 1} \left(\frac{m^2}{2}\right)^K N_{\mathrm{H},K} \tag{0.5}$$

where $N_{\mathrm{H},K}$ is the number of distinct configurations of K-HAWs on $\mathcal{M}$, reads (e.g., on the torus)

$$\mathcal{Z}_{\mathrm{H}} = 2 \det(-\Delta + m^2) \tag{0.6}$$

This is the direct generalization of Kasteleyn's relation (0.2). It also exemplifies the physical Hamiltonian system to which there corresponds the addition of a mass term to the free field theory: $m^2/2$ is the contractible HAW fugacity. We give the explicit formula for the multiple correlation functions of the "*contractible*" Hamiltonian melt. They are *determinants* of the free field two-point correlation function. Now, with a free field being critical at $m^2 = 0$ (zero fugacity), a *finite* number of adjacent HAWs filling an (infinite) Manhattan lattice form a 2D *critical* system, i.e., a free field theory, with logarithmic divergences. This is studied in detail in this article.

On the other hand, the unrooted and "nested" system B can be transformed exactly[25] into a *critical* Q-state Potts-like model, where now $Q^{1/2}$ is the HAW fugacity. Hence it remains critical in the finite interval[26] $Q \in [0, 4]$. In addition to the critical exponents, we give here in particular the exact continuum limit of the partition function on the torus.

In the zero-fugacity limit ($m^2 \to 0$, $Q \to 0$) both systems (A and B) are critical and describe different topological aspects of a same 2D critical system: a *few* HAWs filling $\mathcal{M}$. In 2D conformal invariance,[27] its central charge is then $c = -2$.

In the present work, the study of the Manhattan HAW properties is made in connection with the techniques of critical phenomena in 2D: exact solutions by determinants, 2D free fields, conformal invariance and modular invariance on the torus,[28] spectral theory of the Laplacian, Potts and $O(n)$ models, Coulomb gas methods.

The organization of the paper is as follows.

Part A is devoted to *adjacent* HAWs.

In Section 1, Kasteleyn's remark is generalized to multiple adjacent rooted circuits, which are shown to be in one-to-one relation to multiple rooted spanning trees.

In Section 2, we derive some general theorems concerning rooted spanning trees on unoriented connected graphs. Closed expressions of the multiple tree generating function and correlation functions are given in terms of the graph connection matrix.[8]

Section 3 is devoted to the application of these results to adjacent HAWs on the Manhattan torus and to their free field representation. The first terms of (0.5) are calculated. Their continuum limit is worked out in detail. Close to criticality (a finite number of walks filling $\mathcal{M}$) the finite-size scaling limit of $\mathcal{Q}_H$ (0.5) is calculated. It has a compact modular invariant form,[28] which yields the large-lattice limit of $N_{H,K}$ for any K, generalizing Barber's asymptotics. The relation to modular invariance on a torus[28] and conformal invariance in two dimensions is discussed. The second case is when the *number* of HAWs becomes infinite with the lattice size, which we call the Hamiltonian *melt*. Its exact entropy is given. The exact multiple

correlation functions are given, with a detailed study of their critical and melt limits.

In Section 4, the effect of boundary conditions relevant for a dense system is considered. On a Manhattan rectangle with *free* edges, the exact number of single HAWs is calculated as well as its asymptotic form. It exhibits a new *perimeter* term, and, more surprisingly, a new exponent γ.

In Section 5, we further elaborate on HAWs with free boundary conditions, relating them to Neumann conditions for the Laplacian, and finally to Dirichlet ones. This leads into Section 6, where other geometries for Manhattan oriented lattices are considered, such as the Kagomé and triangular ones. The spectral theory of the Dirichlet Laplacian on domains with arbitrary shapes is used to derive directly the asymptotic number of single HAWs for any geometry, and in particular its critical exponent γ, which is shape-dependent.

Section 7 concludes with a special application of the Manhattan HAW. We compare two Manhattan even–even and odd–odd rectangles $\mathbf{M} \times \mathbf{N}$ and $(\mathbf{M}+1) \times (\mathbf{N}+1)$ and calculate their respective numbers $N_{\mathrm{H},1}$, which do not have the same analytic form. An exact surface critical exponent is derived. Quite interestingly, it is just the surface exponent for dense polymers obtained elsewhere[22,25] by Coulomb gas methods, giving a direct check of the universality.

This is precisely the subject of Part B, treating *unrooted* and *nested* multiple walks, possibly *not contractible* on the $\mathscr{M}$ torus. Section 8 describes briefly the new aspects of this system, which corresponds exactly to a critical Potts model.[25] An infinite set of exact critical exponents is thus obtained. The relation is made to the subcritical $O(n)$ model and the universality discussed. The exact modular invariant partition function, in the continuum limit, of multiple nested HAWs on the torus is given in Section 9 from results of conformal invariance and Coulomb gas methods. Finally, in Section 10 we compare Manhattan HAWs to dense polymers in 2D. Some exact results for HAWs are used to conjecture new ones for dense polymer networks.

A. ADJACENT AND CONTRACTIBLE MULTIPLE WALKS

1. EQUIVALENCE OF HAMILTONIAN WALKS TO SPANNING TREES

1.1. Single Hamiltonian Walk

Let us consider a *periodic* $\mathbf{M} \times \mathbf{N}$ Manhattan lattice $\mathscr{M}$ (Fig. 2). The periodic boundary conditions and the alternating orientation rule require

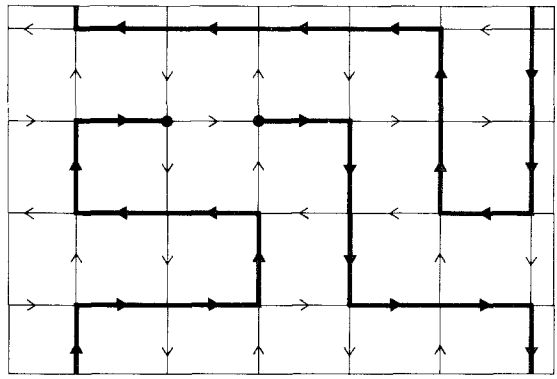

Fig. 2. Hamiltonian open walk on the 4×6 Manhattan lattice. It necessarily ends at one lattice spacing of its origin.

M and **N** to be *even*. As remarked by Kasteleyn, any Hamiltonian walk on $\mathcal{M}$ (Fig. 2) is "almost closed": the special Manhattan orientation forces the walk to end at one lattice spacing from its origin. Indeed, suppose that the walk starts at 0 (Fig. 3). Let A and B be the two neighboring sites from which one can go to 0 in accordance to the Manhattan orientation. *If* A and B are not end points of the Hamiltonian walk, the latter must pass through sites A and B at some time and leave them. But not being allowed to return to 0 by hypothesis, it must leave A following out-line *a and* B by out-line b (Fig. 3). These two lines are *confluent* at site C (Fig. 3) and this contradicts the self-avoidance constraint. Hence, either A or B is an end point. The walk can be closed simply by adding the oriented bond joining the end point A or B to 0.

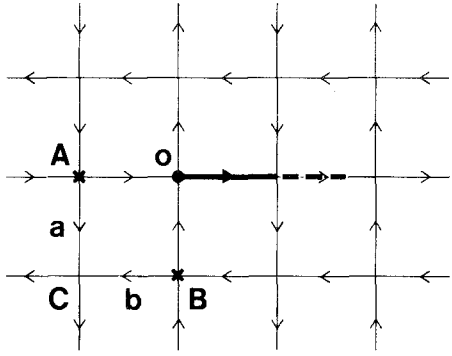

Fig. 3. A Hamiltonian walk starting at 0 must end at A or B. Otherwise it would have to follow lines a and b and cross itself at c.

So, *to each oriented open walk corresponds exactly one closed walk*, where the origin is *distinguished.* We shall also distinguish closed walks (which are rooted) from *circuits*, where the origin is *not* considered.

On a torus, the problem of counting open Manhattan Hamiltonian walks thus reduces to that of closed walks. This will not be true in the case of free boundary conditions, where real open walks will be possible, as treated later in this work.

Now, following Kasteleyn,[4] we notice that a Hamiltonian circuit of $\mathcal{M}$ is either clockwise or counterclockwise oriented. It is useful to consider among all the set of square *plaquettes* building $\mathcal{M}$ the two peculiar subsets where the plaquettes are clockwise or counterclockwise oriented (Fig. 4). These plaquettes are like vortices (or antivortices) and a Hamiltonian circuit encircles the clockwise or counterclockwise set, depending upon whether it is itself clockwise or counterclockwise. (Figs. 4a, 4b). The centers

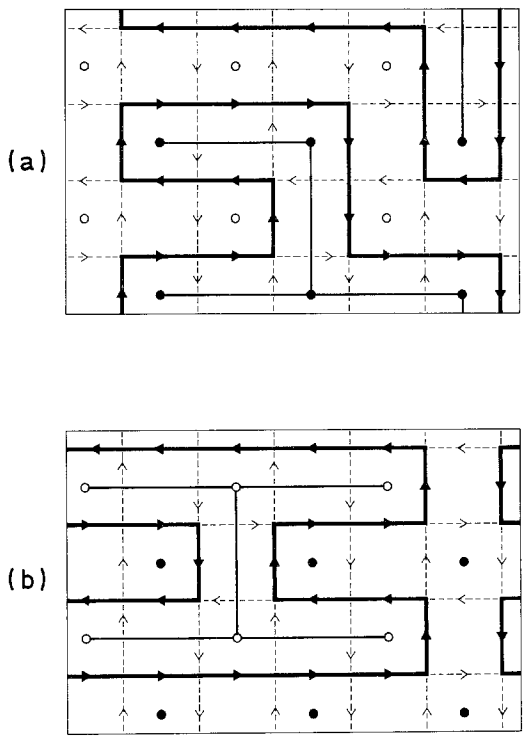

Fig. 4. The periodic 4×6 Manhattan lattice $\mathcal{M}$ and the two unoriented square lattices $\mathcal{L}_A$ (solid dots) and $\mathcal{L}_B$ (open dots), the sites of which are the centers of clockwise and counterclockwise plaquettes of $\mathcal{M}$. A clockwise (resp. counterclockwise) Hamiltonian circuit on $\mathcal{M}$ encircles in a one-to-one correspondence a spanning tree on (a) $\mathcal{L}_A$ [(b) resp. on $\mathcal{L}_B$].

of clockwise (resp. counterclockwise) plaquettes build an unoriented square lattice $\mathscr{L}_A$ (resp. $\mathscr{L}_B$), whose mesh is twice that of $\mathscr{M}$ (Fig. 4). Then each clockwise Hamiltonian circuit on $\mathscr{M}$ encircles in a one-to-one correspondence a *spanning tree* on $\mathscr{L}_A$ (Fig. 4a), counterclockwise Hamiltonian circuits corresponding to spanning trees of the other sublattice $\mathscr{L}_B$ (Fig. 4b).

We shall distinguish here the number $N_{\mathrm{H},1}$ of single Hamiltonian *open walks*, which is the same as that of *closed walks* with the origin specified, from the number $N^0_{\mathrm{H},1}$ of *circuits* without origin. We have

$$N_{\mathrm{H},1} = \mathscr{N} N^0_{\mathrm{H},1} \tag{1.1}$$

where

$$\mathscr{N} = \mathbf{MN} \tag{1.2}$$

is the number of sites of $\mathscr{M}$, as well as the length of a Hamiltonian circuit on $\mathscr{M}$.

Let similarity $N_{T,1}$ denote the number of *rooted* spanning trees on $\mathscr{L}_A$ (or $\mathscr{L}_B$) and $N^0_{T,1}$ the number of *unrooted* spanning trees. These tree numbers are related by

$$N_{T,1} = \mathscr{N}_S N^0_{T,1} \tag{1.3}$$

where $\mathscr{N}_S$ is the number of sites of lattice $\mathscr{L}_A$ (or $\mathscr{L}_B$), given in terms of the number of sites of $\mathscr{M}$ by

$$\mathscr{N} = 4\mathscr{N}_S \tag{1.4}$$

According to the preceding discussion, one has the relation between Hamiltonian circuits on $\mathscr{M}$ and unrooted spanning trees on $\mathscr{L}_A$ or $\mathscr{L}_B$

$$N^0_{\mathrm{H},1} = 2N^0_{T,1} \tag{1.5}$$

where the factor 2 accounts for the two possible orientations of the walks, i.e., for the two lattices $\mathscr{L}_A$ and $\mathscr{L}_B$. One has a similar relation between Hamiltonian closed walks with specified origin on $\mathscr{M}$ and rooted spanning trees on $\mathscr{L}_A$ (or $\mathscr{L}_B$),

$$N_{\mathrm{H},1} = 2 \cdot 4N_{T,1} \tag{1.6}$$

where the factor 4 comes from the number of possible origins on the walk per root on the spanning tree.

1.2. Multiple Walks (Adjacent and Contractible)

We can generalize the preceding results by considering now K ($K \geqslant 1$) Hamiltonian ("nearly closed" or closed) walks on $\mathscr{M}$, which completely fill the lattice. Since we want to preserve the equivalence to spanning (multiple) trees, we impose two conditions (Fig. 5):

1. The walks are *adjacent*, i.e., none encircles another circuit.
2. On the Manhattan torus, some walks could *wind* around the torus. We forbid this by requiring that all walks are *contractible to a point*, i.e., *homotopic to zero.*

The general situation where circuits can encircle others and where they can wind around the torus is also very interesting and will be considered later (Part B). Note also that since the circuits are homotopic to zero (condition 2), condition 1 is now equivalent to requiring that all circuits have the same orientation (either clockwise or counterclockwise). This will decide whether all K circuits are in correspondence to a multiple spanning tree on $\mathscr{L}_A$ or $\mathscr{L}_B$. We now define on $\mathscr{M}$ the restricted partition function or *K-correlator*

$$N_{\mathrm{H}}(x_1,\ldots, x_K) = \#K\text{-adjacent contractible walks rooted at } \{x_1,\ldots, x_K\}, \qquad x_i \in \mathscr{M} \tag{1.7}$$

where the x_i are K points on $\mathscr{M}$ which the ith walk passes through (Fig. 6).

It will be natural to introduce similar quantities for the K-spanning trees on either lattice $\mathscr{L}_A$ or $\mathscr{L}_B$.

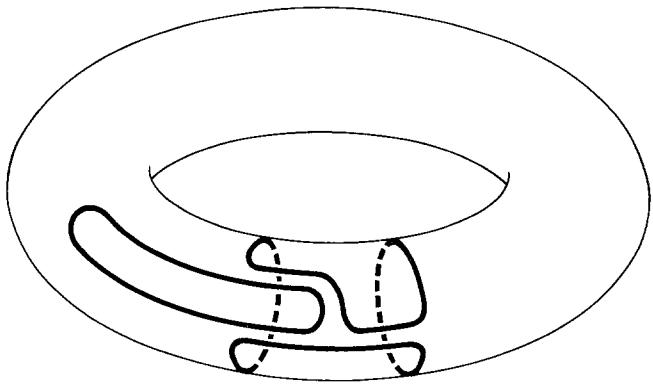

Fig. 5. Depiction of $K=2$ HAWs adjacent and contractible to a point on the torus.

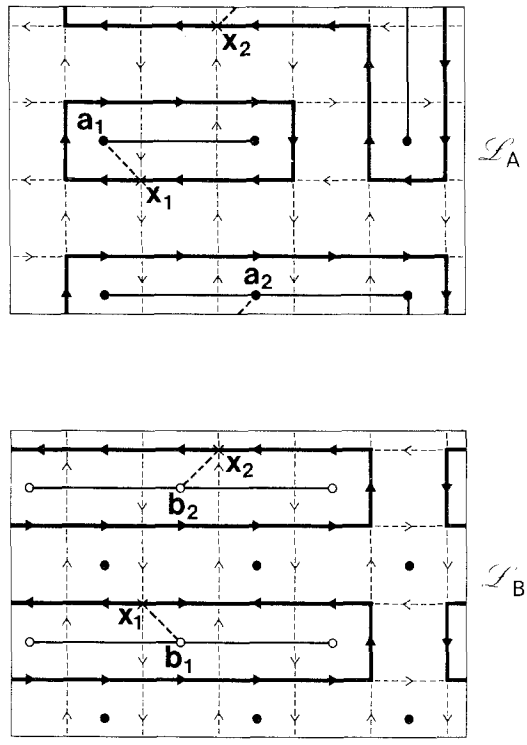

Fig. 6. Two sets of K-Hamiltonian walks, for $K=2$, contributing to $N_H(x_1, x_2)$. They correspond to two sets of 2-spanning trees either on $\mathscr{L}_A$ or $\mathscr{L}_B$, contributing, respectively, to $N_T^A(a_1, a_2)$ and $N_T^B(b_1, b_2)$.

Definition. A K-spanning tree T on lattice graph $\mathscr{L}$ is a tree that covers all sites of $\mathscr{L}$ and has K connected components $T_1,..., T_K$.

Then the partition function of K *rooted* spanning trees is defined on lattice $\mathscr{L}$ as

$$N_T(a_1,..., a_K) = \#K\text{-spanning trees } \{T_1,..., T_K\} \text{ with respective roots } a_1,..., a_K, \qquad a_1,..., a_K \in \mathscr{L} \quad (1.8)$$

where the a_i are K distinct points on $\mathscr{L}$ ($=\mathscr{L}_A$ or $\mathscr{L}_B$).

Now, the Hamiltonian walk and tree partition functions (1.7) and (1.8) are related to each other by the following rules. We first note that the walks contributing to (1.7) split into two classes, where the K walks are all clockwise or all counterclockwise oriented. When clockwise (resp., counterclockwise) they encircle a spanning tree on $\mathscr{L}_A$ (resp. $\mathscr{L}_B$) with K connected

components. The roots of the K-spanning tree on $\mathscr{L}_A$ (or $\mathscr{L}_B$) are easily found by a *proximity rule.*

Indeed, we remark that on a Manhattan lattice $\mathscr{M}$, we may associate in a unique way to any point x a site $a(x)$ on $\mathscr{L}_A$ and another site $b(x)$ on $\mathscr{L}_B$ (Fig. 7),

$$x \to \begin{cases} a(x) \in \mathscr{L}_A \\ b(x) \in \mathscr{L}_B \end{cases} \tag{1.9}$$

where $a(x)$ [resp. $b(x)$] is the center of the unique clockwise (resp. counterclockwise) plaquette from which x is a corner.

Now, to the set $\{x_i\}$ in (1.7) we associate two sets $\{a_i\}$ and $\{b_i\}$ by (1.9), which are roots in (1.8) of K-trees on $\mathscr{L}_A$ or $\mathscr{L}_B$. Then the basic relation between walks and trees is

$$N_{\mathrm{H}}(x_1,..., x_K) = N_T^A(a_1,..., a_K) + N_T^B(b_1,..., b_K) \tag{1.10}$$

where the two terms correspond to the spanning trees encircled by the nonoverlapping sets of clockwise or counterclockwise K-walks on $\mathscr{M}$ contributing to (1.7) (Fig. 6). Let us note that if two different x_i have the same a (or b), then N_T^A (or N_T^B) is automatically zero.

From the correlations (1.7), (1.8) we now derive other quantities of interest.

1.3. Partial Partition Functions

For K'-Hamiltonian walks with fixed roots $x_1,..., x_{K'}$ on $\mathscr{M}$, immersed in K'' other walks with arbitrary roots, we have the partition function

$$N_{\mathrm{H}}(x_1,..., x_{K'}; K'') \equiv \frac{1}{K''!} \sum_{\{y_1,..., y_{K''}\}} N_{\mathrm{H}}(x_1,..., x_{K'}, y_1,..., y_{K''}), \qquad K' + K'' = K \tag{1.11}$$

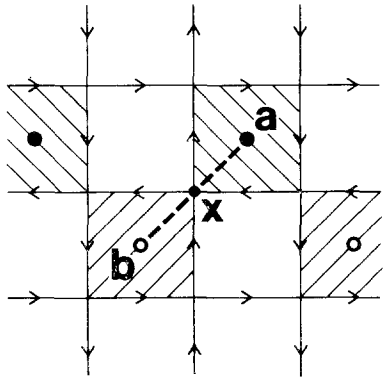

Fig. 7. The proximity rule. To each $x \in \mathscr{M}$ there corresponds exactly one pair of points $a \in \mathscr{L}_A$, $b \in \mathscr{L}_B$ that are the closest centers of clockwise and counterclockwise plaquettes.

Similarly, it will be useful to consider K' trees with fixed roots $a_1,..., a_{K'}$ in the presence of K'' other trees without specified roots on $\mathscr{L}_A$ (or $\mathscr{L}_B$),

$$N_T(a_1,..., a_{K'}; K'') \equiv \frac{1}{K''!} \sum_{a'_1,...,a'_{K''}} N_T(a_1,..., a_{K'}, a'_1,..., a'_{K''}) \tag{1.12}$$

When $K'=0$, $K''=K$ in definitions (1.11), (1.12) one obtains, respectively, the total number $N_{\mathrm{H},K}$ of rooted K-Hamiltonian walks on $\mathscr{M}$ and $N_{T,K}$ of rooted K-spanning trees on $\mathscr{L}$ ($=\mathscr{L}_A$ or $\mathscr{L}_B$),

$$\begin{aligned} N_{\mathrm{H},K} &\equiv N_{\mathrm{H}}(\varnothing; K) \\ N_{T,K} &\equiv N_T(\varnothing; K) \end{aligned} \tag{1.13}$$

where $\varnothing$ is the empty set.

From the fundamental relation (1.10), one deduces relations between the partial partition functions (1.11), (1.12):

$$N_{\mathrm{H}}(x_1,..., x_{K'}; K'') = 4^{K''}[N_T^A(a_1,..., a_{K'}; K'') + N_T^B(b_1,..., b_{K'}; K'')] \tag{1.14}$$

where the factor $4^{K''}$ arises from the fact that each plaquette $a \in \mathscr{L}_A$ (and $b \in \mathscr{L}_B$) has four corners x on $\mathscr{M}$ when inverting the mapping (1.9). Hence, formally,

$$\sum_{\{x_1,..., x_{K''}\}} = 4^{K''} \sum_{\{a_1,..., a_{K''}\}} \tag{1.15}$$

For the total number of rooted walks $N_{\mathrm{H},K}$ and trees $N_{T,K}$ we have finally

$$N_{\mathrm{H},K} = 2 \cdot 4^K N_{T,K} \tag{1.16}$$

where the factor 2 comes from the two equal contributions of lattices $\mathscr{L}_A$ and $\mathscr{L}_B$.

1.4. Grand Canonical Partition Functions

We now define the generating function or grand canonical partition function of the K-Hamiltonian walks on $\mathscr{M}$,

$$\mathscr{Z}_{\mathrm{H}}(\lambda) = \sum_{K=1}^{\mathscr{N}_S} \lambda^K N_{\mathrm{H},K} \tag{1.17}$$

The maximum value of K in the sum is obtained when each walk encircles an elementary plaquette of $\mathscr{M}$, and is thus the number of sites of $\mathscr{L}_A$ or $\mathscr{L}_B$, $\mathscr{N}_S = \mathbf{MN}/4$. According to (1.16), $\mathscr{Z}_{\mathrm{H}}(\lambda)$ can be immediately rewritten as

$$\mathscr{Z}_{\mathrm{H}}(\lambda) = 2\mathscr{Z}_T(4\lambda) \tag{1.18}$$

where $\mathcal{Q}_T$ is the generating function for rooted K-spanning trees on the unoriented lattice $\mathcal{L}_A$ (or $\mathcal{L}_B$)

$$\mathcal{Q}_T(m^2) \equiv \sum_{K=1}^{\mathcal{N}_S} m^{2K} N_{T,K} \tag{1.19}$$

The notation m^2 for the tree fugacity has been chosen for the following reason: as we shall see later, the generating function $\mathcal{Q}_T$ may be written as the partition function of a free field with mass m on the lattice $\mathcal{L}_A$ and $\mathcal{L}_B$.

Finally, we can also introduce grand canonical partition functions with specified roots for Hamiltonian walks

$$\mathcal{Q}_{\mathrm{H}}(x_1,..., x_K; \lambda) = \sum_{K' \geqslant 0} \lambda^{K'} N_{\mathrm{H}}(x_1,..., x_K; K') \tag{1.20}$$

and for spanning trees on $\mathcal{L}$ ($=\mathcal{L}_A$ or $\mathcal{L}_B$)

$$\mathcal{Q}_T(a_1,..., a_K; m^2) = \sum_{K' \geqslant 0} m^{2K'} N_T(a_1,..., a_K; K') \tag{1.21}$$

According to Eq. (1.14), the following identity holds between walks on $\mathcal{M}$ and trees on $\mathcal{L}_A$ and $\mathcal{L}_B$:

$$\mathcal{Q}_{\mathrm{H}}(x_1,..., x_K; \lambda) = \mathcal{Q}_T^A(a_1,..., a_K; 4\lambda) + \mathcal{Q}_T^B(b_1,..., b_K; 4\lambda) \tag{1.22}$$

which generalizes (1.18).

2. SOME RESULTS ON THE ENUMERATION OF TREES ON GRAPHS

In this section we derive some general results on the enumeration of trees on general graphs, which will be used in the next sections. These results are merely elaborations of classical results, which may be found, for instance, in refs. 5–8. We recall them for completeness.

Let us first fix some notations and definitions.

Definition 1. A *subgraph* S of G is a subset of vertices $\{a_i\}$ and of lines $\{l_i\}$ of G such that it forms a graph (that is, if a line l belongs to S, vertices.

Definition 1. A *subgroup* S of G is a subset of vertices $\{a_i\}$ and of lines $\{l_i\}$ of G such that it forms a graph (that is, if a line l belongs to S, the two vertices at the ends of l belong to S).

Remark. With this definition, a subgraph S is not necessarily connected, and an isolated vertex may form a subgraph or a connected part of a subgraph.

Definition 2. Given a (sub)graph S, we denote, respectively, by $N_0(S)$, $N_1(S)$, and $N_c(S)$ the numbers of vertices, lines, and connected parts of S.

Definition 3. Given a (sub)graph S, the number of internal loops $N_2(S)$ is defined by the Euler relation:

$$N_2(S) = N_c(S) - N_0(S) + N_1(S) \tag{2.1}$$

Definition 4. A subgraph S of a graph G is a *spanning-K-tree* of G if

$$\begin{aligned} N_0(S) &= N_0(G) \\ N_2(S) &= 0 \\ N_c(S) &= K \end{aligned} \tag{2.2}$$

that is, if every vertex of G belongs to S, S has no internal loops, and S has K connected components.

Definition 5. Given a graph G, the connection matrix $\mathbf{C}_G$ is an $N_0(G) \times N_0(G)$ matrix, where elements C_{ab} are labeled by the vertices of G and are defined as follows:

$$\begin{aligned} C_{ab} &= -\text{number of lines joining } a \text{ to } b \qquad \text{if} \quad a \neq b \\ C_{aa} &= -\sum_{b \neq a} C_{ab} = \text{number of lines attached to } a \text{ by} \\ &\qquad \text{one (and only one) extremity} \qquad \text{if} \quad a = b \end{aligned} \tag{2.3}$$

With these definitions, the problem of enumerating spanning-K-trees of a graph G is related to the properties of the connection matrix $\mathbf{C}_G$ by the following fundamental theorem.

Theorem 1. Let G be a graph, $A = \{a_1, ..., a_K\}$ a subset of K distinct vertices of G, and $N_T(a_1, ..., a_K)$ the number of spanning-K-trees S of G such that each vertex a_i of A belongs to a different connected component S_i of S. We have

$$N_T(a_1, ..., a_K) = \det(\mathbf{C}_{G/A}) \tag{2.4}$$

where $\mathbf{C}_{G/A}$ is the $[N_0(G) - K] \times [N_0(G) - K]$ submatrix of $\mathbf{C}$ obtained by removing all lines and columns labeled by elements of A.

Proof. The proof is a simple generalization of a classical theorem by Kirchhoff (which holds for $K = 1$). Let us choose an arbitrary orientation

for each line of G and define the $N_0(G) \times N_1(G)$ incidence matrix $\mathbf{E}$, where elements E_{al} are labeled by a vertex a and a line l of G and are defined as

$$\begin{aligned} E_{al} &= +1 \quad \text{if line } l \text{ flows toward } a \\ &= -1 \quad \text{if line } l \text{ flows outward } a \\ &= 0 \quad \text{otherwise} \end{aligned} \tag{2.5}$$

It is easy to see that $\mathbf{C} = \mathbf{E} \cdot \mathbf{E}^t$. From the Binet–Cauchy theorem we can write $\det \mathbf{C}_{G/A}$ as a sum over all subsets L of $N_0(G) - K$ lines of G,

$$\det(\mathbf{C}_{G/A}) = \sum_L [\det(\mathbf{E}_{G/A,L})]^2 \tag{2.6}$$

$\mathbf{E}_{G/A,L}$ is the square matrix obtained from $\mathbf{E}$ by keeping only the elements of $\mathbf{E}$ attached to vertices of G/A and to lines of L.

By extension, we shall also denote by L the subgraph of G containing *every vertex of* G, but *only the lines* l *in* L. One can show that if at least one connected component of L does not contain any vertex of A, then $\det(\mathbf{E}_{G/A,L}) = 0$. Thus, the sum in (2.6) is reduced to L such that each connected component of L contains at least one vertex of A. Thus, $N_c(L) \leqslant K$, since A has K vertices. Since $N_0(L) = N_0(G)$ and $N_1(L) = N_0(G) - K$, the Euler relation (2.1) gives $N_2(L) \leqslant 0$. This implies that $N_2(L) = 0$ (thus, L is a spanning tree) and that each vertex of A must belong to a different connected component of L (thus, L is a spanning-K-tree). Then one can show that since L is a tree, $\det(\mathbf{E}_{G/A,L}) = \pm 1$ (the sign depends on the orientation of the lines of L). Conversely, every spanning-K-tree contributes to the sum in (2.6). Theorem 1 follows.

Remark. In the simplest case $K = 1$, $N_T(a) = N_{T,1}^0$ is independent of the chosen vertex a and is simply the number of connected spanning trees on G.

Theorem 1 can be extended in the following way.

Theorem 2. Let G and $A = \{a_1, ..., a_K\}$ as in Theorem 1. The characteristic polynomial of the restricted matrix $\mathbf{C}_{G/A}$ reads

$$\begin{aligned} \det(\mathbf{C}_{G/A} + \lambda \mathbf{1}) &= \mathscr{Q}_T(a_1, ..., a_K; \lambda) \\ &= \sum_{K'} \lambda^{K'} N_T(a_1, ..., a_K; K') \end{aligned} \tag{2.7}$$

where $N_T(a_1, ..., a_K; K')$ is expressed as a sum over spanning-$(K + K')$-trees S of G such that each vertex a_i of A belongs to a different connected component of S,

$$N_T(a_1, ..., a_K; K') = \sum_S \prod_1^{K'} N_0(S_i) \tag{2.8}$$

where in (2.8) the product runs over the K' connected components of S that do not contain any vertex of A, and where $N_0(S_i)$ is the number of vertices of each connected component.

Proof. Expanding the determinant on the lhs of (2.7), we get

$$N_T(a_1,..., a_K; K') = \sum_{B=\{b_1,...,b_{K'}\}} \det(\mathbf{C}_{G/A\cup B}) \tag{2.9}$$

where $b_1 \cdots b_{K'}$ are K' vertices of G/A. Using Theorem 1 and regrouping the sum over B into a sum over $K+K'$ spanning trees, we get (2.8).

Important Remark. Theorem 2 is still valid if $K=0$ (A is the empty set $\varnothing$). Then the sum in (2.8) reduces to spanning-K'-trees. The fact that the first term $N_T(\varnothing; 0)$ vanishes is a consequence of the existence of a zero eigenvalue for $\mathbf{C}$, which implies that $\det \mathbf{C}=0$. In that particular case we shall denote the term of the expansion by

$$\det(\mathbf{C}_G + \lambda \mathbf{1}) = \sum_{K'} P_{K'} \lambda^{K'} = P(\lambda) \tag{2.10}$$

We have from Theorem 2

$$\begin{aligned} P_0 &= 0 \\ P_1 &= N_0(G) \cdot N^0_{T,1} = N_{T,1} \end{aligned} \tag{2.11}$$

where $N^0_{T,1}$ is the number of (unrooted) connected spanning trees on G.

The matrix $\mathbf{C}$ is equal to minus the combinatoric Laplacian on the graph G. It is then natural to express the "correlation function" $N_T(a_1,..., a_K; \lambda)$ in terms of the "propagator," that is, of the inverse of $(\mathbf{C}+\lambda \mathbf{1})$.

Definition 6. We define the "massive propagator" matrix $\mathbf{G}(\lambda)$ as the inverse $\mathbf{C}+\lambda \mathbf{1}$,

$$\mathbf{G}(\lambda)_{ab} = (\mathbf{C}+\lambda \mathbf{1})^{-1}|_{ab} \tag{2.12}$$

Theorem 3. For G and $A=\{a_1,..., a_K\}$ as in Theorem 1, $\mathcal{Z}_T(a_1,..., a_K; \lambda)$ defined as in (2.7) and $P(\lambda)$ as in (2.10), we have

$$\mathcal{Z}_T(a_1,..., a_K; \lambda) = P(\lambda) \cdot \det(\mathbf{G}(\lambda)|_A) \tag{2.13}$$

where $\mathbf{G}(\lambda)|_A$ is the $K\times K$ matrix obtained by restricting to A the propagator matrix $\mathbf{G}(\lambda)$.

Proof. Let us decompose the matrix $(\mathbf{C}_G + \lambda \mathbf{1})$ into blocks relative to elements of A and elements of G/A,

$$[\mathbf{C}_G + \lambda \mathbf{1}] = \begin{bmatrix} A & B \\ B^t & C \end{bmatrix} \tag{2.14}$$

We have

$$P(\lambda) = \det(\mathbf{C}_G + \lambda \mathbf{1}) = \det(C) \cdot \det(A - BC^{-1}B^t) \tag{2.15}$$

but $C = (\mathbf{C}_{G/A} + \lambda \mathbf{1})$ and inverting (2.14) leads to

$$\mathbf{G}(\lambda) = \begin{bmatrix} (A - BC^{-1}B^t)^{-1} & -(A - BC^{-1}B^t)^{-1} BC^{-1} \\ -C^{-1}B^t(A - BC^{-1}B^t)^{-1} & C^{-1} + C^{-1}B^t(A - BC^{-1}B^t)^{-1} BC^{-1} \end{bmatrix} \tag{2.16}$$

Thus, $(A - BC^{-1}B^t)^{-1}$ is nothing but $\mathbf{G}(\lambda)|_A$.

For the "massless" case $\lambda = 0$, we have to take into account the zero mode of $\mathbf{C}$, which causes $P(\lambda)$ to vanish and the propagator $\mathbf{G}(\lambda)$ to diverge. The projector onto the zero mode will be denoted by $\mathbf{P}_0$ and has matrix elements

$$(\mathbf{P}_0)_{ab} = \frac{1}{N_0(G)} \tag{2.17}$$

Then in the limit $\lambda \to 0$ the propagator matrix $\mathbf{G}(\lambda)$ defined by (2.12) has the expansion

$$\mathbf{G}(\lambda) = \frac{1}{\lambda} \mathbf{P}_0 + (\mathbf{C} + \mathbf{P}_0)^{-1} - \mathbf{P}_0 + O(\lambda) \tag{2.18}$$

Hence

$$\tilde{\mathbf{G}} = (\mathbf{C} + \mathbf{P}_0)^{-1} - \mathbf{P}_0 \tag{2.19}$$

is the finite part of $\mathbf{G}(\lambda)$ and is infrared finite. We have the following theorem, which generalizes a classical result by Kirchhoff for $K = 2$.

Theorem 4. With the notations of Theorem 3,

$$N_T(a_1, \ldots, a_K) = N_{T,1}^0 \det_{(K-1)\times(K-1)}(\mathbf{D}) \tag{2.20}$$

where $\mathbf{D}$ is the $(K-1) \times (K-1)$ matrix whose elements are

$$\mathbf{D}_{ij} = \tilde{\mathbf{G}}_{a_i a_j} - \tilde{\mathbf{G}}_{a_i a_K} - \tilde{\mathbf{G}}_{a_K a_j} + \tilde{\mathbf{G}}_{a_K a_K} \tag{2.21}$$

The $\det(\mathbf{D})$ does not depend on the labeling of the vertices in A, and $N_{T,1}^0$ is the number of unrooted, connected spanning trees on G.

Proof. Starting from (2.13), we can write

$$\det_{K\times K}[\mathbf{G}(\lambda)|_A] = \{\det_{(K-1)\times(K-1)}[\mathbf{D}(\lambda)]\} \times \mathbf{G}(\lambda)_{a_K a_K} \tag{2.22}$$

with the matrix $\mathbf{D}$ defined as

$$\mathbf{D}_{ij}(\lambda) = \mathbf{G}_{a_i a_j}(\lambda) - \mathbf{G}_{a_i a_K}(\lambda) \cdot \mathbf{G}_{a_K a_j}(\lambda)/\mathbf{G}_{a_K a_K}(\lambda) \tag{2.23}$$

now as $\lambda \to 0$, $\mathbf{D}(\lambda)$ is finite and goes to the matrix $\mathbf{D}$ defined by (2.21) from (2.18), while

$$\mathbf{G}(\lambda)_{a_K a_K} \sim \frac{1}{\lambda N_0(G)} \tag{2.24}$$

and from (2.11)

$$P(\lambda) \sim \lambda N_0(G) \cdot N_{T,1}^0 \tag{2.25}$$

This ends the proof.

3. APPLICATION TO THE MANHATTAN TORUS

3.1. General Formulas

In the case of the Manhattan torus, we now apply the general results of Section 2 for trees on a general graph to the particular case where the graph G is the $\mathbf{M}/2 \times \mathbf{N}/2$ periodic square lattice $\mathscr{L} = \mathscr{L}_A$ (or $\mathscr{L}_B$). We denote by

$$M = \mathbf{M}/2, \qquad N = \mathbf{N}/2, \qquad N_0(\mathscr{L}) = \mathscr{N}_S = MN \tag{3.1}$$

the dimensions of lattice $\mathscr{L}$, with a total number of sites $\mathscr{N}_S$. The $\mathscr{N}_S \times \mathscr{N}_S$ matric $\mathbf{C}$ of (2.3) is then (minus) the combinatoric Laplacian on $\mathscr{L}$. Its eigenvalues on this periodic lattice are

$$\begin{aligned} &\lambda_{\mathbf{k}} = 4 - 2\cos\frac{2\pi k}{M} - 2\cos\frac{2\pi l}{N} \\ &\mathbf{k} = \left(\frac{2\pi k}{M}, \frac{2\pi l}{N}\right), \qquad 0 \leqslant k \leqslant M-1, \quad 0 \leqslant l \leqslant N-1 \end{aligned} \tag{3.2}$$

The zero mode corresponds to $\mathbf{k} = \mathbf{0}$.

Let us now recall the essential results of the preceding section, now applied to the periodic lattice $\mathscr{L}$.

3.1.1. Partition Function. The exact form of the generating function for rooted K-spanning trees is [Eq. (2.10)]

$$\mathscr{Z}_T(m^2) = \sum_{K=1}^{\mathscr{N}_S} m^{2K} N_{T,K} = \det(\mathbf{C} + m^2 \mathbf{1})_{\mathscr{L}} \tag{3.3}$$

Note that the first term, i.e., the number of singly connected, rooted trees $N_{T,1}$, reads

$$N_{T,1} = \det' \mathbf{C}_{\mathscr{L}} = \mathscr{N}_S \det \mathbf{C}_{\mathscr{L}/\{a\}} \tag{3.4}$$

where the prime denotes the product of nonzero eigenvalues, while $\det \mathbf{C}_{\mathscr{L}/\{a\}}$ is the minor of any point $\{a\}$ in $\mathbf{C}$, and equals the number of unrooted 1-spanning trees on $\mathscr{L}$ [see (2.11)]

$$N^0_{T,1} = \det \mathbf{C}_{\mathscr{L}/\{a\}} \tag{3.5}$$

3.1.2. Correlation Functions. The grand canonical multipoint correlation function

$$\mathscr{Z}_T(a_1,..., a_K; m^2) = \sum_{K' \geqslant 0} m^{2K'} N_T(a_1,..., a_K; K')$$

of a set $A = \{a_1,..., a_K\}$ rooting K trees, and immersed into $K' \geqslant 0$ other rooted trees, reads in $\mathscr{L}$ [Eq. (2.7)]

$$\mathscr{Z}_T(a_1,..., a_K; m^2) = \det[(\mathbf{C} + m^2 \mathbf{1})_{\mathscr{L}/A}] \tag{3.6}$$

It also can be expressed as the correlation function [Eq. (2.13)]

$$\frac{\mathscr{Z}_T(a_1,..., a_K; m^2)}{\mathscr{Z}_T(m^2)} = \det{}_{K \times K}[\mathbf{G}_{a_i a_j}(m^2)]$$

in terms of the massive propagator

$$\mathbf{G}_{a_i a_j}(m^2) = (\mathbf{C} + m^2 \mathbf{1})^{-1}_{a_i a_j} \tag{3.7}$$

The zero-mass limit will be of particular interest later. The number of K-spanning trees rooted at $\{a_1,..., a_K\}$ is, on square lattice $\mathscr{L}$,

$$N_T(a_1,..., a_K) \equiv \mathscr{Z}_T(a_1,..., a_K; m^2 = 0) = \det \mathbf{C}_{\mathscr{L}/A} \tag{3.8}$$

It also has an expression in terms of the finite part of the propagator at zero mass [Eq. (2.20)]

$$\frac{N_T(a_1,\ldots,a_K)}{N_{T,1}^0} = \det_{(K-1)\times(K-1)} \mathbf{D}_{a_i a_j}, \qquad i,j=1,\ldots,K-1 \tag{3.9}$$

$$\mathbf{D}_{a_i a_j} = \tilde{\mathbf{G}}_{a_i a_j} - \tilde{\mathbf{G}}_{a_i a_K} - \tilde{\mathbf{G}}_{a_K a_j} + \tilde{\mathbf{G}}_{a_K a_K}$$

$$\tilde{\mathbf{G}}_{ab} = (\mathbf{C}+\mathbf{P}_0)^{-1}_{ab} - \frac{1}{MN} \tag{3.10}$$

where $(\mathbf{P}_0)_{ab} = 1/MN$ is the projector on the zero mode of $\mathbf{C}$.

The corresponding partition functions and correlation functions for Hamiltonian walks on Manhattan $\mathscr{M}$ can now be calculated directly in terms of those of spanning trees of $\mathscr{L}$, by using the relations established in Section 1, Eqs. (1.10), (1.14), (1.18), and (1.22).

Before proceeding further on the elaboration of results, let us make some basic remarks. We see that all formulas (3.3)–(3.10) are free field formulas. Hence, the problem of (adjacent and rooted) Hamiltonian walks on Manhattan oriented lattice $\mathscr{M}$ has been entirely reduced to a *free field* theory on the unoriented square lattice $\mathscr{L}$. The square mass m^2 of the field just plays the role of the grand canonical fugacity λ associated with the number of Hamiltonian walks, since from (1.18) one has

$$m^2 = 4\lambda$$

This identification opens different directions for exploiting the results. First, for fixed value $\mathbf{M}, \mathbf{N}$ of the lattice size, expanding all free field quantities in powers of m^2, one can evaluate on the *discrete* lattice all moments, i.e., the various numbers and correlation functions of HAWs, with some constraints (see Sections 3.2 and 3.3).

Of particular interest is the massless case, $m^2 = 0$. One knows indeed that a free field with zero mass is, in the *continuum limit*, a particular example of a *critical system*. On the Manhattan lattice or on $\mathscr{L}$, we shall reach the continuum limit by taking the infinite-volume limit $\mathbf{M}, \mathbf{N} \to \infty$ (since the lattice spacing has been fixed to one). The critical zero-mass limit will thus correspond to a finite set of HAWs filling the infinite lattice $\mathscr{M}$.

We discuss the critical continuum limit in Section 3.4, through its link to conformal invariance theory on the two-dimensional torus. This leads to a new way of seeing Manhattan Hamiltonian walks, which appear as a physical realization of a two-dimensional critical free field theory.

Away from the critical point, at $m^2 \neq 0$, one can also consider the continuum limit of the theory. The *finite-size scaling limit* is then particularly

interesting, where the mass m^2 goes to zero, while $\mathbf{M}, \mathbf{N} \to \infty$, keeping $m(\mathbf{MN})^{1/2}$ finite. We consider in detail this FSS limit in Section 3.5. From this limit all critical enumeration properties of finite sets of HAWs can be derived.

In Section 3.6 we calculate the critical correlation functions of trees or Hamiltonian walks on the continuum torus. Finally, another limit, m^2 fixed, $\mathbf{M}, \mathbf{N} \to \infty$, i.e., the massive infinite-volume limit, is also interesting. It corresponds physically to an infinite set of walks filling the infinite lattice, and is considered in Section 3.7.

3.2. Moments of Partition Functions

Let us evaluate the exact numbers of K-spanning trees $N_{T,K}$ and Hamiltonian walks $N_{\mathrm{H},K}$ on the discrete lattices $\mathscr{L}$ and $\mathscr{M}$, respectively. Due to (3.2) and (3.3), the tree-generating function $\mathscr{Q}_T$ reads explicitly, on the square periodic lattice,

$$\begin{aligned}\mathscr{Q}_T(m^2) &= \prod_{\substack{0 \leqslant k \leqslant M-1 \\ 0 \leqslant l \leqslant N-1}} \left(4 + m^2 - 2\cos\frac{2\pi k}{M} - 2\cos\frac{2\pi l}{N}\right) \\ &= \prod_{\mathbf{k}} (\lambda_{\mathbf{k}} + m^2) \end{aligned} \tag{3.11}$$

Expanding in powers of m^2 yields the first moments $N_{T,K}$,

$$N_{T,1} = \prod_{\mathbf{k}}{}' \lambda_{\mathbf{k}} \tag{3.12}$$

$$\frac{N_{T,2}}{N_{T,1}} = \sum_{\mathbf{k}}{}' \frac{1}{\lambda_{\mathbf{k}}} \tag{3.13}$$

$$\frac{N_{T,3}}{N_{T,1}} = \frac{1}{2}\left[\left(\sum_{\mathbf{k}}{}' \frac{1}{\lambda_{\mathbf{k}}}\right)^2 - \sum_{\mathbf{k}}{}' \frac{1}{\lambda_{\mathbf{k}}^2}\right] \tag{3.14}$$

$$\cdots$$

where the prime means that the zero mode $\mathbf{k} = \mathbf{0}$ is removed. The corresponding numbers of Hamiltonian walks on $\mathscr{M}$ are obtained from Eq. (1.16) and read

$$N_{\mathrm{H},1} = 8 \prod_{\substack{0 \leqslant k \leqslant M-1 \\ 0 \leqslant l \leqslant N-1 \\ (k,l) \neq (0,0)}} \left(4 - 2\cos\frac{2\pi k}{M} - 2\cos\frac{2\pi l}{N}\right) \tag{3.15}$$

$$\frac{N_{\mathrm{H},2}}{N_{\mathrm{H},1}} = 4 \sum_{\substack{0 \leqslant k \leqslant M-1 \\ 0 \leqslant k \leqslant N-1 \\ (k,l) \neq (0,0)}} \left(4 - 2\cos\frac{2\pi k}{M} - 2\cos\frac{2\pi l}{N}\right)^{-1} \tag{3.16}$$

$$\frac{N_{\mathrm{H},3}}{N_{\mathrm{H},1}} = 8\left[\sum_{k,l}{}' \left(4 - 2\cos\frac{2\pi k}{M} - 2\cos\frac{2\pi l}{N}\right)^{-1}\right]^2 - 8\left[\sum_{k,l}{}' \left(4 - 2\cos\frac{2\pi k}{M} - 2\cos\frac{2\pi l}{N}\right)^{-2}\right] \tag{3.17}$$

Of course, higher numbers $N_{\mathrm{H},K}$ can be calculated as well. These results generalize the celebrated exact value (3.15), (0.1) by Kasteleyn.

The large-lattice limit $\mathbf{M}, \mathbf{N} \to \infty$, or $M, N \to \infty$, with $\mathbf{M}/\mathbf{N} = M/N$ finite, can be seen either as the thermodynamic limit or the continuum limit, since the lattice mesh is fixed. The asymptotic value of $N_{\mathrm{H},1}$ is known.[9] We have evaluated directly the asymptotic expressions of (3.12)–(3.17) by a different method (Appendix A). They will also be obtained later by the evaluation of generating function (3.11) in the finite-size continuum limit. These asymptotics are

$$\ln N_{T,1} = MN\frac{4G}{\pi} + \ln MN + 4\ln[P(q)q^{1/24}\xi^{1/4}] + O\left(\frac{1}{(MN)^{1/2}}\right) \tag{3.18}$$

where

$$G = \int_0^{\pi/2} dx \ln[\sin x + (1 + \sin^2 x)^{1/2}]$$

$$= 1 - \frac{1}{3^2} + \frac{1}{5^2} + \cdots \tag{3.18a}$$

is Catalan's constant[4] and where ξ is the modular ratio of the torus[27,28]

$$\xi = \frac{M}{N} = \frac{\mathbf{M}}{\mathbf{N}} \qquad \text{and} \qquad q = e^{-2\pi M/N} \tag{3.19}$$

and

$$P(q) = \prod_{n=1}^{\infty} (1 - q^n) \tag{3.20a}$$

One uses also Dedekind's function

$$\eta(q) = P(q)q^{1/24} \tag{3.20b}$$

For the number of Hamiltonian walks on the $\mathbf{M} \times \mathbf{N}$ Manhattan lattice, this gives

$$N_{\mathrm{H},1} = \prod_{\mathbf{k} \neq \mathbf{0}} \lambda_{\mathbf{k}} \cong 2e^{G\mathbf{MN}/\pi} \mathbf{MN} \eta^4(q) \xi \tag{3.21}$$

This is just another form of Barber's result,[9] which can be transformed into the present one by using the properties of elliptic Jacobi θ-functions. For the next moment we find (Appendix A)

$$\sum_{\mathbf{k}}{}' \frac{1}{\lambda_{\mathbf{k}}} \cong \frac{MN}{4\pi} \left\{ \ln MN + 2 \ln \left(\frac{\sqrt{2}}{\pi} e^{\gamma} \right) - 4 \ln[P(q)\, q^{1/24} \xi^{1/4}] \right\} \tag{3.22}$$

(γ is the Euler constant).

Hence, the number of two-component Hamiltonian walks (3.16) reads asymptotically ($\mathbf{MN} = 4MN$)

$$N_{\mathrm{H},2} \cong N_{\mathrm{H},1} \frac{\mathbf{MN}}{4\pi} \ln \left(\mathbf{MN} \frac{e^{2\gamma}}{2\pi^2 \eta^4(q) \xi} \right) \tag{3.23}$$

The presence of a logarithmic growing factor, besides a term $\mathbf{MN}$, is characteristic of the enumeration of rooted walks or trees. This will appear clearly below in Part B, where two-component walks with no roots will be enumerated.[25] Finally, the evaluation of the third moment gives, after a rather long algebra (Appendix A),

$$\sum_{\mathbf{k}}{}' \frac{1}{\lambda_{\mathbf{k}}^2} \cong \left(\frac{MN}{2\pi} \right)^2 \left[\frac{1}{2^4 \times 45} (2\pi\xi)^2 + \frac{\zeta(3)}{2(2\pi\xi)} + \frac{1}{2\pi\xi} \sum_{n \geqslant 1} \frac{1}{n^3} \frac{q^n}{1-q^n} + \sum_{n \geqslant 1} \frac{1}{n^2} \frac{q^n}{(1-q^n)^2} \right] \tag{3.24}$$

From Eqs. (3.16), (3.17), (3.23), and (3.24) we finally find for the asymptotic number of rooted three-component Hamiltonian walks:

$$\frac{N_{\mathrm{H},3}}{N_{\mathrm{H},1}} = \frac{1}{2} \left(\frac{\mathbf{MN}}{4\pi} \right)^2 \left[\ln^2 \left(\mathbf{MN} \frac{e^{2\gamma}}{2\pi^2 \eta^4(q) \xi} \right) - \frac{1}{2^2 \times 45} (2\pi\xi)^2 - \frac{2\zeta(3)}{2\pi\xi} - \frac{4}{2\pi\xi} \sum_{n \geqslant 1} \frac{1}{n^3} \frac{q^n}{1-q^n} - 4 \sum_{n \geqslant 1} \frac{1}{n^2} \frac{q^n}{(1-q^n)^2} + \cdots \right] \tag{3.25}$$

By construction, the problem considered here is symmetric under the exchange of M and N (or $\mathbf{M}$ and $\mathbf{N}$). It is actually possible to check that expressions (3.18) and (3.21)–(3.25) are *invariant* in this exchange. For

(3.21), (3.23) this is easily seen, since they involve only the Dedekind combination $\eta^4(q)\xi$, which is known to be invariant.[28,29] For the result (3.25) this is less obvious, but true. This simple invariance is a particular case of the more general *modular invariance*[28] on a torus, which is valid for any critical system. The latter also holds true here, since we are actually dealing with a critical 2D free field theory. The expressions above are indeed *fully modular invariant*. Their complex analytic form can be obtained by letting q become complex[28] and reestablishing complex conjugates in the above real expressions. This will be studied in more detail later (Sections 3.4–3.6).

3.3. Correlation Functions

Let us first make explicit the general structure of multipoint correlation functions of order K. According to Eqs. (3.6) and (3.8), they can be obtained for the minor of order K of $\mathbf{C}$ on the periodic square lattice. Equivalently, they are computed in terms of the propagator $\mathbf{G}$ on the discrete lattice $\mathscr{L}$, (3.7) and (3.9). As we have seen, the form of the correlation functions depends upon whether $m^2 = 0$ or $m^2 \neq 0$.

Let us first consider the massless critical case: $m^2 = 0$. Then, the first correlation functions (3.9), (3.10) read for trees on $\mathscr{L}$

$$K=2: \quad N_T(a,b) = 2N^0_{T,1}[\tilde{\mathbf{G}}_{aa} - \tilde{\mathbf{G}}_{ab}] \tag{3.26}$$

$$K=3: \quad N_T(a,b,c) = N^0_{T,1} \det \begin{bmatrix} \mathbf{D}_{aa} & \mathbf{D}_{ba} \\ \mathbf{D}_{ab} & \mathbf{D}_{bb} \end{bmatrix} \tag{3.27}$$

with

$$\mathbf{D}_{aa} = 2[\tilde{\mathbf{G}}_{aa} - \tilde{\mathbf{G}}_{ac}]$$
$$\mathbf{D}_{bb} = 2[\tilde{\mathbf{G}}_{aa} - \tilde{\mathbf{G}}_{bc}]$$
$$\mathbf{D}_{ab} = \mathbf{D}_{ba} = \tilde{\mathbf{G}}_{ab} - \tilde{\mathbf{G}}_{ac} - \tilde{\mathbf{G}}_{bc} + \tilde{\mathbf{G}}_{aa}$$

On a periodic lattice $\mathbf{G}_{aa}$ is a constant independent of a. It is then convenient to introduce a shifted propagator (with a change of sign)

$$\mathbf{G}'_{ab} = \tilde{\mathbf{G}}_{aa} - \tilde{\mathbf{G}}_{ab} \tag{3.28}$$

Then one finds

$$N_T(a,b,c) = N^0_{T,1} \det \begin{bmatrix} 2\mathbf{G}'_{ac} & \mathbf{G}'_{ac} + \mathbf{G}'_{bc} - \mathbf{G}'_{ab} \\ \mathbf{G}'_{ac} + \mathbf{G}'_{bc} - \mathbf{G}'_{ab} & 2\mathbf{G}'_{bc} \end{bmatrix}$$
$$= N^0_{T,1}\{2\mathbf{G}'_{ac}\mathbf{G}'_{bc} + 2\mathbf{G}'_{ab}\mathbf{G}'_{ac} + 2\mathbf{G}'_{ab}\mathbf{G}'_{bc} - \mathbf{G}'^2_{ab} - \mathbf{G}'^2_{ac} - \mathbf{G}'^2_{bc}\} \tag{3.29}$$

which can be represented diagrammatically as in the Mayer expansion for real gases

$$\frac{N_T(a,b,c)}{N^0_{T,1}} = 2(\quad + \quad + \quad) - (\quad + \quad + \quad) \tag{3.30}$$

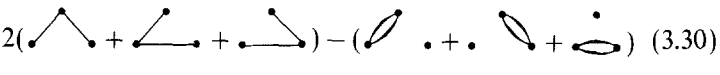

Higher order correlation functions can be calculated from (3.9), and have the same typical cluster structure.

For evaluating the correlation functions of the pure ($\lambda = 0$) Hamiltonian walks on a Manhattan lattice, one has simply to use the correspondence (1.6), (1.9), (1.10). One finds, to first order from (3.26), (3.29),

$$N_H(x, y) = \tfrac{1}{4} N^0_{H,1} [\mathbf{G}'_{a(x)\,a(y)} + \mathbf{G}'_{b(x)\,b(y)}] \tag{3.26bis}$$

$$N_H(x, y, z) = \tfrac{1}{8} N^0_{H,1}$$

$$\times \left\{ \det \begin{bmatrix} 2\mathbf{G}'_{a(x)\,a(z)} & \mathbf{G}'_{a(x)\,a(y)} - \mathbf{G}'_{a(x)\,a(z)} - \mathbf{G}'_{a(y)\,a(z)} \\ \mathbf{G}'_{a(x)\,a(y)} - \mathbf{G}'_{a(x)\,a(z)} - \mathbf{G}'_{a(y)\,a(z)} & 2\mathbf{G}'_{a(y)\,a(z)} \end{bmatrix} \right.$$

$$\left. + \text{id. with } b(x), b(y), b(z) \right\} \tag{3.29bis}$$

Let us recall that $N_H(x, y, z,...)$ is the total number of possible K-Hamiltonian circuits filling the lattice $\mathcal{M}$ such that one circuit passes through x, a second one through y, etc. (Fig. 4), $x, y, z,...$ being sites of $\mathcal{M}$.

On the square periodic lattice $\mathcal{L}$ the finite part $\tilde{\mathbf{G}}$, (3.10), of the massless propagator reads, from the eigenvectors and eigenvalues (3.2) of $\mathbf{C}$,

$$\tilde{\mathbf{G}}_{ab} = \sum_{\substack{0 \leqslant k \leqslant M-1 \\ 0 \leqslant l \leqslant N-1 \\ (k,l) \neq (0,0)}} \frac{\exp[2\pi i(k/M)(x_a - x_b) + 2\pi i(l/N)(y_a - y_b)]}{4 - 2\cos(2\pi k/M) - 2\cos(2\pi l/N)} \tag{3.31}$$

where $\mathbf{a} = (x_a, y_a)$ and $\mathbf{b} = (x_b, y_b)$ are the positions of points a and b on the discrete lattice $\mathcal{L}$. The zero mode is simply subtracted out.

Accordingly, the other propagator $\mathbf{G}'$, (3.28), reads formally

$$\mathbf{G}'_{ab} = \sum_{\mathbf{k} \neq \mathbf{0}} \frac{1}{\lambda_{\mathbf{k}}} \{1 - \exp[i\mathbf{k} \cdot (\mathbf{a} - \mathbf{b})]\} \tag{3.32}$$

with $\mathbf{k} = (2\pi k/M, 2\pi l/N)$.

Let us finally consider the massive case. Equations (3.7) giving the multipoint correlation function are now simpler. The massive propagator $\mathbf{G}_{a_i a_j}$ reads explicitly on $\mathscr{L}$

$$\mathbf{G}_{ab} = \sum_{\substack{0 \leqslant k \leqslant M-1 \\ 0 \leqslant l \leqslant N-1}} \frac{\exp[i\mathbf{k}(\mathbf{a}-\mathbf{b})]}{4+m^2-2\cos(2\pi k/M)-2\cos(2\pi l/N)} \tag{3.33}$$

The presence of a mass term makes the theory noncritical. At large distances, $\mathbf{G}_{ab}$ will have an exponential decay with a correlation length $\sim m^{-1}$. Hence, the correlations between trees or Hamiltonian circuits will be *screened* by the presence of a thermodynamic number of other trees or walks. Let us write the *grand canonical* correlation functions (1.20) of Hamiltonian circuits of $\mathscr{M}$, using the correspondence (1.18), (1.22) to trees. The result (3.7) for trees then gives immediately for HAWs on $\mathscr{M}$

$$\frac{\mathscr{Q}_{\mathrm{H}}(x_1,\ldots,x_K;\lambda)}{\mathscr{Q}_{\mathrm{H}}(\lambda)} = \frac{1}{2}\left[\det_{K\times K}\mathbf{G}_{a(x_i)\,a(x_j)}(m^2) + \det_{K\times K}\mathbf{G}_{b(x_i)\,b(x_j)}(m^2)\right] \tag{3.34}$$

with $m^2 = 4\lambda$, and where the points $\{a(x_i),\ i=1,\ldots,K\}$ of $\mathscr{L}_A$ and $\{b(x_i),\ i=1,\ldots,K\}$ of $\mathscr{L}_B$ are obtained by the lattice correspondence (1.9) (Figs. 6 and 7).

3.4. Critical Point and Conformal Properties

Here we study in more detail the general relation of the Manhattan Hamiltonian walk problem in the critical continuum limit to conformal invariance theory. We shall indicate the way HAWs are described within this formalism, by focusing on modular invariance on the torus and on central charge. In particular, we shall see the interpretation of Kasteleyn–Barber result (3.21) in terms of standard two-dimensional critical field theory.

In the preceding sections we saw that the generating functions $\mathscr{Q}_{\mathrm{H}}$ of (1.17) and $\mathscr{Q}_T$ of (1.19) read formally

$$\mathscr{Q}_{\mathrm{H}}(\lambda) = 2\mathscr{Q}_T(4\lambda) = 2\det(-\Delta + m^2)|_{m^2=4\lambda} \tag{3.35}$$

since $-\mathbf{C} = \Delta$ is the combinatoric Laplacian. Consider now a continuum free field theory, whose partition function on the torus $\mathbf{T}$ is defined by the functional integral

$$Z(m) = \int_{\text{periodic}} [D\varphi] \exp\left[-\int_{\mathbf{T}} d^2x\, \frac{1}{2}\varphi(-\Delta + m^2)\varphi\right] \tag{3.36}$$

where φ is periodic along the torus. This Gaussian integral reads formally

$$Z(m) \sim [\det(-\Delta + m^2)]_{\mathbf{T}}^{-1/2} \tag{3.37}$$

Therefore the generating function of HAWs reads

$$\mathcal{Q}_{\mathrm{H}}(m^2/4) \sim Z^{-2}(m) \tag{3.38}$$

In the limit $m \to 0$ the free field theory is the simplest example of a *critical* theory. This describes a finite set of Hamiltonian walks filling an infinite Manhattan lattice. Hence the properties of such Hamiltonian walks are those of a (two-dimensional) *critical system* and are *conformally invariant.*[27]

The critical limit allows us to escape from the simple rectangular periodic lattice and to consider the continuum torus parametrized[28-30] by its two complex periods ω_1, ω_2 with a modular ratio τ,

$$\tau = \omega_2/\omega_1, \qquad q = e^{2\pi i \tau} \tag{3.39}$$

Then the continuum, massless, free-field partition function on the torus, which has been much considered recently,[29,30] reads (in ζ-function regularization[29,30]

$$Z(m) = \frac{1}{m} Z_1 + \cdots, \qquad m \to 0 \tag{3.40}$$

with

$$Z_1 \equiv [\det'(-\Delta)]^{-1/2} = \frac{1}{\mathscr{A}^{1/2} (\operatorname{Im} \tau)^{1/2} \eta(q) \eta(\bar{q})} \tag{3.41}$$

where $\mathscr{A}$ is the area of the torus

$$\mathscr{A} = \operatorname{area}(\mathbf{T}) = |\omega_1|^2 \operatorname{Im} \tau \tag{3.42}$$

In the zero-mass limit we have, by definition of $\mathcal{Q}_{\mathrm{H}}$ in (1.17),

$$\mathcal{Q}_{\mathrm{H}}(m^2/4) = \tfrac{1}{4} m^2 N_{\mathrm{H},1} + \cdots$$

Hence we find, by comparing (3.38) and (3.40),

$$N_{\mathrm{H},1} = 4 Z_1^{-2} = 4 \mathscr{A} \operatorname{Im} \tau \, \eta^2(q) \eta^2(\bar{q}) \tag{3.43}$$

This formula is the modular invariant form[28] of the result (3.21), which

we obtained by a direct asymptotic evaluation of (3.15). Indeed, the periodic rectangular lattice $\mathscr{L}$ corresponds to

$$\begin{aligned} \omega_1 &= N, \qquad \omega_2 = iM \\ \tau &= iM/N, \qquad q = e^{-2\pi M/N} \\ \mathscr{A} &= MN = \mathbf{MN}/4 \end{aligned} \tag{3.44}$$

and Eqs. (3.21) and (3.43) coincide, except for the leading nonuniversal (dominant) term $\exp[(G/\pi)\,\mathbf{MN}]$. This is natural, since the field-theoretic approach (3.36) requires that one renormalizes continuum partition functions. Terms like $\exp[(G/\pi)\mathbf{MN}]$ are the exponentials of terms that diverge as powers of the cutoff. Those terms are set to zero in analytic regularization, such as the so-called ζ-function regularization.[29-31] It amounts here to simply setting $G=0$ for Catalan's constant. We shall return to this comparison of lattice and ζ-function regularizations in the next section, when we evaluate the complete generating function $\mathscr{Q}_T(m^2)$.

Let us finally consider the universal central charge[27] of the critical Hamiltonian system. This central charge[27] c governs in particular the universal finite-size scaling behavior of a critical system on an *infinite strip*. This geometry corresponds to the limit $q \to 0$ on the torus. Then the partition function of a critical system behaves as

$$Z \sim (q\bar{q})^{-c/24} \qquad (q \to 0)$$

For a free field [Eq. (3.41)] one has the well-known result $c=1$. Then the identities (3.38), (3.40), (3.41) show that for Hamiltonian walks the central charge is[20,21]

$$c = -2 \tag{3.45}$$

In Part B of this article, we shall obtain a further confirmation of this value, from an entirely different approach with the Potts model. Note that $c=-2$ is also the universal central charge of dense polymers,[20-22] which already signals the universality properties of HAWs on the Manhattan lattice.[25]

3.5. Finite-Size Effect, Continuum Limit Close to Criticality

3.5.1. Finite-Size Scaling Limit. We would like to have information on all the moments $N_{\mathrm{H},K}$ of $\mathscr{Q}_{\mathrm{H}}(m^2/4)$ in the large-lattice limit. These configuration numbers correspond to finite numbers $K \geqslant 1$ of walks occupying the infinite lattice. (The size of the walks grows with MN, not

their number.) For a gas of walks with fugacity m^2, the correlation length between walks is $\xi = m^{-1}$ (see Section 3.3) and gives the scale of the distance between points belonging to different walks. For a *finite* number of walks, this distance, or correlation length, is proportional to the system size $(MN)^{1/2}$. Hence, we are explicitly dealing with the *finite-size scaling limit* (FSS) where $MN \to \infty$, $m^2 \to 0$, together with keeping the product $m^2 MN$ *finite*. We shall obtain in this limit the exact generating function $\mathcal{Z}_{\mathrm{H}}(m^2/4)$ of the Hamiltonian walks on the continuum torus.

To perform the calculation, we introduce the FSS variable

$$t = m \frac{|\omega_1|}{2\pi} = m \frac{N}{2\pi} \tag{3.46}$$

and we want to evaluate for t fixed, in the infinite-lattice limit, the tree-generating function

$$\ln \mathcal{Z}_T(m^2) = \ln \det(-\Delta + m^2)|_{\mathbf{T}} = \sum_{\substack{0 \leqslant m' \leqslant M-1 \\ 0 \leqslant n \leqslant N-1}} \ln(4 - 2c_{m'} - 2c_n + m^2) \tag{3.47}$$

with

$$c_{m'} \equiv \cos \frac{2\pi m'}{M}, \qquad c_n = \cos \frac{2\pi n}{N}$$

To simplify the notations, we note the logarithm of the determinant on the torus

$$\ln D = \ln \det(-\Delta + m^2)|_{\mathbf{T}} \tag{3.48}$$

3.5.2. Series Representation. We first use the Fourier representation

$$\ln[2(\mathrm{ch}\, t' - \cos\theta)] = t' - \sum_{k \in \mathbf{Z}^*} \frac{e^{-|k|t'}}{|k|} e^{ik\theta} \tag{3.49}$$

We now set

$$2\,\mathrm{ch}\, t_n = 4 + m^2 - 2\cos\theta_n \qquad (t_n > 0) \tag{3.50}$$
$$\theta_n = 2\pi n/N$$

and rewrite (3.47) as

$$\ln D = \sum_{\substack{0 \leqslant m' \leqslant M-1 \\ 0 \leqslant n \leqslant N-1}} \left(t_n - \sum_{k \in \mathbf{Z}^*} e^{2\pi i k m'/M} e^{-|k| t_n}/|k| \right)$$

We perform the summation on momenta m' with

$$\sum_{0 \leqslant m' \leqslant M-1} e^{2\pi i k m'/M} = M \sum_{k' \in \mathbf{Z}} \delta_{k,k'M}$$

and find

$$\begin{aligned} \ln D &= \sum_{0 \leqslant n \leqslant N-1} \left(M t_n - 2 \sum_{k' \in \mathbf{N}^*} \frac{e^{-k'Mt_n}}{k'} \right) \\ &= \sum_{0 \leqslant n \leqslant N-1} [M t_n + 2 \ln(1 - e^{-Mt_n})] \end{aligned} \tag{3.51}$$

3.5.3. FSS Calculation. So we are led to evaluate the asymptotics of a single sum, parametrized by (3.50). To perform a finite-size scaling expansion around $m = 0$, we rewrite Eq. (3.50) in terms of the FSS variable t, (3.46),

$$\operatorname{ch} t_n = 2 + \left(\frac{2\pi}{N}\right)^2 \frac{t^2}{2} - \cos\theta_n, \qquad \theta_n = \frac{2\pi n}{N} \tag{3.52}$$

The zero-mass value $t_n^{(0)}$ of t_n is obtained from the equation

$$\operatorname{ch} t_n^{(0)} = 2 - \cos\theta_n \tag{3.53}$$

For N *large* and t *fixed*, we can expand, according to Eq. (3.52), t_n around $t_n^{(0)}$,

$$t_n = t_n^{(0)} + \delta t_n + \cdots \tag{3.54}$$

and find

$$\delta t_n = \left(\frac{2\pi}{N}\right)^2 \frac{t^2}{2} \frac{1}{\operatorname{sh} t_n^{(0)}}, \qquad \text{for} \quad n \neq 0 \tag{3.55}$$

For $n = 0$, we have simply

$$t_0 = \frac{2\pi}{N} t + \cdots \tag{3.56}$$

So we rewrite the first sum in (3.51) as

$$\begin{aligned} S &\equiv \sum_{0 \leqslant n \leqslant N-1} t_n \\ &= t_0 + \sum_{n \neq 0} t_n^{(0)} + \sum_{n \neq 0} \delta t_n + \sum_{n \neq 0} [t_n - t_n^{(0)} - \delta t_n] \end{aligned} \tag{3.57}$$

It is worth noting that instead of the Brillouin zone $n \in [0, N-1]$, the symmetric one $n \in [-N/2, N/2]$ is more convenient near the continuum limit, since the singularities will then stay near the origin.

Now, the two first sums in Eq. (3.57) will be evaluated separately. The third one has a finite continuum limit. Indeed for t fixed, $N \to \infty$, and n fixed, we find from (3.52)

$$t_n \to \frac{2\pi}{N}(n^2+t^2)^{1/2} \tag{3.58a}$$

$$t_n^{(0)} \to \frac{2\pi}{N} n \tag{3.58b}$$

$$\delta t_n \to \frac{2\pi}{N}\frac{t^2}{2n} \tag{3.58c}$$

Hence, the continuum limit of the last sum of Eq. (3.57) involves the convergent series

$$\sum_{1 \leqslant n \leqslant N-1} [t_n - t_n^{(0)} - \delta t_n] \to 2 \sum_{n=1}^{\infty} \frac{2\pi}{N}\left[(n^2+t^2)^{1/2} - n - \frac{t^2}{2n}\right] \tag{3.59}$$

1. For evaluating $\sum_n t_n^{(0)}$, we use the Euler–MacLaurin formula

$$\sum_{1 \leqslant n \leqslant N-1} f(n) = \int_0^N f(n)\, dn - \frac{1}{2}[f(0)+f(N)] + \sum_{n \geqslant 1} (-1)^{n-1} \frac{B_{2n}}{(2n)!}[f^{(2n-1)}(N) - f^{(2n-1)}(0)] \tag{3.60}$$

where the B_{2n} are Bernoulli numbers, $B_2 = 1/6$, $B_4 = -1/30$,.... For $t_n^{(0)}$, we have

$$\operatorname{ch} t(\theta) = 2 - \cos\theta$$

$$\theta = \frac{2\pi n}{N} \in [0, 2\pi]$$

$$t'(\theta) = \frac{\sin\theta}{\operatorname{ch} t(\theta)}, \qquad t'(0^+) = -t'(2\pi^-) = 1$$

and we obtain

$$\sum_{1 \leqslant n \leqslant N-1} t_n^{(0)} = N \int_0^{2\pi} t(\theta)\frac{d\theta}{2\pi} + \frac{1}{12}\frac{2\pi}{N}[t'(2\pi^-) - t'(0^+)] + \cdots$$

or

$$\sum_{1 \leqslant n \leqslant N-1} t_n^{(0)} = N\frac{4G}{\pi} - \frac{1}{6}\frac{2\pi}{N} + \cdots \tag{3.61}$$

where G is Catalan's constant

$$G = \frac{1}{4}\int_0^{\pi} d\theta\, t(\theta) = \int_0^{\pi/2} dx \ln[\sin x + (1+\sin^2 x)^{1/2}]$$

$$= 1 - \frac{1}{3^2} + \frac{1}{5^2} - \frac{1}{7^2} + \cdots \tag{3.62}$$

2. For evaluating finally $\sum_{n \neq 0} \delta t_n$ in (3.57), we have to subtract from it its dominant part near the origin, which diverges in the continuum limit. So we set

$$\sum_{1 \leqslant n \leqslant N/2} (\operatorname{sh} t_n^{(0)})^{-1} = S_1 + S_2$$

$$S_1 = \sum_{n=1}^{N/2} \left(\frac{1}{\operatorname{sh} t_n^{(0)}} - \frac{N}{2\pi n}\right) = -\frac{N}{2\pi}\ln\frac{\pi}{2\sqrt{2}} + \cdots$$

$$S_2 = \sum_{n=1}^{N/2} \frac{N}{2\pi n} = \frac{N}{2\pi}\left(\ln\frac{N}{2} + \gamma + \cdots\right)$$

and thus, from (3.55),

$$\sum_{1 \leqslant n \leqslant N-1} \delta t_n^{(0)} \cong \frac{2\pi}{N} t^2 \ln\left(Ne^{\gamma}\frac{\sqrt{2}}{\pi}\right) \tag{3.63}$$

Finally, it remains to evaluate in (3.51) the sum

$$S' = \sum_{0 \leqslant n \leqslant N-1} 2\ln(1 - e^{-Mt_n}) \tag{3.64a}$$

This is easily done, since the continuum limit (3.58a) yields a convergent sum. Hence

$$S' \to \sum_{n=-\infty}^{\infty} 2\ln\left\{1 - \exp\left[-2\pi\frac{M}{N}(n^2 + t^2)^{1/2}\right]\right\} \tag{3.64b}$$

where the sum over $n \in \mathbf{Z}$ comes from the two extremities of the Brillouin zone.

Collecting our results (3.56), (3.57), (3.59), (3.61), (3.63), and (3.64), we find the finite-size scaling limit of the massive free field determinant

$$\ln \det(-\Delta + m^2)|_{\mathbf{T}} = MN\frac{4G}{\pi} + 2\pi\frac{M}{N}\left[t - f(t) - \frac{1}{6} + t^2 \ln\left(Ne^{\gamma}\frac{\sqrt{2}}{\pi}\right)\right] + 2\sum_{n=-\infty}^{\infty} \ln\left\{1 - \exp\left[-2\pi\frac{M}{N}(n^2+t^2)^{1/2}\right]\right\} + \cdots \tag{3.65}$$

with

$$f(t) = \sum_{n=1}^{\infty}\left[2n + \frac{t^2}{n} - 2(n^2+t^2)^{1/2}\right] \tag{3.66}$$

and $t = mN/2\pi$.

This result is reminiscent of that found by Ferdinand and Fisher[32] for the Ising partition function on a torus. These authors used a different asymptotic method. This is not surprising, since close to criticality the Ising model is equivalent to a massive free fermion theory, which in turn is expressed in terms of bosonic degrees of freedom, with special boundary conditions.[32,30]

3.5.4. Modular Form and ζ-Regularization. It is interesting to rewrite this continuum partition function in a modular form. Indeed, by construction it is invariant under the exchange of M and N, and this is a nontrivial property of the result (3.65). In the continuum limit, one can also use the torus parametrization (3.39) with geodesics ω_1, ω_2. Using the identities (3.44), we obtain $\det(-\Delta + m^2)_{\mathbf{T}}$ in the form

$$\det(-\Delta + m^2)|_{\mathbf{T}} = \exp\left(\frac{4G}{\pi}\mathscr{A} - 2\pi \operatorname{Im}\tau\left\{\frac{1}{6} - t + f(t) + t^2 \ln\left[\frac{\pi}{\sqrt{2}}e^{-\gamma}\left(\frac{\operatorname{Im}\tau}{\mathscr{A}}\right)^{1/2}\right]\right\}\right) \times \prod_{n\in\mathbf{Z}}\{1 - \exp[-2\pi(n^2+t^2)^{1/2}\operatorname{Im}\tau]\}^2 \tag{3.67}$$

where τ is pure imaginary. A similar result on the torus has been recently obtained[33] by the different *ζ-regularization method.*[31] It reads

$$\det(-\Delta + m^2)|_{\zeta\text{-reg}} = \exp\left(-2\pi \operatorname{Im}\tau\left\{\frac{1}{6} - t + \frac{t^4}{2}\int_0^1 d\lambda\,(1-\lambda)\sum_1^{\infty}\frac{1}{(n^2+\lambda t)^{3/2}} + t^2 \ln\left[4\pi e^{-\gamma}\left(\frac{\operatorname{Im}\tau}{\mathscr{A}}\right)^{1/2}\right]\right\}\right) \times \prod_{n\in\mathbf{Z}}\{1 - \exp[2\pi i n \operatorname{Re}\tau - 2\pi(n^2+t^2)^{1/2}\operatorname{Im}\tau]\}^2 \tag{3.68}$$

valid for any complex modular ratio $\tau = \omega_2/\omega_1$. It is not difficult to see that

$$\frac{t^4}{2}\int_0^1 d\lambda\,(1-\lambda)\sum_1^\infty \frac{1}{(n^2+\lambda t)^{3/2}} = f(t) \tag{3.69}$$

where $f(t)$ is the function in (3.66). Hence, comparing (3.67) and (3.68), we are able to relate directly the lattice and ζ-regularized partition functions

$$\det(-\Delta + m^2)|_{\text{lattice reg}} = \exp\left[\frac{4G}{\pi}\mathscr{A} + \frac{5}{2}\ln 2(2\pi \operatorname{Im}\tau)t^2\right]\det(-\Delta+m^2)|_{\zeta\text{-reg}}$$

$$= \exp\left[\frac{4G}{\pi}\mathscr{A} + m^2\mathscr{A}\frac{5}{4\pi}\ln 2\right]\det(-\Delta+m^2)|_{\zeta\text{-reg}}$$

The first term is characteristic of the ultraviolet properties of the square lattice and yields Kasteleyn's result. It is of course unattainable by the ζ-method. Next, the appearance of a mass term difference $m^2\mathscr{A}$ between the two regularizations reflects the need for an ultraviolet renormalization of the "specific heat," i.e., the second derivative of $\ln Z$ in (3.37) with respect to m. The mass term $m^2\mathscr{A}$ is indeed associated with the logarithmic term $m^2\mathscr{A}\ln\mathscr{A}$, which thus has a different scale in the two regularizations.

The final, most general modular form of our lattice-regularized tree partition function $\mathscr{Z}_T(m^2)$, (3.47), is finally given in the continuum limit by

$$\ln \mathscr{Z}_T(m^2) = \ln\det(-\Delta+m^2)|_{\mathbf{T}}$$

$$= \frac{4G}{\pi}\mathscr{A} - 2\pi\operatorname{Im}\tau\left[\frac{1}{6} - t + f(t) + t^2\ln C\right]$$

$$+ \sum_{n\in\mathbf{Z}} 2\ln\{1-\exp[2\pi i n\operatorname{Re}\tau - 2\pi(n^2+t^2)^{1/2}\operatorname{Im}\tau]\} \tag{3.70}$$

where C is the constant

$$C = \frac{\pi}{\sqrt{2}}e^{-\gamma}\left(\frac{\operatorname{Im}\tau}{\mathscr{A}}\right)^{1/2} \tag{3.71}$$

and $t = m|\omega_1|/2\pi$.

3.5.5. Small-Mass Limit in FSS. As already discussed, the series expansion in powers of t of the finite-size scaling expression of $\mathscr{Z}_T(m^2)$, (3.70), yields the number of K-trees $N_{T,K}$ or of Hamiltonian walks $N_{\mathrm{H},K}$ in the continuum limit or infinite-lattice limit for any *finite* value of K. Straightforward but lengthy algebra yields the series

$$\ln \det(-\Delta + m^2)|_{\mathrm{T}} = \frac{4G}{\pi}\mathscr{A} - \frac{x}{6} + 2\ln P(q)\,P(\bar{q}) + \ln x^2 t^2$$
$$+ \frac{1}{12}x^2t^2 - xt^2 \ln[P(q)\,P(\bar{q})C]$$
$$- \frac{1}{2^5 \cdot 45}x^4t^4 - xt^4\frac{1}{4}\zeta(3)$$
$$- \frac{1}{4}xt^4\left[\sum_{n\geqslant 1}\frac{q^n}{1-q^n}\frac{1}{n^3} + \text{c.c.}\right]$$
$$- \frac{1}{4}x^2t^4\left[\sum_{n\geqslant 1}\frac{q^n}{(1-q^n)^2}\frac{1}{n^2} + \text{c.c.}\right] + O(t^6) \qquad (3.72)$$

where

$$x \equiv 2\pi \operatorname{Im}\tau, \qquad xt^2 = m^2\mathscr{A}/2\pi$$

Use of the formal expansion

$$\ln \det(-\Delta + m^2) = \ln m^2 + \sum_{\mathbf{k}\neq\mathbf{0}} \ln \lambda_{\mathbf{k}} + \sum_{p\geqslant 1}\frac{(-1)^{p-1}}{p}m^{2p}\sum_{\mathbf{k}\neq\mathbf{0}}(\lambda_{\mathbf{k}})^{-p} \qquad (3.73)$$

allows to identify the first moments (3.18), (3.22), and (3.24). QED. This checks the exactness of the general formula (3.70). From this, the Hamiltonian walk numbers $N_{\mathrm{H},1}$ of (3.21), $N_{\mathrm{H},2}$ of (3.23) and $N_{\mathrm{H},3}$ of (3.25) are recovered. With patience, any tree number $N_{T,K}$ or HAW number $N_{\mathrm{H},K}$ can then be obtained in the large-lattice limit from the expansion (3.70).

3.5.6. Large-Mass Limit in FSS. It is finally interesting to consider the large-fugacity limit of $\mathscr{Z}_{\mathrm{H}}$ or $\mathscr{Z}_T$ where more and more walks start to fill the lattice. This corresponds to the large-t expansion of $\ln D$ of (3.70) in finite-size scaling. We first need the large-t expansion of function $f(t)$ [(3.66), (3.69)]. After some calculations involving the Euler–MacLaurin formula, it is obtained as

$$f(t) = t^2\left(\ln t - \ln 2 + \gamma - \frac{1}{2}\right) + t - \frac{1}{6} + \frac{1}{360}\frac{1}{t} + \cdots, \qquad t\to\infty \qquad (3.74)$$

Since the last series in (3.70) gives only exponentially small corrections, we find

$$\ln D|_{\mathrm{FSS}} = \frac{4G}{\pi}\mathscr{A} - 2\pi \operatorname{Im}\tau\, t^2 \ln\left[t\pi 2^{-3/2}e^{-1/2}\left(\frac{\operatorname{Im}\tau}{\mathscr{A}}\right)^{1/2}\right]$$
$$+ \frac{1}{360t} + \cdots, \qquad t\to\infty \qquad (3.75a)$$

Using now definitions (3.42) and (3.46) gives

$$\ln D|_{\mathrm{FSS}} = \frac{4G}{\pi}\mathscr{A} - \frac{1}{2\pi}m^2\mathscr{A}\ln(m2^{-5/2}e^{-1/2}) + O\left(\frac{1}{m|\omega_1|}\right), \qquad t \to \infty \tag{3.75b}$$

This limit corresponds to a *large* but still not thermodynamic number of walks filling the infinite Manhattan lattice. We shall use it later for evaluating the effective Hamiltonian entropy as a function of the walk concentration. As we shall see now, this large-mass limit in FSS is also identical to the small-mass limit of the *standard* thermodynamic limit of $\ln D$ or $\ln \mathscr{Q}_{\mathrm{H}}$. By *standard*, we mean that the large-lattice-size limit is taken at fixed value of m^2. Hence, the correlation length m^{-1} remains infinitesimally small with respect to the torus size. The mean number $\langle K \rangle$ of Hamiltonian walks is then thermodynamically large, and allows the definition of a walk (or circuit) concentration $\langle K \rangle / \mathscr{A}$, where $\mathscr{A}$ is the area of the torus. We shall thus call this limit in brief the *Hamiltonian melt*, and study it now.

3.6. Hamiltonian Melt Entropy

We thus consider the standard thermodynamic limit, which consists in taking

$$M, N \to \infty, \qquad m^2 \text{ fixed} \tag{3.76}$$

We have to return to the exact representation of $\ln D$ in (3.51) before it was evaluated in the FSS limit:

$$\ln D = \sum_{0 \leqslant n \leqslant N-1} Mt_n + 2\ln(1 - e^{-Mt_n}) \tag{3.77}$$

$$2 \operatorname{ch} t_n = 4 + m^2 - 2\cos\theta_n, \qquad \theta_n = 2\pi n/N$$

Taking the straightforward thermodynamic continuum limit gives

$$\ln \mathscr{Q}_T(m^2) \to \ln D_\infty = MN \int_0^\pi \frac{d\theta}{\pi} t(\theta) \tag{3.78a}$$

with

$$\operatorname{ch} t(\theta) = 2 + \tfrac{1}{2}m^2 - \cos\theta \tag{3.78b}$$

This limit is exact, up to exponentially small correction terms, coming both from the corrections of the Euler–MacLaurin formula for a *periodic*

function like $t(\theta)$ and from the second term of (3.77). It is then interesting to define a grand canonical potential, which is an intensive quantity

$$\mathscr{Q} = \lim_{\mathscr{A} \to \infty} \frac{1}{\mathscr{A}} \ln \mathscr{Q}_{\mathrm{H}} = \frac{1}{\mathscr{A}} \ln D_{\infty} \tag{3.79}$$

(Note that we choose for convenience to take as a reference area $\mathscr{A}$ the number of sites of the underlying square lattices $\mathscr{L}_A$ and $\mathscr{L}_B$ and not that of the Manhattan torus $4\mathscr{A}$.)

Hence

$$\mathscr{Q} = \frac{1}{\pi} \int_0^{\pi} d\theta\, t(\theta), \qquad \operatorname{ch} t = 2 + \frac{m^2}{2} - \cos\theta \tag{3.80}$$

Let us recall that according to Eqs. (1.17) and (1.19) we have

$$\mathscr{Q}_{\mathrm{H}}(\lambda) = \sum_{K \geqslant 1} \lambda^K N_{\mathrm{H},K} = 2D(m^2 = 4\lambda)$$

The grand canonical potential (3.79) is thus of purely entropic nature and we define an average concentration for the number of Hamiltonian paths per unit of area,

$$\mathscr{C} = \frac{\langle K \rangle}{\mathscr{A}} = \lambda \frac{\partial}{\partial \lambda} \frac{1}{\mathscr{A}} \ln \mathscr{Q}_{\mathrm{H}} = m^2 \frac{\partial}{\partial m^2} \frac{\ln D_{\infty}}{\mathscr{A}} \tag{3.81}$$

From (3.80) we find its parametric form

$$\mathscr{C} = \frac{m^2}{2\pi} \int_0^{\pi} d\theta \frac{1}{\operatorname{sh} t(\theta)} \tag{3.82}$$

Since $\mathscr{Q}_{\mathrm{H}}$ resums numbers of configurations, we can define a (grand canonical) entropy by Legendre-transforming (3.79) with respect to the chemical potential $\ln \lambda$

$$\mathscr{S} = \mathscr{Q} - \ln \lambda \frac{\partial}{\partial \ln \lambda} \mathscr{Q}, \qquad \mathscr{C} = \frac{\partial}{\partial \ln \lambda} \mathscr{Q}, \qquad \ln \lambda = -\frac{\partial \mathscr{S}}{\partial \mathscr{C}} \tag{3.83a}$$

We can also write

$$\mathscr{S} = \mathscr{Q} - \mathscr{C} \ln(m^2/4) \tag{3.83b}$$

There are now two interesting limits of $\ln D_{\infty}$:

$$m^2 \to 0, \qquad m^2 \to \infty$$

3.6.1. Small-Walk-Concentration Limit. Due to the existence of a critical point at $m^2 = 0$, $\ln D$ develops a weak logarithmic singularity near the origin. Expanding (3.78) near $m^2 = 0$ yields

$$\ln D_\infty = \mathscr{A}\left[\frac{4G}{\pi} - \frac{1}{4\pi} m^2 \ln m^2 + O(m^2)\right], \qquad m^2 \to 0 \tag{3.84}$$

where G is Catalan's constant, i.e., the zero-mass value (3.62). Comparing (3.84) for the standard thermodynamic limit at m^2 small and the finite-size scaling form $\ln D|_{\text{FSS}}$ from (3.75b) for t large, we see that they just coincide. These two limits describe the same crossover region where one goes from finite-size scaling to standard thermodynamics. This is even clearer if one considers the concentration of Hamiltonian walks (3.81). From (3.75b) we find

$$\mathscr{C} = -\frac{1}{4\pi} m^2 \ln(m^2 2^{-5}) \tag{3.85}$$

So, in FSS the regime $t^2 \sim m^2 \mathscr{A}$ being large means $\mathscr{C}\mathscr{A} = \langle K \rangle$ large, while in standard thermodynamics ($\mathscr{A} = \infty$) the limit $m^2 \to 0$ means $\mathscr{C}a^2$ small (a is the lattice spacing, here taken equal to 1). So these two situations both correspond physically to a number of chains becoming thermodynamic, but with a very small concentration at the lattice spacing scale.

Eliminating m^2 between (3.84) and (3.85) yields for the potential $\mathscr{Q}$ the expansion at small concentrations

$$\mathscr{Q} = \frac{4G}{\pi} + \mathscr{C} - \frac{\mathscr{C}}{\ln \mathscr{C}} + \cdots, \qquad \mathscr{C} \to 0 \tag{3.86}$$

So we see that the concentration dependence is nonanalytic at $\mathscr{C} = 0$, reflecting the existence of the free field *critical point*. The entropy (3.83b) has a slightly different singular behavior

$$\mathscr{S} = \frac{4G}{\pi} - \mathscr{C} \ln \mathscr{C} + O(\mathscr{C}) \tag{3.87}$$

valid for $\mathscr{C}$ small. As expected, for a vanishing concentration, the entropy (per site of $\mathscr{L}$) $4G/\pi$ just recovers (four times) the Kasteleyn connectivity constant (0.3) of the single Hamiltonian walk.

3.6.2. High-Concentration Limit. This limit will drive the Hamiltonian system to its *saturation*, i.e., to the maximum number of disconnected paths filling the lattice. It is obtained by expanding (3.78b) for m^2 large:

$$t(\theta) = \ln m^2 + (4 - 2\cos\theta) m^{-2} + O(m^{-4})$$

which gives in (3.78a)

$$\mathscr{Q} = \frac{1}{\mathscr{A}} \ln D_\infty = \ln m^2 + 4m^{-2} + O(m^{-4}) \tag{3.88a}$$

The Hamiltonian concentration (3.81) reads therefore

$$\mathscr{C} = 1 - 4m^{-2} + O(m^{-4}) \tag{3.88b}$$

and finally

$$\mathscr{Q} \cong \ln\left(\frac{4}{1-\mathscr{C}}\right) + 1 - \mathscr{C} \tag{3.89}$$

where the concentration is close to its upper maximum value $\mathscr{C}_{\max} = 1$. The occurrence of this maximum concentration is easy to understand. It occurs when all Hamiltonian loops form MN elementary plaquettes of length 4 on $\mathscr{M}$, encircling either all the $\mathscr{A} = MN$ sites of $\mathscr{L}_A$ or all those of $\mathscr{L}_B$ (Fig. 4). Close to this saturation limit, the entropy (3.83b) is easily found from (3.88b),

$$\mathscr{S} \cong \ln 4 + (1-\mathscr{C})[1 + \ln(1-\mathscr{C})^{-1}] \tag{3.90}$$

for $\mathscr{C} \to 1^-$. The limiting entropy $\ln 4$ is, as expected, just given by the number of choices of the origin of the circuit on each of the plaquettes of $\mathscr{M}$. This value is reached with a logarithmically diverging slope.

The full curve giving the entropy $\mathscr{S}$ as a function of concentration $\mathscr{C}$ for $0 \leqslant \mathscr{C} \leqslant 1$ has been calculated numerically, using the parametric form

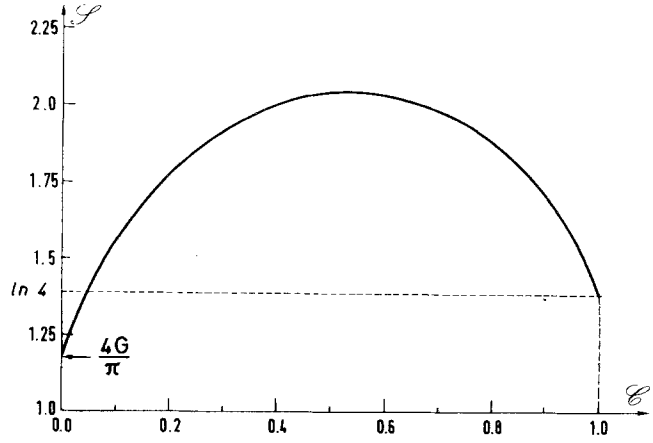

Fig. 8. The entropy $\mathscr{S}$ versus the walk concentration $\mathscr{C}$ in the thermodynamic (melt) limit.

(3.80), (3.82), (3.83). This curve (Fig. 8) has a characteristic convex shape with a maximum value at $\mathscr{C} \cong 0.536591$. When the walk concentration $\mathscr{C}$ increases from zero, this maximum value of the entropy results from a competition between the increase of entropy due to the increase of the number of free extremities of walks and an entropic decrease due to the reduction of exchanges of positions between the different walks.

3.7. Continuum Correlation Functions

One can repeat for all the multipoint correlation functions, whose exact forms are given in Section 3.3, the analysis of the continuum limit presented above for the generating functions $\mathscr{Z}_T$ or $\mathscr{Z}_H$. In particular, one would have to distinguish the FSS limit (Section 3.5) from the standard thermodynamic limit (Section 3.6). We shall not perform here all the intermediate FSS analysis, which is involved. Instead we concentrate on the two interesting extreme cases.

1. The critical limit, where one looks at the correlations of any finite set of K walks filling the continuum torus. (Note that the FSS is only the resummation of this case.)

2. The standard thermodynamic limit (infinite-volume limit) with a finite concentration of walks in the melt.

3.7.1. Exact Critical Multipoint Correlation Functions. The formal expressions of the Hamiltonian and tree correlation functions in the massless case are given in Section 3.3. They are built [Eqs. (3.26)–(3.29)] as determinants of the finite part of the free field propagators $\tilde{\mathbf{G}}_{ab}$, (3.31), or $\mathbf{G}'_{ab}$, (3.32). The Laplacian of $\mathbf{G}'_{ab}$ reads, from (3.32),

$$\Delta \mathbf{G}'_{ab} = \sum_{\mathbf{k} \neq \mathbf{0}} \frac{\mathbf{k}^2}{\lambda_{\mathbf{k}}} \exp[i\mathbf{k} \cdot (\mathbf{a} - \mathbf{b})] \tag{3.91}$$

In the continuum limit, we have for the eigenvalues (3.2)

$$\lambda_{\mathbf{k}} \cong (2\pi)^2 \left(\frac{k^2}{M^2} + \frac{l^2}{N^2} \right) \equiv \mathbf{k}^2 \tag{3.92}$$

Adding and subtracting the zero-mode contribution to (3.91) and taking the continuum limit yields the equation

$$\Delta \mathbf{G}' = \mathscr{A} \delta^2(\mathbf{a} - \mathbf{b}) - 1$$

Now, the solution of the Poisson equation on the *continuum* torus

$$\Delta G = \delta(\mathbf{r}) - 1/\mathscr{A} \tag{3.93}$$

has been much studied in the realm of conformal invariance.[30,34] We use the standard parametrization (3.39) of the geodesics of the torus by generators ω_1, ω_2 and denote by z the complex affix of a point $\mathbf{r} = \mathbf{a} - \mathbf{b}$ on the torus. Setting

$$y = e^{2\pi i z/\omega_1}, \qquad q = e^{2\pi i \omega_2/\omega_1}, \qquad \mathrm{Im}(\omega_2/\omega_1) > 0$$

we find for G exactly

$$G(\mathbf{r}) = \frac{1}{2}\left(\frac{\mathrm{Im}^2(z/\omega_1)}{\mathrm{Im}\,\tau} + \mathrm{Im}\,\frac{z}{\omega_1}\right) - \frac{1}{2\pi}\ln\left|\frac{F(z)}{F'(0)}\right| \tag{3.94}$$

with

$$\begin{aligned} F(z) &= \sum_{m \in \mathbf{Z}} (-y)^m q^{m(m+1)/2} \\ &= (1 - y^{-1}) \prod_{n \geqslant 1} (1 - q^n)(1 - yq^n)(1 - y^{-1}q^n) \\ F'(0) &= \frac{2\pi i}{\omega_1} P^3(q), \qquad P(q) = \prod_{n \geqslant 1} (1 - q^n) \end{aligned} \tag{3.95}$$

and the correlation function $\tilde{\mathbf{G}}$ or $\mathbf{G}'$ reads (up to an additive constant)

$$\mathbf{G}' = \mathscr{A} G \tag{3.96}$$

At short distance, $|z|/\omega_1 \to 0$, one recovers

$$\begin{aligned} G &= -\frac{1}{2\pi}\ln|z| + \cdots \\ \mathbf{G}' &= -\frac{\mathscr{A}}{2\pi}\ln|z| + \cdots \end{aligned} \tag{3.97}$$

i.e., the standard Coulomb potential in the infinite plane. When considering the discrete torus, this limit is valid for distances large with respect to the lattice spacing, but small with respect to the torus generators. For intermediate finite-size distances, the general aspect of the lines of equicorrelation is given on Fig. 9.

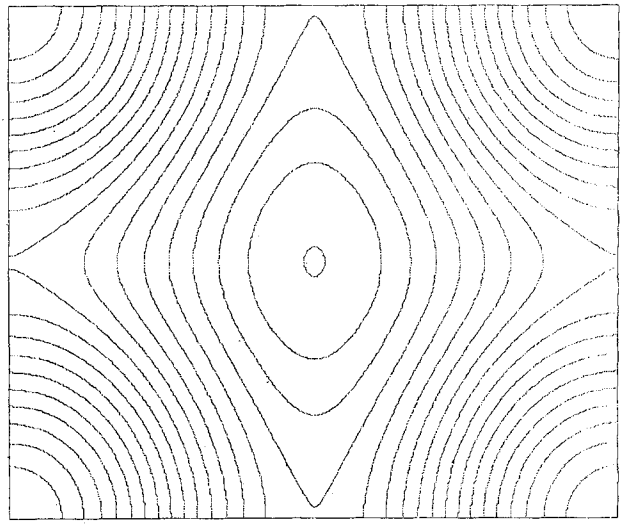

Fig. 9. The *critical* continuum correlation function $G(\mathbf{r})$ of (3.94) on the torus (courtesy of J. M. Luck). The lines are *equiprobability* lines of finding a second HAW passing through $\mathbf{r}$, knowing that a first one passes through the origin 0. One observes the restoration of the radial symmetry near the origin, where $G(\mathbf{r}) \sim -\ln r$, implying a weak logarithmic *repulsion* of two walks.

In the continuum limit, we do not distinguish of course lattices $\mathscr{L}_A$ and $\mathscr{L}_B$. Then the two- and three-point Hamiltonian correlation functions (3.26bis) and (3.29bis) read

$$\frac{N_{\mathrm{H}}(x, y)}{N^0_{\mathrm{H},1}} = \frac{1}{2}\mathbf{G}'(x-y)$$

$$\frac{N_{\mathrm{H}}(x, y, z)}{N^0_{\mathrm{H},1}} = \frac{1}{4}\det\begin{bmatrix} 2\mathbf{G}'(x-z) & \mathbf{G}'(x-z)+\mathbf{G}'(y-z)-\mathbf{G}'(x-y) \\ \mathbf{G}'(x-z)+\mathbf{G}'(y-z)-\mathbf{G}'(x-y) & 2\mathbf{G}'(y-z) \end{bmatrix}$$

The short-distance (planar) limit gives, for instance, explicitly

$$\frac{N_{\mathrm{H}}(x, y)}{N^0_{\mathrm{H},1}} \cong -\frac{1}{4\pi}\mathscr{A}\ln|x-y| \tag{3.98}$$

$$\begin{aligned}\frac{N_{\mathrm{H}}(x, y, z)}{N^0_{\mathrm{H},1}} \cong \frac{1}{4}\frac{\mathscr{A}^2}{(2\pi)^2}\,&(2\ln|x-z|\ln|z-y| + 2\ln|x-y|\ln|y-z| \\ &+ 2\ln|x-y|\ln|x-z| - \ln^2|x-y| \\ &- \ln^2|y-z| - \ln^2|z-x|)\end{aligned} \tag{3.99}$$

for distances $|x-y|$, $|y-z|$, $|z-x|$ small with respect to $|\omega_1|$, $|\omega_2|$. Therefore we see that the correlation functions of a few (adjacent) Hamiltonian walks filling the Manhattan lattice are essentially *determinants of logarithms.*

It is striking to note that this exact logarithmic form agrees with some logarithm behavior obtained[35] in the study of two-dimensional polymer melts within the quite different realm of the nonlinear σ-model. We believe that the present results, while attached to the specific model of Manhattan HAWs, embodies some essential physics of the two-dimensional polymer melts. We return to this later, when studying the universality properties of the model.

The full continuum exact expression of the critical correlation functions on the torus is obtained by plugging (3.94) and (3.95) into the above correlators.

3.7.2. Exact Correlation Functions in the Melt. The correlation functions in the massive case are given by the determinant formulas (3.7), (3.33), (3.34). Now, in the infinite-volume case $M, N \to \infty$, m^2 fixed, the continuum limit of the free field propagator $\mathbf{G}_{ab}$ of (3.33) reads simply

$$\mathbf{G}_{ab} \cong \frac{MN}{(2\pi)^2} \int d^2k \frac{\exp[i\mathbf{k}\cdot(\mathbf{a}-\mathbf{b})]}{m^2+k^2}$$

and in two dimensions is known to be the Bessel function

$$\mathbf{G}(r) = \frac{\mathscr{A}}{2\pi} K_0(mr) \tag{3.100}$$

with $\mathbf{r} = \mathbf{a} - \mathbf{b}$.

Hence we find the grand canonical multiple correlation functions for Hamiltonian walks (3.34) in the standard thermodynamic limit, i.e., for a *Hamiltonian melt,*

$$\frac{\mathscr{Q}_{\mathrm{H}}(x_1,\ldots,x_K;m^2/4)}{\mathscr{Q}_{\mathrm{H}}(m^2/4)} = \left(\frac{\mathscr{A}}{2\pi}\right)^K \det_{K\times K}\{K_0(m|x_i-x_j|)\} \tag{3.101}$$

This quantity represents the (grand canonical) probability of finding K distinct Hamiltonian walks passing through the points x_i, $i=1,\ldots,K$, in a Manhattan Hamiltonian melt. Let us recall that the grand canonical partition function $\mathscr{Q}_{\mathrm{H}}(m^2/4)$, (1.17), is given, in the standard infinite-volume case, by the parametric equations (3.78)

$$\mathscr{Q}_{\mathrm{H}}(m^2/4) = 2\exp\left[(\mathscr{A}/\pi)\int_0^\pi d\theta\, t(\theta)\right]$$

where $t(\theta)$ is given in (3.78b). The melt *correlation length* is m^{-1} and is related to the walk concentration $\mathscr{C}$ by the parametric equation (3.82). According to the preceding section, we have for small concentration [Eq. (3.85)]

$$m^2/4 \cong \pi\mathscr{C}/\ln(\pi\mathscr{C}), \qquad m^2 \to 0 \tag{3.102}$$

while the concentration reaches its maximum value $\mathscr{C} \to 1$ [Eq. (3.88b)] when

$$m^2/4 \cong 1/(1-\mathscr{C}), \qquad m^2 \to \infty \tag{3.103}$$

It is interesting to consider the two limits of the correlation functions (3.101), at short and large distances, respectively.

Critical Short-Distance Behavior. For z small, we have $K_0(z) = -\ln(z/2)[1+O(z)]$.

The two-point correlation function therefore reads

$$\mathbf{G}(\mathbf{r}) \cong -(\mathscr{A}/2\pi)\ln(mr/2)[1+O(mr)] \tag{3.104}$$

This is in full agreement with the *critical* two-point correlation function (3.97) at small distances, as it should be. Only the length scale of the logarithmic behavior has changed. It was given at criticality by the torus periods ω_1, ω_2, while here it is given by the inverse fugacity m^{-1}, or by the concentration (3.102), (3.103). The multipoint correlation function at short distances in the melt is therefore

$$\frac{\mathscr{Q}_{\mathrm{H}}(x_1,\ldots,x_K,m^2/4)}{\mathscr{Q}_{\mathrm{H}}(m^2/4)} \cong \left(\frac{\mathscr{A}}{2\pi}\right)^K \det_{K\times K}\left[-\ln\left(|x_i-x_j|\frac{m}{2}\right)\right] \tag{3.105}$$

Classical Long-Distance Screening. For $z \to \infty$,

$$K_0(z) = (\pi/2z)^{1/2}e^{-z}[1+O(z^{-1})]$$

Hence, at large distances, $rm \gg 1$, one has

$$\mathbf{G}(\mathbf{r}) \cong \frac{\mathscr{A}}{2\pi}\left(\frac{\pi}{2mr}\right)^{1/2} e^{-mr} \tag{3.106}$$

and

$$\frac{\mathscr{Q}_{\mathrm{H}}(x_1,\ldots,x_K,m^2/4)}{\mathscr{Q}_{\mathrm{H}}(m^2/4)} \cong \left(\frac{\mathscr{A}}{2\pi}\right)^K \left(\frac{\pi}{2m}\right)^{K/2} \det_{K\times K}\left(\frac{e^{-m|x_i-x_j|}}{|x_i-x_j|^{1/2}}\right) \tag{3.107}$$

The correlations are exponentially screened at distances larger than the correlation length. Hence the *melt of (adjacent) Manhattan Hamiltonian walks, at a finite walk concentration, is in a normal fluid phase.*

4. FREE BOUNDARY CONDITIONS (EVEN–EVEN LATTICE)

4.1. General Considerations

Until now, we have considered closed Hamiltonian walks on a torus. When considering instead a rectangle with *free edges*, interesting new boundary effects appear. This situation has not yet been studied in detail, except for numerical work by Malakis.[10] But the numerical enumeration of single HAWs was done only on small Manhattan lattices and the fit to a conjectured asymptotic form was not very precise. Here we derive the exact asymptotic number of single HAWs.

We consider an even–even $\mathbf{M} \times \mathbf{N}$ (sites) Manhattan lattice with free edges,

$$\mathbf{M} = 2M, \qquad \mathbf{N} = 2N$$

The even–even lattice allows to arrange on it *closed* Hamiltonian walks (Fig. 10), which can be related to spanning trees as before. When one of the sides of the lattice $\mathcal{M}$ has an odd number of sites, the situation is quite different, since only completely *open* HAWs are possible. They are no longer in direct correspondence to trees, and must be studied by a slightly different technique (Section 7). For the even–even lattice, the Manhattan orientation must be properly chosen for closed HAWs to be possible. The lattice external perimeter must form a closed oriented loop (Fig. 10).

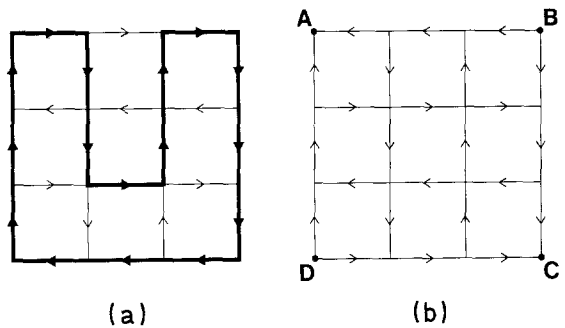

Fig. 10. (a) A 4×4 Manhattan lattice with free edges. The relative orientation of the horizontal and vertical boundary lines is chosen so that there is one large oriented perimeter loop encircling the lattice. Then HAWs are possible. (b) The other choice of boundary orientations; HAWs are impossible, since they should start at *B and D*, end at *A and C*.

As for the torus, one introduces the grand canonical partition function of K disconnected Hamiltonian walks with free boundary conditions

$$\mathcal{Q}^{\mathrm{f}}_{\mathrm{H}}(\lambda) = \sum_{K \geqslant 1} \lambda^K N^{\mathrm{f}}_{\mathrm{H},K} \tag{4.1}$$

where $N^{\mathrm{f}}_{\mathrm{H},K}$ is the number of K-HAWs with rooted origins. Let us recall that the walks can be either open, with the origin and extremity at one lattice spacing, or closed (Fig. 3). In the latter case, the position of the origin of the closed walk is counted.

The only difference from the periodic case lies in the fact that only one of the sublattices $\mathscr{L}_A$ or $\mathscr{L}_B$ is now relevant. All Hamiltonian walks will indeed circulate in the same sense, defined by the lattice perimeter, and this selects either $(+)$ or $(-)$ plaquettes on $\mathscr{M}$, whose centers are sites of $\mathscr{L}_A$ or $\mathscr{L}_B$ (Fig. 11). Here again there is a one-to-one correspondence to rooted spanning trees on $\mathscr{L}$ $(=\mathscr{L}_A$ or $\mathscr{L}_B$ exclusively), with free boundary conditions. Hence we write

$$\begin{aligned} \mathcal{Q}^{\mathrm{f}}_{\mathrm{H}}(\lambda) &= \mathcal{Q}^{\mathrm{f}}_{\mathscr{T}}(m^2 = 4\lambda) \\ &= \det(\mathbf{C}^{\mathrm{f}} + m^2 \mathbf{1})_{\mathscr{L}} \end{aligned} \tag{4.2}$$

where $\mathbf{C}^{\mathrm{f}}$ is the connection matrix (2.3) of the $M \times N$ unoriented square lattice $\mathscr{L}$, with *free* edges. For a one-dimensional lattice of M sites, $\mathbf{C}^{\mathrm{f}}$ reads explicitly

$$\mathbf{C}^{\mathrm{f}}_M = \begin{bmatrix} 1 & -1 & 0 & & & 0 \\ -1 & 2 & -1 & & & 0 \\ 0 & & & & & 0 \\ 0 & & & -1 & 2 & -1 \\ 0 & & & 0 & -1 & 1 \end{bmatrix} \begin{matrix} \\ \\ M \\ \\ \\ \end{matrix} \tag{4.3}$$

$$\underbrace{\qquad\qquad\qquad\qquad\qquad\qquad}_{M}$$

On the rectangle lattice $M \times N$, $\mathbf{C}^{\mathrm{f}}$ is the tensorial product $\mathbf{C}^{\mathrm{f}}_M \otimes \mathbf{C}^{\mathrm{f}}_N$.

The eigenvalues of $\mathbf{C}^{\mathrm{f}}_M \otimes \mathbf{C}^{\mathrm{f}}_N$ are

$$\begin{aligned} &\lambda_{m,n} = 4 - 2\cos\frac{m\pi}{M} - 2\cos\frac{n\pi}{N} \\ &m \in [0, M-1], \quad n \in [0, N-1] \end{aligned} \tag{4.4}$$

Hence

$$\mathcal{Q}^{\mathrm{f}}_{\mathrm{H}}(\lambda = m^2/4) = \prod_{\substack{0 \leqslant m' \leqslant M-1 \\ 0 \leqslant n \leqslant N-1}} (\lambda_{m',n} + m^2) \tag{4.5}$$

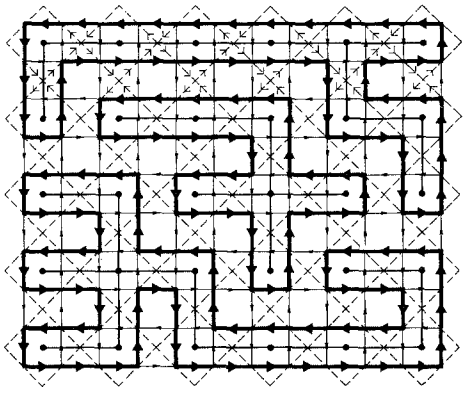

Fig. 11. Three disconnected, closed Hamiltonian walks with free boundary conditions. Their skeletons are disconnected spanning trees on the sublattice $\mathscr{L}_B$, whose sites are centers of counterclockwise square plaquettes of the Manhattan lattice. The other lattice $\mathscr{L}_A$ (clockwise plaquettes) does not play any role here.

In particular, the number of single HAWs (with varying origins) on the free edge lattice reads

$$N^{\mathrm{f}}_{\mathrm{H},1} = 4 \det' \mathbf{C}^{\mathrm{f}} = \prod_{\substack{0 \leqslant m \leqslant M-1 \\ 0 \leqslant n \leqslant N-1 \\ (m,n) \neq (0,0)}} \lambda_{m,n} \tag{4.6}$$

4.2. Asymptotic Number of Hamiltonian Walks

It would be interesting to evaluate the asymptotics of the massive free-field determinant (4.5) in the case of free edges, as we did in Section 3 for the torus. For the sake of simplicity, we only evaluate here the first moment (4.6), via its logarithm

$$\ln \det' \mathbf{C}^{\mathrm{f}} \equiv \ln D_{\mathrm{f}} = \sum_{\substack{0 \leqslant m \leqslant M-1 \\ 0 \leqslant n \leqslant N-1 \\ (m,n) \neq (0,0)}} \ln\left(4 - 2\cos\frac{m\pi}{M} - 2\cos\frac{n\pi}{N}\right) \tag{4.7}$$

To avoid the singularity brought in by the zero mode, we split the sums into

$$\ln D_{\mathrm{f}} = \ln D + \sum_{m=1}^{M-1} \ln(2 - 2c_m) + \sum_{n=1}^{N-1} \ln(2 - 2c_n) \tag{4.8}$$

$$\ln D = \sum_{\substack{1 \leqslant m \leqslant M-1 \\ 1 \leqslant n \leqslant N-1}} \ln(4 - 2c_m - 2c_n) \tag{4.8a}$$

with $c_m = \cos(m\pi/M)$, $c_n = \cos(n\pi/N)$.

We make use again of

$$\ln[2\,(\mathrm{ch}\,t-\cos\theta)]=t-\sum_{k\in\mathbf{Z}^*}\frac{e^{-|k|t}}{|k|}e^{ik\theta}$$

setting

$$2\,\mathrm{ch}\,t_n=4-2c_n=4-2\cos\frac{n\pi}{N},\qquad 1\leqslant n\leqslant N-1 \tag{4.9}$$

Then

$$\ln D=(M-1)\sum_n t_n-\sum_n\sum_{k\in\mathbf{Z}^*}\frac{e^{-|k|t_n}}{|k|}S_k \tag{4.10}$$

where the sum over n means from now on $1\leqslant n\leqslant N-1$, and where

$$S_k=\sum_{m=1}^{M-1}e^{ikm\pi/M}$$

One finds

$$S_k=\begin{cases}M-1 & \text{if}\quad k\in 2M\mathbf{Z}\\ -1 & \text{if}\quad k\in 2\mathbf{Z},\quad k\notin 2M\mathbf{Z}\\ -\mathrm{cotg}\,\dfrac{k\pi}{2M} & \text{if}\quad k\in 2\mathbf{Z}+1\end{cases}$$

The sum brought in (4.10) by S_k for the odd values $k\in 2\mathbf{Z}+1$ adds to zero by parity. The two other contributions of S_k are easily evaluated, yielding finally

$$\ln D=\sum_{n=1}^{N-1}[(M-1)t_n+\ln(1-e^{-2Mt_n})-\ln(1-e^{-2t_n})]$$

which we rewrite as

$$\ln D=\sum_{n=1}^{N-1}[Mt_n-\ln(2\,\mathrm{sh}\,t_n)+\ln(1-e^{-2Mt_n})] \tag{4.11}$$

1. The first sum

$$\sigma_1=M\sum_{n=1}^{N-1}t_n \tag{4.12}$$

is evaluated with the help of the Euler–MacLaurin formula (3.60). We find

$$\sigma_1 = \frac{MN}{\pi}\int_0^{\pi} d\theta \ln[2+\cos\theta+(3+4\cos\theta+\cos^2\theta)^{1/2}]$$
$$-\frac{1}{2}M\ln(3+2\sqrt{2})-\frac{\pi}{12}\frac{M}{N}+\cdots$$

which we rewrite in term of the Catalan constant G, (3.18a),

$$\sigma_1 = MN\frac{4G}{\pi}-\mathscr{B}M-\frac{\pi}{12}\frac{M}{N}+\cdots \tag{4.13}$$

with

$$\mathscr{B}=\ln(1+\sqrt{2}) \tag{4.13a}$$

2. The second sum

$$\sigma_2 = -\sum_{n=1}^{N-1}\ln(2\,\mathrm{sh}\,t_n) \tag{4.14}$$

cannot be evaluated by the Euler–MacLaurin approach under this form, since the derivatives diverge at the origin. So we introduce the regular part

$$f(n) = -\ln(2\,\mathrm{sh}\,t_n)+\ln\frac{n\pi}{N} \tag{4.15}$$

where the behavior of t_n in (4.9), $t_n = n\pi/N+\cdots$, near the origin is subtracted out.

We rewrite σ_2 as

$$\sigma_2 = \sigma_2' + \sigma_2'' \tag{4.16}$$

$$\sigma_2' = \sum_{n=1}^{N-1} f(n) \tag{4.16a}$$

$$\sigma_2'' = -\sum_{n=1}^{N-1}\ln\frac{n\pi}{N} = -N(\ln\pi-1)-\frac{1}{2}\ln N-\ln\left(\frac{2}{\pi}\right)^{1/2}-\frac{1}{12N}+\cdots \tag{4.16b}$$

Now σ_2' can be evaluated by means of the Euler–MacLaurin formula (3.60) applied to (4.15). We find after some calculations

$$\sigma_2' = -N\left(I-\frac{1}{\pi}\int_0^{\pi} dx\ln x\right)+\frac{1}{2}\ln\left(\frac{8\sqrt{2}}{\pi}\right)+\frac{1}{12N}+\cdots$$

with

$$I=\frac{1}{\pi}\int_0^{\pi} dx \ln[2(3+4\cos x+\cos^2 x)^{1/2}] \tag{4.17}$$

We finally find for σ_2 from (4.14), (4.16)

$$\sigma_2 = -NI+\frac{1}{2}\ln(4\sqrt{2})-\frac{1}{2}\ln N+O\left(\frac{1}{N^2}\right) \tag{4.18}$$

Integral I in (4.17) is actually calculable by factorization, $I=\mathscr{B}=\ln(1+\sqrt{2})$. This was expected for restoring the symmetry between the perimeter terms M in (4.13) and N in (4.18).

3. The last sum in (4.11)

$$\sigma_3=\sum_{n=1}^{N-1}\ln(1-e^{-2Mt_n})$$

converges exponentially rapidly to its continuum limit, obtained by retaining only the behavior of t_n in (4.9) near the origin, $t_n=n\pi/N+\cdots$, which yields

$$\sigma_3=\sum_{n=1}^{\infty}\ln(1-e^{-2\pi nM/N})=\ln P(q) \tag{4.19}$$

We finally find for $\ln D$ in (4.11), using (4.13), (4.18), and (4.19),

$$\ln D = MN\frac{4G}{\pi}-(M+N)\ln(1+\sqrt{2})-\frac{1}{4}\ln MN+\frac{1}{2}\ln(4\sqrt{2})$$
$$+\ln\left[q^{1/24}P(q)\left(\frac{M}{N}\right)^{1/4}\right] \tag{4.20}$$

It remains to add to $\ln D$ the contribution of boundary sums appearing in (4.8),

$$\mathscr{S}_N=\ln\prod_{n=1}^{N-1}2\left(1-\cos\frac{n\pi}{N}\right) \tag{4.21}$$

A well-known identity gives

$$\prod_{n=1}^{N-1}2\left(1-\cos\frac{n\pi}{N}\right)=N \tag{4.22}$$

and $\mathscr{S}_N\equiv\ln N$.

Hence, we finally find from (4.20) and (4.22)

$$\begin{aligned}\ln D_{\mathrm{f}} &= \ln D + \mathscr{S}_M + \mathscr{S}_N \\ &= MN\frac{4G}{\pi} - (M+N)\ln(1+\sqrt{2}) + \frac{3}{4}\ln MN \\ &\quad + \frac{1}{2}\ln(4\sqrt{2}) + \ln\left[q^{1/24}P(q)\left(\frac{M}{N}\right)^{1/4}\right] + \cdots \end{aligned} \tag{4.23}$$

The asymptotic number (4.6) of open Hamiltonian walks on the even–even $\mathbf{M}\times\mathbf{N}$ Manhattan lattice with free boundary conditions is therefore

$$\begin{aligned} N_{\mathrm{H},1}^{\mathrm{f}} &= 4\det'\mathbf{C}^{\mathrm{f}} \\ &\cong 2^{7/4}e^{G\mathbf{MN}/\pi}(1+\sqrt{2})^{-(\mathbf{M}+\mathbf{N})/2}(\mathbf{MN})^{3/4}\,\eta(q)\left(\frac{\mathbf{M}}{\mathbf{N}}\right)^{1/4} \end{aligned} \tag{4.24}$$

4.3. Discussion

Perimeter term. One notes the appearance of a subleading perimeter correction term $a^{-(\mathbf{M}+\mathbf{N})}$, as conjectured by Malakis.[10] This author found numerically the approximate value $a \simeq 1.515 \pm 0.015$, in reasonable agreement with the exact value $(1+\sqrt{2})^{1/2} = 1.55377\ldots$. When comparing expression (4.24) to the Kasteleyn–Barber result (3.21) for the torus,

$$N_{\mathrm{H},1} \cong 2e^{G\mathbf{MN}/\pi}\,\mathbf{MN}\eta^4(q)\frac{\mathbf{M}}{\mathbf{N}} \tag{3.21}$$

we see that the *bulk* dominant contribution with connectivity constant $\mu = e^{G/\pi}$ is the same, as expected. This is a purely local term, which is boundary-independent.

Critical exponent. A power law correction term $(\mathbf{MN})^{\bar{\gamma}}$ also appears in (4.24) and (3.21), with a critical exponent depending on boundary conditions: $\bar{\gamma}_{\mathrm{free}} = \frac{3}{4}$, $\bar{\gamma}_{\mathrm{periodic}} = 1$. This exponent is similar to the usual configuration exponent γ of polymers, and its dependence on boundaries is a new effect, characteristic of a *dense* system.[22] The relevance of these results for dense polymers in 2D is discussed in detail elsewhere[22] (also see Section 10).

Conformal invariance. We also observe the different modular dependences of $N_{\mathrm{H},1}$ and $N_{\mathrm{H},1}^{\mathrm{f}}$, as $\eta^4(q)$ and $\eta(q)$ respectively. The change of power by a factor 4 was expected. If we consider indeed the scaling

behavior on a strip of width N and length $M \to \infty$, i.e., the limit $q = e^{-2\pi M/N} \to 0$, we have from (3.20b)

$$N_{\mathrm{H},1} \sim q^{1/6}, \qquad H^{\mathrm{f}}_{\mathrm{H},1} \sim q^{1/24} \tag{4.25}$$

Quite generally,[36] for a *critical* system, with finite-size partition function $Z(M, N)$, the free energy of the strip reads, for periodic boundary conditions,

$$\lim_{M \to \infty} \frac{1}{M} \ln Z(M, N) = Nf_0 + \pi \frac{c}{6N} + \cdots \tag{4.26}$$

and for free boundary conditions

$$= Nf_0 + f_S + \frac{\pi}{24} \frac{c}{N} + \cdots \tag{4.27}$$

where $-f_0$ and $-f_S$ are, respectively, the nonuniversal bulk and surface free energies per unit of volume, and c is the universal *central charge*[27] of the critical model.

We get in both cases from (4.25) a value $c = -2$, which recovers[20,25,22] the universal central charge of Hamiltonian walks, as discussed in Section 2.

5. NEUMANN OR DIRICHLET BOUNDARY CONDITIONS

In order to discuss in the next section Hamiltonian walks on Manhattan lattices with arbitrary external shapes and free boundary conditions, we discuss in more detail here their relation to standard Neumann or Dirichlet problems. For simplicity we consider only the enumeration of single closed walks, which will be reducible to that of spanning trees on some underlying lattice (Section 6). We first show that the evaluation of spanning trees with free boundary conditions is actually equivalent to a *Neumann* problem.

5.1. Free or Neumann Boundary Conditions

The number of rooted 1-spanning trees on a general graph G is given in terms of the connectivity matrix $\mathbf{C}_G$ of (2.3) [Eqs. (2.10), (2.11), (3.4)]

$$N_{T,1} = \det' \mathbf{C}_G \tag{5.1}$$

We shall see that for a graph G corresponding to the underlying lattice of some domain $\mathscr{D}$ with boundary on the Manhattan lattice, $\mathbf{C}_G$ corresponds

to minus the discrete combinatoric Laplacian with free, i.e., Neumann, boundary conditions on the boundary of $\mathscr{D}$ ($\partial_n \varphi = 0$, where ∂_n is the normal derivative to the boundary). Thus,

$$\mathbf{C}_G \to -\Delta|_{G,\,\text{Neumann}} \tag{5.2}$$

To see the equivalence, it is sufficient to consider the Gaussian integral

$$\mathscr{I} = \int_{-\infty}^{+\infty} \prod_{i=1}^{N_0(G)} d\varphi(i) \exp\left\{ -\frac{1}{2} \sum_{\langle i,j \rangle} [\varphi(i) - \varphi(j)]^2 \right\} \delta(\varphi(o)) \tag{5.3}$$

where a field $\varphi(i)$ is defined for each of the $N_0(G)$ sites $i \in G$, one ($\varphi(o)$) being fixed for eliminating the zero mode. $\langle i, j \rangle$ denotes nearest neighbors on G. In terms of the connectivity matrix $\mathbf{C}_G$ of G, $\mathscr{I}$ reads

$$\mathscr{I} = \int \prod_{i=1}^{N_0(G)} d\varphi(i) \exp\left(-\frac{1}{2} {}^t\varphi \mathbf{C}_G \varphi \right) \delta(\varphi(o)) \tag{5.4}$$

On the other hand, the continuum limit of (5.3) can be written as a functional integral over fields $\varphi(x)$ defined on a domain D with boundary ∂D

$$\mathscr{I} = \int [D\varphi] \exp\left[-\frac{1}{2} \int (\nabla\varphi)^2 \, d^2x \right] \delta(\varphi(o)) \tag{5.5}$$

and if one imposes the vanishing of the normal derivatives at the boundary $\partial_n \varphi = 0$, then

$$\mathscr{I} = \int [D\varphi] \exp\left[\frac{1}{2} \int \varphi \, \Delta\varphi \, d^2x \right] \delta(\varphi(o)) \tag{5.6}$$

which is just (5.2).

5.2. Dirichlet Manhattan Rectangle

The Laplacian with Dirichlet boundary conditions ($\varphi = 0$ on the boundary) on a rectangle is therefore not described by the matrix $\mathbf{C}$ in (4.3). Let us consider a larger $(M+1) \times (N+1)$ site rectangle $\mathscr{L}^*$, with sites $i = (m, n)$, $1 \leqslant m \leqslant M+1$, $1 \leqslant n \leqslant N+1$ (Fig. 12). A lattice field $\varphi(i)$ is defined such that $\varphi(i) = 0$ at the boundary edges $i \in \partial\mathscr{L}^*$, $i = (1, n)$, $(M+1, n)$, $(m, 1)$, or $(m, N+1)$. We introduce the *Dirichlet* Gaussian integral

$$\mathscr{I}_D = \int \prod_{i \notin \partial\mathscr{L}^*} d\varphi(i) \exp\left\{ -\frac{1}{2} \sum_{\langle i,j \rangle}^{(0)} [\varphi(i) - \varphi(j)]^2 \right\} \tag{5.7}$$

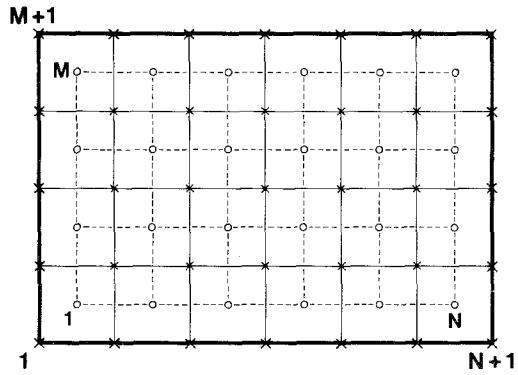

Fig. 12. (○) Original $M \times N$ site lattice $\mathscr{L}_A$ or $\mathscr{L}_B$ on which the connectivity matrix $\mathbf{C}^{\mathrm{f}}$ is defined. (×) Dual $(M+1)\times(N+1)$ site lattice with Dirichlet conditions on the external perimeter, for which $\det(-\Delta)|_{\mathrm{D}}$ is calculated.

where $\langle i, j\rangle$ denotes all nearest neighbors, the superscript (0) *including* sites at $\partial\mathscr{L}^*$. One has

$$\mathscr{I}_{\mathrm{D}} = \int \prod_{i \notin \partial\mathscr{L}^*} d\varphi(i) \exp\left(-\frac{1}{2}\, {}^t\varphi \mathbf{C}^D \varphi\right) \tag{5.8}$$

where the new Dirichlet matrix $\mathbf{C}^{\mathrm{D}}$ reads $\mathbf{C}^{\mathrm{D}} = \mathbf{C}^{\mathrm{D}}_{M-1} \otimes \mathbf{C}^{\mathrm{D}}_{N-1}$, with

$$\mathbf{C}^{\mathrm{D}}_{M-1} = \left.\begin{bmatrix} 2 & -1 & 0 & 0 \\ -1 & 2 & -1 & 0 \\ & & & 0 \\ 0 & -1 & 2 & -1 \\ 0 & 0 & -1 & 2 \end{bmatrix}\right\} M-1 \qquad \begin{matrix} \\ \\ \\ \\ M-1 \end{matrix} \tag{5.9}$$

for the one-dimensional Dirichlet Laplacian. This matrix differs from $\mathbf{C}^{\mathrm{f}}_M$ of (4.3). Going to the continuum limit in (5.7), we identify C^{D} as the combinatoric Laplacian with *Dirichlet* boundary conditions

$$\mathbf{C}^{\mathrm{D}} = -\Delta|_{\mathscr{L}^*,\,\mathrm{Dirichlet}} \tag{5.10}$$

The eigenvalues of $\mathbf{C}^{\mathrm{D}}$ are simply found from (5.9),

$$\lambda_{m,n} = 4 - 2\cos\frac{m\pi}{M} - 2\cos\frac{n\pi}{N}, \qquad 1 \leqslant m \leqslant M-1, \quad 1 \leqslant n \leqslant N-1 \tag{5.11}$$

and are contained in the larger set $0 \leqslant m \leqslant M-1$, $0 \leqslant n \leqslant N-1$ of eigenvalues (4.4) of $\mathbf{C}^{\mathrm{f}}$. We therefore observe that the partial determinant $\ln D$ in (4.8a) calculated above is just that of the Laplacian $\mathbf{C}^{\mathrm{D}}$ on $\mathscr{L}^*$,

$$\ln \det(-\Delta)|_{\mathscr{L}^*,\,\mathrm{Dirichlet}} = \ln D \tag{5.12}$$

The other Neumann determinant, $\det' \mathbf{C}^{\mathrm{f}}$ [(4.7), (4.8)], of the connectivity matrix $\mathbf{C}^{\mathrm{f}}$ of the original rectangle $\mathscr{L}$ (Fig. 12) is thus given by [use Eq. (4.22)]

$$\det' \mathbf{C}^{\mathrm{f}} = MN \det(-\Delta)|_{\mathscr{L}^*,\,\mathrm{Dirichlet}} \tag{5.13}$$

5.3. Duality

The result (5.13), obtained directly for the rectangle, is actually a particular case of a general duality property between Neumann boundary conditions on a given lattice G and Dirichlet ones on the dual lattice G^* (Fig. 12). It is shown in Appendix B that

$$\begin{aligned} \det' \mathbf{C}_G &\equiv \det'(-\Delta)|_{G,\,\mathrm{Neumann}} \\ &= N_0(G) \det(-\Delta)|_{G^*,\,\mathrm{Dirichlet}} \end{aligned} \tag{5.14}$$

where $N_0(G)$ is the number of sites of G, or of faces of its dual G^*. In the next section this result will find an interesting application to Manhattan lattices with various geometries.

6. OTHER GEOMETRIES

6.1. General Considerations

As remarked by Kasteleyn,[4] the enumeration of Hamiltonian walks on an oriented lattice is always possible when this lattice is the covering graph $\mathscr{G}^{\mathrm{c}}$ of any oriented graph $\mathscr{G}$. By the *covering graph* $\mathscr{G}^{c}$ of $\mathscr{G}$ we understand[1,4] the oriented graph obtained by: (1) replacing each oriented line or edge of $\mathscr{G}$ by its medial point, (2) joining two such medial points, if the corresponding original lines in $\mathscr{G}$ were *consecutive*, by an new oriented line. The orientation of this new line of $\mathscr{G}^{\mathrm{c}}$ is chosen in accordance to those of the source lines of $\mathscr{G}$.

For instance, the Manhattan lattice $\mathscr{M}$ is the covering graph of an oriented diagonal square lattice, with specific orientations (Fig. 11).

Then there is a one-to-one-correspondence between the Hamiltonian circuits on the covering $\mathscr{G}^{\mathrm{c}}$ $(=\mathscr{M})$ and the Eulerian circuits on the covered graph $\mathscr{G}$.[4] Systematic successive coverings of the Manhattan lattice have

been studied in detail by Malakis.[10] Here we first give other examples of Manhattan-like graphs and of Hamiltonian walks on them. Later we give a general analytical result for their enumeration.

6.2. Kagomé Lattice

Let us consider the oriented Kagomé lattice $\mathscr{K}$ where all hexagons are oriented in the same direct sense (Fig. 13). By joining the midpoints of the edges of the hexagons, one obtains the oriented covering graph $\mathscr{K}^c$ of the Kagomé lattice $\mathscr{K}$, which is diamondlike (Fig. 13). The orientations on $\mathscr{K}^c$ are chosen in accordance with those on $\mathscr{K}$. We imagine that a free perimeter is delimited on $\mathscr{K}$, by retaining only a connected set of Kagomé hexagons, i.e., a connected set G of hexagon centers (Fig. 13). This choice on $\mathscr{K}$ then induces free edges on $\mathscr{K}^c$. Then, looking at Hamiltonian circuits on $\mathscr{K}^c$ with these boundaries, it is not difficult to convince oneself that they are in one-to-one correspondence to Eulerian closed walks on $\mathscr{K}$ (Fig. 14a). In turn, these Eulerian walks are in one-to-one correspondence with (unrooted) spanning trees on graph G, which is made up of the hexagon centers of $\mathscr{K}$ or $\mathscr{K}^c$ (Fig. 14b). So we have, as for the rectangular Manhattan lattice,

$$N^0_{H,1}(\mathscr{K}^c) = N^0_{T,1}(G) \tag{6.1}$$

Enumerating unrooted trees is done by using formulas (3.4), (3.5):

$$N^0_{T,1}(G) = \frac{1}{N_0(G)} \det' \mathbf{C}_G \tag{6.2}$$

where $\mathbf{C}_G$ is the connectivity matrix (2.3) of the unoriented graph of hexagon centers (Fig. 14).

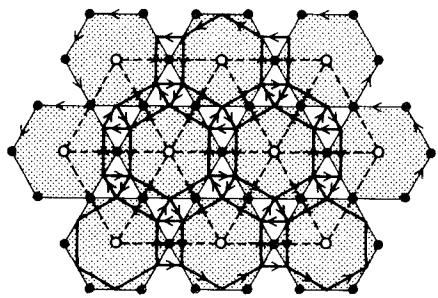

Fig. 13. Oriented Kagomé lattice $\mathscr{K}$ (solid dots) and its oriented covering graph $\mathscr{K}^c$, which is diamondlike and made up of adjacent hexagons, squares, and triangles.

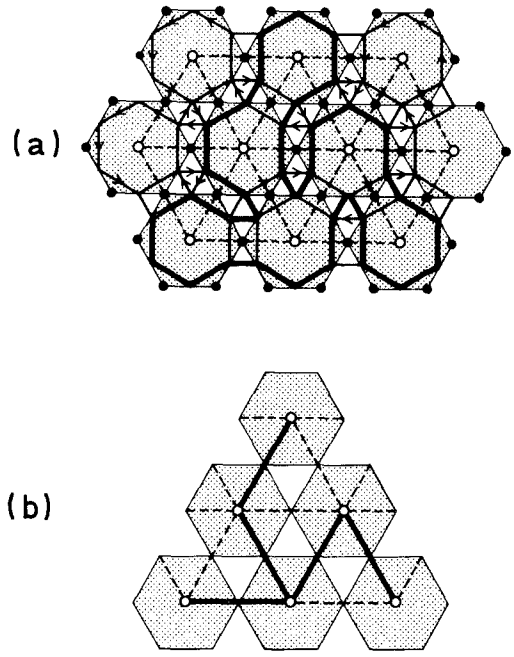

Fig. 14. (a) The Kagomé lattice with free edges. Here we have chosen a triangular shape. A Hamiltonian loop circulates on the covering lattice $\mathscr{K}^c$. (b) A Hamiltonian loop is in one-to-one correspondence with a Eulerian circuit on $\mathscr{K}$, itself determined by a spanning tree on the triangular set G of hexagon centers.

This discussion is quite general and is independent of the external shape of $\mathscr{G}$ we have chosen. On Fig. 13b we have chosen a particular *triangular* shape of $\mathscr{K}$, $\mathscr{K}^c$, and G. The fact that the sites of G (open dots in Fig. 14b) lie on the triangular lattice enables us to introduce another oriented lattice on which we shall consider HAWs, the *triangular Manhattan lattice* $\mathscr{T}$, which we study now.

6.3. Triangular Manhattan Lattice

This lattice $\mathscr{T}$ (Fig. 15) is the generalization of the rectangular $\mathscr{M}$. The external shape could be generalized to be polygonal. As on $\mathscr{M}$, the circulation alternates along each strate of $\mathscr{T}$. The open dots are the centers of (counterclockwise) oriented plaquettes. They are also identical by construction with the centers of hexagons in the previous Kagomé lattice.

Now, as before for the free Manhattan lattice $\mathscr{M}$, the Hamiltonian walks of $\mathscr{T}$ are in one-to-one correspondence with spanning trees on the

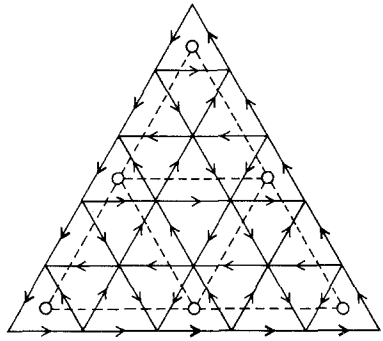

Fig. 15. The triangular Manhattan lattice $\mathscr{T}$. The set G of centers of (counterclockwise) oriented triangular plaquettes (open dots) is the same as that of the centers of (oriented) hexagons in the former Kagomé lattice $\mathscr{K}$.

graph G made up of the centers of (here counterclockwise) oriented plaquettes. An example is given in Fig. 16. Since the graph G is the same as that associated with the Kagomé lattice, we conclude that the Hamiltonian problems are topologically the same on $\mathscr{K}^c$ and $\mathscr{T}$. Hence

$$N^0_{H,1}(\mathscr{K}^c) = N^0_{H,1}(\mathscr{T}) = \frac{1}{N_0(G)} \det' \mathbf{C}_G \tag{6.3}$$

From Eq. (6.3) we could compute the exact asymptotic number of Hamiltonian circuits on $\mathscr{K}^c$ or $\mathscr{T}$ in the particular case of a triangular boundary. It is important to realize, however, that the Hamiltonian property is purely topological. In particular, the boundary lines are parallel to the lattice axes. Hence, when we go to the thermodynamic or continuum

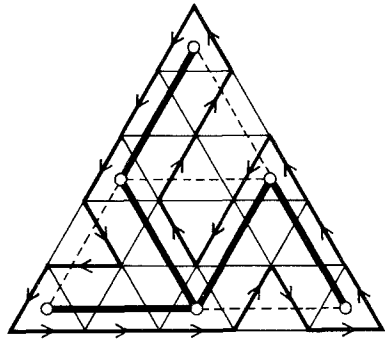

Fig. 16. A Hamiltonian circuit on $\mathscr{T}$, topologically equivalent to the covering Kagomé HAW (Fig. 14).

limit, we obtain a continuum triangle whose angles are all $\pi/3$ and are not arbitrary. The spectrum of the Laplacian in the triangles is not known in general, though a lot of work has been devoted to it.[37] For an equilateral one, the eigenvalues of the Neumann connectivity matrix $\mathbf{C}_G$ are known, and the determinant $\det' \mathbf{C}_G$ could be evaluated asymptotically as in Section 4 for the free $\mathscr{M}$, but we do not intend to reproduce the whole analysis. Instead we give a quite general result, obtained from spectral theory.

6.4. Hamiltonian Number in a Domain of Arbitrary Shape

We expect in general for single, oriented Hamiltonian *circuits* or spanning trees in a large domain $\mathscr{D}$ with boundary the asymptotic numbers

$$N^0_{\mathrm{H},1} = N^0_{T,1} \sim \mu^{\mathscr{A}} \mu_S^{\mathscr{P}} \mathscr{A}^{\bar{\gamma}_0 - 1} \tag{6.4}$$

where $\mathscr{A}$ is the "area" of $\mathscr{D}$, i.e., its number of sites, or the number of points of the Hamiltonian circuit, $\mathscr{P}$ is the perimeter of the boundary, i.e., the number of points of the Hamiltonian walk on the perimeter, and μ and μ_S are, respectively, the bulk and surface Hamiltonian connectivity constants. $\bar{\gamma}_0$ is a *critical exponent*, like the usual γ for SAWs.[22]

For example, in the case of the rectangular Manhattan lattice $\mathscr{M}$, Eqs. (3.21) and (4.24) give

$$\mu = e^{G/\pi}, \qquad \mu_S = (1+\sqrt{2})^{-1/2} \tag{6.5}$$

$$\bar{\gamma}_0 = 1 \quad \text{(torus)}, \qquad \bar{\gamma}_0 = 3/4 \quad \text{(free rectangle)} \tag{6.6}$$

The constants μ, μ_S are strongly lattice-dependent. However, they do not depend on the *topology* of the Hamiltonian walk (open or closed, or even branched[22]), and they are ultraviolet local quantities, depending only on the connectivity of the lattice. In contrast, the critical exponent $\bar{\gamma}_0$ depends on the *topology* of the domain and also on the *geometrical shape* of the boundary. This interesting shape dependence of $\bar{\gamma}_0$ is now discussed. We shall see that the exact value of $\bar{\gamma}_0$ can be deduced from classical results of spectral theory for a domain with an arbitrary shape.

6.5. Spectral Theory

For any oriented Hamiltonian problem that can be transformed into counting (unoriented) spanning trees on a graph G (as on $\mathscr{M}$, $\mathscr{K}^c$, $\mathscr{T}$,...) with free boundaries the number of circuits $N^0_{\mathrm{H},1}$ is given by

$$N^0_{\mathrm{H},1} = \frac{1}{N_0(G)} \det' \mathbf{C}_G \tag{6.7}$$

We now use the duality relation (5.14), which relates $\mathbf{C}_G$ to the combinatoric Laplacian on the dual lattice G^* with Dirichlet conditions (Fig. 17)

$$N^0_{\mathrm{H},1} = \det(-\Delta)|_{G^*,\,\mathrm{Dirichlet}} \tag{6.8}$$

We are interested in the large-lattice or continuum limit. In this limit, the shape of G and that of its dual G^* become *identical* (Fig. 17). The spectrum of the continuum Laplacian in a finite domain $\mathscr{D}$ ($=G$ or G^*) has been very much studied in the mathematical literature.[38,31]

In particular, the determinant of $-\Delta$ with Dirichlet boundary conditions is defined by the so-called ζ-function regularization.[29,31] The ζ-function of the eigenvalue spectrum $\{\lambda_n\}$ of Δ is defined by the infinite series

$$\zeta(s) = \sum_n \lambda_n^{-s} \tag{6.9}$$

which converges for s sufficiently large and positive. The important property[29,31] is that it can be analytically continued toward $s=0$.

Then the ζ-regularized determinant of the Laplacian is defined as

$$\det(-\Delta) = e^{-\zeta'(0)} \quad \left(= \prod_n \lambda_n\right) \tag{6.10}$$

Now suppose one dilates all dimensions of the continuum domain $\mathscr{D}$ by a factor α. The new spectrum of Δ is then $\{\alpha^{-2}\lambda_n\}$, and $\zeta_\alpha(s) = \alpha^{2s}\zeta(s)$. The dilated determinant (6.10) then reads

$$\det(-\Delta)|_{\alpha\mathscr{D}} = \alpha^{-2\zeta(0)} \det(-\Delta)|_{\mathscr{D}}$$

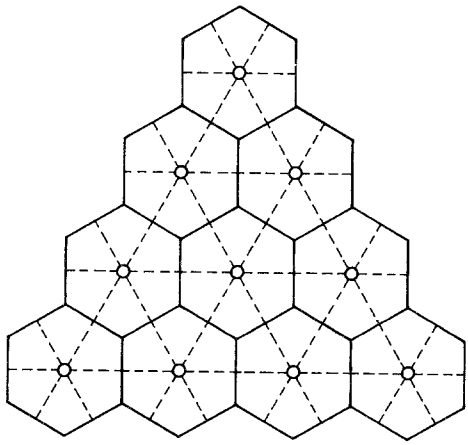

Fig. 17. The triangular lattice G (dashed lines) and the dual honeycomb G^*. The external perimeter of G^* is still triangular and becomes an equilateral triangle in the continuum limit.

Since the area of the two-dimensional domain scales like α^2, we conclude that in two dimensions the area dependence of the Laplace determinant (6.10) with Dirichlet boundary conditions is (up to regularization-dependent exponential leading factors)

$$\det(-\Delta)|_{\mathscr{D}} \sim \mathscr{A}^{-\zeta(0)} \tag{6.11}$$

where $\mathscr{A}$ is the area of $\mathscr{D}$. Thus, $\zeta(0)$ is nothing but $1-\bar{\gamma}_0$, where $\bar{\gamma}_0$ is the geometrical index characteristic of the domain $\mathscr{D}$, introduced in Eq. (6.4).

This result gives the solution, since the value of $\zeta(0)$ is known[31,38] to be only a function of the geometrical shape of the boundary for a domain with the topology of a disk. In particular, let us consider a boundary $\partial\mathscr{D}$ made up of rectifiable arcs γ_i joined at corners of angles α_j. For instance, for the rectangular Manhattan lattice $\mathscr{M}$ or the Manhattan triangle $\mathscr{T}$ above we have, respectively,

$$\begin{aligned} &\alpha_i = \pi/2, \qquad i = 1,\ldots,4 \quad \{\mathscr{M}\} \\ &\alpha_i = \pi/3, \qquad i = 1,2,3 \quad \{\mathscr{T}\} \end{aligned} \tag{6.12}$$

The contribution of corners to the asymptotic Dirichlet problem was found by D. B. Roy (described in McKean and Singer[38]). The general result[38] reads in the ζ-formalism

$$\zeta(0) = \sum_j \frac{1}{24}\left(\frac{\pi}{\alpha_j} - \frac{\alpha_j}{\pi}\right) + \sum_i \frac{1}{12\pi}\int_{\gamma_i} \frac{dl}{\rho} \tag{6.13}$$

where ρ is the curvature along the smooth arcs γ_i.

Let us apply this result to the determination of the critical exponent $\bar{\gamma}_0$.

6.6. Exact Exponent γ

Equations (6.8) and (6.11) thus yield the general scaling behavior (6.4) of the number of Hamiltonian circuits in a domain with boundaries

$$N^0_{\mathrm{H},1} \sim \mu^{\mathscr{A}} \mu_S^{\mathscr{P}} \mathscr{A}^{\bar{\gamma}_0 - 1}, \qquad \bar{\gamma}_0 - 1 = -\zeta(0) \tag{6.14}$$

where $\zeta(0)$ is given by Eq. (6.13). For the rectangular Manhattan lattice $\mathscr{M}$ we find from (6.12) and (6.13)

$$\bar{\gamma}_{0,\mathscr{M}} - 1 = -\zeta(0) = -1/4 \tag{6.15a}$$

in agreement with the direct evaluation (6.6) and (4.24). For the covering

graph of the Kagomé lattice $\mathscr{K}^c$, which is equivalent to the symmetric triangle $\mathscr{T}$, we have from (6.12) the new result

$$\bar{\gamma}_{0,\mathscr{T}} - 1 = -\zeta(0) = -1/3 \tag{6.15b}$$

Let us recall that the Hamiltonian problem is purely topological, while a formula like (6.13) is metric. To use this metric formula, one has to note that the discrete Manhattan lattice is parallel to the boundary edges and forces the continuum limit to correspond to a regular polygon with *equal* angles. Different continuum angles would require Manhattan lines that would be *cut* by the external edges.

Formulas (6.15a) and (6.15b) can be generalized to a *polygonal* Manhattan lattice (generalizing Figs. 10 and 15), where the boundary is a closed polygon with P sides and P equal angles $\alpha = \pi(P-2)/P$. Then

$$\bar{\gamma}_0 - 1 = -\zeta(0) = -\tfrac{1}{6}(P-1)/(P-2) \tag{6.15c}$$

In Section 10 we discuss the relation of this exponent to those of dense polymers.

7. OPEN HAMILTONIAN WALKS ON MANHATTAN LATTICE

7.1. Description

We return to the original Manhattan rectangular lattice with free edges. In Section 4 we considered free boundary conditions for an even–even $(\mathbf{M} = 2M) \times (\mathbf{N} = 2N)$ lattice, where *closed* Hamiltonian walks were possible (Figs. 10 and 11). It is quite interesting to remark that for an $\mathbf{M}_{\text{odd}} \times \mathbf{N}_{\text{odd}}$ or $\mathbf{M}_{\text{even}} \times \mathbf{N}_{\text{odd}}$ Manhattan lattice, there is always one corner with diverging arrows and one with converging arrows (Fig. 18). This constrains the Hamiltonian walk to travel from the first to the second corner

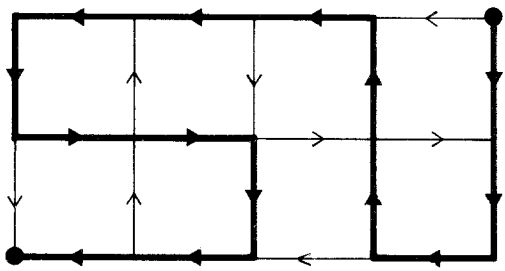

Fig. 18. The odd–odd 3×5 Manhattan lattice ($\mathbf{M} = 2M - 1$, $\mathbf{N} = 2N - 1$, $M = 2$, $N = 3$). All HAWs start at the wedge with diverging arrows and end up at the converging one.

and to be open along the diagonal of $\mathcal{M}$ for $\mathbf{M}_{\text{odd}} \times \mathbf{N}_{\text{odd}}$ and along one edge for $\mathbf{M}_{\text{even}} \times \mathbf{N}_{\text{odd}}$. So we now have an open polymer chain rather than a cyclic polymer. This shows the extreme sensitivity of Hamiltonian walks to boundary conditions.

The number of configurations of such an open walk has been studied numerically by Malakis.[10] Here we want to evaluate it exactly. This is interesting for the following reason. Due to the change of topology of the HAW, which now starts in two corners, we shall be able to extract from our exact results a (universal) *critical wedge exponent*. As we shall see, it is identical with the one derived recently for dense polymers[22] from conformal invariance and Coulomb gas methods.

Consider the odd–odd Manhattan lattice $\mathcal{M}$ with $\mathbf{M} \times \mathbf{N}$ sites,

$$\mathbf{M} = 2M - 1, \qquad \mathbf{N} = 2N - 1 \tag{7.1}$$

and denote by $N_{\mathrm{H}}^{W}(\mathcal{M})$ the total number of open Hamiltonian walks going from the wedge of $\mathcal{M}$ with diverging arows to the one with converging arrows (Fig. 18). The number N_{H}^{W} of open walks can still be evaluated exactly by an extension of the equivalence to spanning trees, as used in Sections 1 and 2 on the torus and in Sections 4 and 5 for free boundary conditions. Indeed, we remark that the *open* wedge-to-wedge walks on odd–odd $\mathcal{M}$ are in one-to-one correspondence to *closed* walks on the extended Manhattan lattice $\mathcal{M}^{+} = \mathcal{M} \cup \partial_{+} \mathcal{M}$ obtained by adding to $\mathcal{M}$ a column and a row of $\mathbf{M}+1$ and $\mathbf{N}+1$ sites sharing one site at their right-angle crossing (Fig. 19a).

Then $\mathcal{M}^{+}$ is an even–even $(\mathbf{M}+1)(\mathbf{N}+1)$ lattice, as in Section 4. Then to any wedge-to-wedge walk $\mathcal{W}$ on $\mathcal{M}$ corresponds a closed walk on $\mathcal{M}^{+}$ obtained by closing $\mathcal{W}$ along the added row and column of $\mathcal{M}^{+}$ (Fig. 19a). So we have

$$N_{\mathrm{H}}^{W}(\mathcal{M}) = N_{\mathrm{H},1}^{0}(\mathcal{M}^{+})|_{\text{borderline}} \tag{7.2}$$

where $N_{\mathrm{H},1}^{0}(\mathcal{M}^{+})|_{\text{borderline}}$ is the total number of unrooted closed HAWs on $\mathcal{M}^{+}$ subjected to the *constraint* that they follow the added square half-borderline, made up of the bottom row and right column. (These closed HAWs form a subclass of the HAWs on $\mathcal{M}^{+}$ with free boundary condition, as calculated in Section 4.)

These special "borderline" HAWs on $\mathcal{M}^{+}$ are now in one-to-one correspondence to a special subclass of (unrooted) spanning trees on the square, unoriented $M \times N$ sublattice $\mathscr{L}$ of $\mathcal{M}^{+}$ (on Figs. 19a and 19b, $\mathscr{L} = \mathscr{L}_{B}$, whose sites are centers of counterclockwise plaquettes of $\mathcal{M}^{+}$). Let us denote by $i = (m', n')$ the sites of $\mathscr{L}$, with $0 \leqslant m' \leqslant M-1$ and $0 \leqslant n' \leqslant N-1$. The bottom row and right column of $\mathscr{L}$ are labeled, respec-

tively, by $(M-1, n')$, $0 \leqslant n' \leqslant N-1$, and by $(m', 0)$, $0 \leqslant m' \leqslant M-2$ (Figs. 19a and 19b), and form the half-borderline $\partial_+ \mathscr{L}$. The other half-borderline, $\partial_- \mathscr{L}$, is formed by the sites $(0, n')$, $1 \leqslant n' \leqslant N-1$, and $(m', N-1)$, $0 \leqslant m' \leqslant M-2$.

Then on $\mathscr{L}$ the spanning trees corresponding to the special "borderline" HAWs on $\mathscr{M}^+$ are those that *bond straight together all sites* of $\partial_+ \mathscr{L}$ (Fig. 19b). Now we remark that these special spanning trees can be

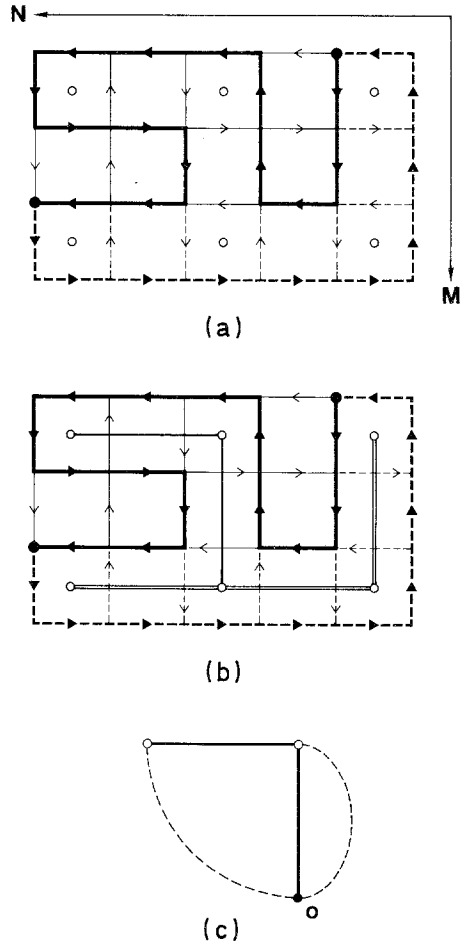

Fig. 19. (a) The open HAW of Fig. 18 has been completed to a closed circuit on $\mathscr{M}^+$ (4×6 Manhattan lattice). (b) This closed circuit is in one-to-one correspondence with a special spanning tree on the unoriented $(M=2) \times (N=3)$ square lattice $\mathscr{L}$ (open dots). All bonds of the half-borderline $\partial_+ \mathscr{L}$ (double lines) belong to the spanning tree. (c) Special spanning trees on $\mathscr{L}$ spanning all bonds of $\partial_+ \mathscr{L}$ are normal spanning trees on the reduced graph $G = \mathscr{L}/\partial_+ \mathscr{L}$ (dotted lines) obtained by coalescing $\partial_+ \mathscr{L}$ to a single point 0.

considered as usual spanning trees on a new graph G obtained from $\mathscr{L}$ by identifying all the sites of $\partial_+ \mathscr{L}$ with a single site (Fig. 19c), which we denote by

$$G = \mathscr{L}/\partial_+ \mathscr{L} \tag{7.3}$$

Then

$$N^0_{\mathrm{H},1}(\mathscr{M}^+)|_{\text{borderline}} = N^0_{T,1}(\mathscr{L}/\partial_+ \mathscr{L}) \tag{7.4}$$

where $N^0_{T,1}(G)$ is the number of unrooted spanning trees on G, with no further constraint. Now, we use Eqs. (3.4) and (3.5) to calculate $N^0_{T,1}(G)$ in terms of the connectivity matrix $\mathbf{C}_G$ of G,

$$N^0_{T,1}(G) = \det \mathbf{C}_{G/\{a\}} = \frac{1}{N_0(G)} \det' \mathbf{C}_G \tag{7.5}$$

where $\det \mathbf{C}_{G/\{a\}}$ is the minor with respect to any point a of G, and det' is the product of all nonvanishing eigenvalues. Note that the number of sites of G is

$$N_0(G) = (M-1)(N-1)+1 \tag{7.6}$$

Now, as in Section 5 and Appendix B, it is convenient to consider the Neumann Gaussian integral (5.3) on graph G

$$\mathscr{I} = \int \prod_{i \in G} d\varphi(i)\, \delta(\varphi(o)) \exp\left\{ -\frac{1}{2} \sum_{\langle i,j \rangle} [\varphi(i) - \varphi(j)]^2 \right\} \tag{7.7}$$

where the site $\{o\}$ is the special site of G obtained by coalescing the half-borderline $\partial_+ \mathscr{L}$ of $\mathscr{L}$. This Neumann integral (7.7) is obtained from Eq. (B.2) of Appendix B as

$$\mathscr{I} = (2\pi)^{[N_0(G)-1]/2} (\det \mathbf{C}_{G/\{a\}})^{-1/2} \tag{7.8}$$

Now, we remark that (7.7) can also be written as an integral over fields living on the sites of $\mathscr{L}$:

$$\mathscr{I} = \int \prod_{i \in \mathscr{L}} d\varphi(i) \prod_{j \in \partial_+ \mathscr{L}} \delta(\varphi(j)) \exp\left\{ -\frac{1}{2} \sum_{\langle i,j \rangle} [\varphi(i) - \varphi(j)]^2 \right\} \tag{7.7bis}$$

where the field φ vanishes along the half-borderline $\partial_+ \mathscr{L}$ and is free along the other half-borderline $\partial_- \mathscr{L}$. Following the same line of argument as in Appendix B, this shows that (7.7bis) corresponds to the discrete Laplacian

on the *infinite* lattice, with Dirichlet boundary conditions on $\partial_+ \mathscr{L}$ and Neumann boundary conditions on $\partial_- \mathscr{L}$. Hence, from (7.8),

$$\det \mathbf{C}_{G/\{a\}} = \det(-\Delta)|_{\substack{\text{Dirichlet } \partial_+ \mathscr{L} \\ \text{Neumann } \partial_- \mathscr{L}}} \tag{7.9}$$

7.2. Spectrum[3]

The spectrum of the bulk discrete Laplacian with these mixed boundary conditions is easy to find by tensorial products. Let us consider first the problem in one dimension, say along a row $0 \leqslant n' \leqslant N-1$. Then the bulk Laplacian is

$$-\Delta\varphi(n') \equiv 2\varphi(n') - \varphi(n'-1) - \varphi(n'+1)$$

We extend any field $\varphi(n')$, $0 \leqslant n' \leqslant N-1$, satisfying $\varphi(0)=0$ with $\varphi(N-1)$ free to the interval $[N, 2N-1]$ by

$$\varphi(2N-1-n') \equiv \varphi(n'), \qquad 0 \leqslant n' \leqslant N-1$$

and then to the interval $[-2N+1, 0]$ by antisymmetry,

$$\varphi(-n') = -\varphi(n'), \qquad 0 \leqslant n' \leqslant 2N-1$$

The extended field is now *periodic* on $\mathbf{Z}$, with period $2(2N-1)$. Hence, the eigenvectors of the above bulk Laplacian can be obtained by the Ansatz

$$\varphi(n') = ae^{2\pi i k n'/2(2N-1)} + be^{-2\pi i k n'/2(2N-1)}$$

with a Brillouin zone $k \in [0, 2N-1]$. The above symmetry equations give

$$a = -b, \qquad k = 2n-1, \quad 1 \leqslant n \leqslant N-1$$

with eigenvalues $2 - 2\cos[(2n-1)/(2N-1)\pi]$.

In two dimensions, the eigenvectors of $-\Delta$ with mixed Dirichlet–Neumann boundary conditions are then factorized into $\sin[\pi m'(2m-1)/(2M-1)]\ \sin[\pi n'(2n-1)/(2N-1)]$ with eigenvalues

$$\lambda_{m,n} = 4 - 2\cos\frac{2m-1}{2M-1}\pi - 2\cos\frac{2n-1}{2N-1}\pi$$
$$1 \leqslant m \leqslant M-1, \qquad 1 \leqslant n \leqslant N-1 \tag{7.10}$$

Note that this gives $(M-1)(N-1)$ nonvanishing eigenvalues for $\mathbf{C}_G$, as expected from (7.6).

[3] This section and Section 7.3 were prepared in collaboration with J. M. Luck.

Collecting Eqs. (7.2)–(7.5), (7.9) and (7.10), we find the exact number of wedge-to-wedge walks

$$N_{\mathrm{H}}^{W} = \det(-\Delta)|_{\substack{\text{Dirichlet } \partial_+ \mathscr{L} \\ \text{Neumann } \partial_- \mathscr{L}}}$$

$$\equiv D' = \prod_{\substack{1 \leqslant m \leqslant M-1 \\ 1 \leqslant n \leqslant N-1}} \left(4 - 2\cos\frac{2m-1}{2M-1}\pi - 2\cos\frac{2n-1}{2N-1}\pi\right) \quad (7.11)$$

7.3. Fourier Transform

The calculation of $\ln D'$ is similar to that of $\ln D$ in (4.8a). We first use

$$\ln[2(\operatorname{ch} t - \cos\theta)] = t - \sum_{k \in \mathbf{Z}^*} \frac{e^{-|k|t}}{|k|} e^{ik\theta} \quad (7.12)$$

and set

$$\operatorname{ch} t_n = 2 - \cos\frac{2n-1}{2N-1}\pi, \qquad 1 \leqslant n \leqslant N-1 \quad (7.12a)$$

For

$$\theta_m = \frac{2m-1}{2M-1}\pi \quad (7.12b)$$

we have the identity

$$\begin{aligned} S_k &= \sum_{m=1}^{M-1} e^{ik\theta_m} + \text{c.c.} \\ &= (-1)^{k+1} \qquad \text{if} \quad k \notin (2M-1)\mathbf{Z} \\ &= (-1)^{k'} 2(M-1) \qquad \text{if} \quad k = k'(2M-1), \quad k' \in \mathbf{Z} \end{aligned} \quad (7.13)$$

Hence we write

$$\begin{aligned} \ln D' &= \sum_{m,n} \ln[2(\operatorname{ch} t_n - \cos\theta_n)] \\ &= \sum_{n=1}^{N-1} \Bigg[(M-1)t_n - \sum_{\substack{k \in \mathbf{N}^* \\ k \neq 0 \bmod(2M-1)}} \frac{e^{-kt_n}}{k}(-1)^{k+1} \\ &\quad - \sum_{k' \in \mathbf{N}^*} \frac{2(M-1)}{2M-1}(-1)^{k'} \frac{e^{-(2M-1)k't_n}}{k'} \Bigg] \\ &= \sum_{n=1}^{N-1} \left[(M-1)t_n + \sum_{k \in \mathbf{N}^*} \frac{e^{-kt_n}}{k}(-1)^k - \sum_{k' \in \mathbf{N}^*} (-1)^{k'} \frac{e^{-(2M-1)k't_n}}{k'} \right] \\ &= \sum_{n=1}^{N-1} [(M-1)t_n - \ln(1+e^{-t_n}) + \ln(1+e^{-(2M-1)t_n})] \end{aligned}$$

It will be convenient to rewrite this sum as

$$\ln D' = \sum_{n=1}^{N-1} \left\{ \left(M - \frac{1}{2} \right) t_n - \ln \left(2 \operatorname{ch} \frac{t_n}{2} \right) + \ln[1 + e^{-(2M-1)t_n}] \right\} \tag{7.14}$$

This is an exact result, which we now evaluate asymptotically.

7.4. Asymptotic Number of Open Walks

Using the notation $t(\theta)$ for the positive solution of $\operatorname{ch} t = 2 - \cos\theta$,

$$t(\theta) = \ln[2 - \cos\theta + (3 - 4\cos\theta + \cos^2\theta)^{1/2}]$$

we have by symmetry with respect to $\theta = \pi$ [see (7.12a)]

$$\sum_{n=1}^{N-1} t_n = \frac{1}{2} [S_{\text{odd}} - t(\pi)] \tag{7.15}$$

where S_{odd} involve the summation over odd l's only

$$S_{\text{odd}} = \sum_{1 \leqslant \text{odd } l \leqslant 2L-1} t\left(\frac{l}{L} \pi \right), \qquad L = 2N - 1 \tag{7.15bis}$$

It is convenient to complete the sum with even terms

$$S(L) \equiv \sum_{1 \leqslant l \leqslant 2L-1} t\left(\frac{l}{L} \pi \right) \tag{7.16}$$

Then, identically,

$$S_{\text{odd}} = S(L) - S(L/2) \tag{7.17}$$

Now $S(L)$ in (7.16) ranging over the period $\theta \in [0, 2\pi]$ is easily evaluated asymptotically with the help of the Euler–MacLaurin formula (3.60),

$$S(L) = 2L \int_0^{2\pi} t(\theta) \frac{d\theta}{2\pi} - t(0) + \frac{1}{12} [-2t'(0)] \frac{\pi}{L} + \cdots \tag{7.18}$$

with $t(0) = 0$, $t'(0) = 1$, and $t(\pi) = 2\ln(1 + \sqrt{2})$.

Hence we finally find from Eqs. (7.15)–(7.18)

$$\left(M - \frac{1}{2} \right) \sum_{n=1}^{N-1} t_n = \left(M - \frac{1}{2} \right) \left(N - \frac{1}{2} \right) \int_0^{\pi} t(\theta) \frac{d\theta}{\pi} - \left(M - \frac{1}{2} \right) \ln(1 + \sqrt{2}) + \frac{\pi}{24} \frac{2M-1}{2N-1} + \cdots \tag{7.19}$$

where, as in (3.62),

$$\int_0^{\pi} t(\theta)\frac{d\theta}{\pi} = \frac{4}{\pi}G \quad (G \text{ Catalan's constant})$$

The second sum in (7.14) is evaluated by the same completion method as in (7.15) and (7.16). We find

$$\begin{aligned}
&\sum_{n=1}^{N-1} \ln\left(2\,\mathrm{ch}\,\frac{t_n}{2}\right) \\
&\quad = \left(N-\frac{1}{2}\right)\int_0^{\pi} \ln\left[2\,\mathrm{ch}\,\frac{t(\theta)}{2}\right]\frac{d\theta}{\pi} - \frac{1}{2}\ln\left[2\,\mathrm{ch}\,\frac{t(\pi)}{2}\right] + O(N^{-1}) \\
&\quad = \left(N-\frac{1}{2}\right)\int_0^{\pi} \frac{d\theta}{\pi}\frac{1}{2}\ln[2(3-\cos\theta)] - \frac{1}{4}\ln 8 + O(N^{-1}) \\
&\quad = \left(N-\frac{1}{2}\right)\ln(1+\sqrt{2}) - \ln 2^{3/4} + O(N^{-1})
\end{aligned} \tag{7.20}$$

Finally, the last sum in (7.14) converges very rapidly and it suffices to approximate t_n by its expansion near the origin $t_n \simeq \theta_n = (2n-1)\pi/(2N-1)$, which gives the infinite-product limit

$$\sum_{n=1}^{N-1} \ln[1+e^{-(2M-1)t_n}] \to \ln \prod_{n=1}^{\infty} (1+q^{n-1/2}) \tag{7.21}$$

with

$$q = e^{-2\pi\xi}, \qquad \xi = \frac{2M-1}{2N-1} = \frac{\mathbf{M}}{\mathbf{N}} \tag{7.22}$$

Collecting Eqs. (7.14) and (7.19)–(7.21) gives finally the asymptotic evaluation

$$\begin{aligned}
\ln D' \cong &\left(M-\frac{1}{2}\right)\left(N-\frac{1}{2}\right)\frac{4G}{\pi} - (M+N-1)\ln(1+\sqrt{2}) \\
&+ \ln\left[2^{3/4}q^{-1/48}\prod_{n=1}^{\infty}(1+q^{n-1/2})\right]
\end{aligned} \tag{7.23}$$

In terms of the number of sites (7.1) of the odd–odd Manhattan lattice, we finally get the number of open Hamiltonian walks (7.11) starting and finishing in the diagonal wedges of $\mathcal{M}$ (Fig. 18),

$$N_{\mathrm{H}}^{W} \simeq e^{G\mathbf{MN}/\pi}(1+\sqrt{2})^{-(\mathbf{M}+\mathbf{N})/2} \times 2^{3/4} q^{-1/48} \prod_{n\geqslant 1} (1+q^{n-1/2}) \tag{7.24}$$

Note the following identity[29,30]:

$$q^{-1/48}\prod_{n\geqslant 1}(1+q^{n-1/2})=\frac{\eta^2(q)}{\eta(q^{1/2})\,\eta(q^2)} \tag{7.24bis}$$

This expression is invariant under the exchange $\mathbf{M}\leftrightarrow\mathbf{N}$ [or $\tau\to -1/\tau$ in the modular invariance formalism (3.39)], as it should be.

Let us now compare the asymptotic numbers $N^{\mathrm{f}}_{\mathrm{H},1}$ [Eq. (4.24)] of Hamiltonian walks on the even–even Manhattan lattice and N^{W}_{H} [Eq. (7.24)] of walks on the odd–odd lattice. They have the same dominant bulk and surface (perimeter) terms, as could be expected, but the power correction terms $(\mathbf{MN})^{\bar\gamma}$ are *different*,

$$\bar\gamma^{\mathrm{f}}=3/4, \qquad \bar\gamma^{W}=0 \tag{7.25}$$

The modular dependence is also different. These exact results on the $\bar\gamma$ exponents are quite interesting, since they will allow us to determine directly a (universal) surface exponent of the Hamiltonian walks.

7.5. An Exact Surface or Wedge Critical Exponent

Consider a *dense* polymer chain of length l in a rectangular box (Fig. 20). The number of sites Λ of the box is such that the occupied fraction $f=l/\Lambda$ remains finite even in the thermodynamic limit. This dense polymer system, or melt, has been studied in detail in refs. 20–22 in two dimensions and its exact critical exponents determined.

Let $\omega_l(\mathbf{r},\mathbf{r}')$ be the number of configurations of the chain of length l joining $\mathbf{r}$ to $\mathbf{r}'$. It has the critical behavior[22]

$$\omega_l(\mathbf{r},\mathbf{r}')\sim\omega_{0,l}\,|\mathbf{r}-\mathbf{r}'|^{-2x_1} \tag{7.26}$$

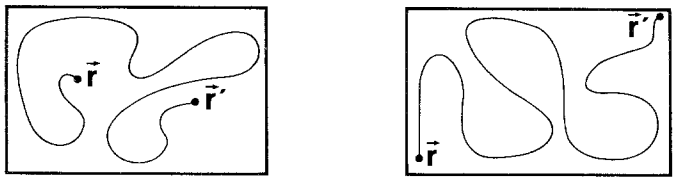

Fig. 20. (a) A dense, self-avoiding chain in a box. The extremities repell each other, with the number of configurations increasing with distance $\omega(\mathbf{r},\mathbf{r}')\sim|r-r'|^{3/8}$, for $\mathbf{r}$ and $\mathbf{r}'$ in the bulk. (b) The analog for a dense SAW in corners ($\alpha=\pi/2$) of Fig. 18 for HAW. Then $\omega(\mathbf{r},\mathbf{r}')\sim|\mathbf{r}-\mathbf{r}'|^{1/2}$.

where $\omega_{0,l}$ is the number of configurations of a dense loop of length l with fixed origin in the same box, and x_1 is a critical exponent, whose value in 2D is, for dense polymers,[20–22]

$$x_1 = -3/16 \tag{7.27}$$

and has been obtained[20,22] from Nienhuis' results[24] and checked numerically.[21] Its negative value is related[24] to the $n=0$ limit of the $O(n)$ model describing polymers. Dense polymers correspond furthermore to the *critical low-temperature phase* of the $O(n=0)$ model.[20–22] This negative value mans that in a *melt* the extremities of a chain *repell* each other. The behavior (7.26), (7.27) holds as long as the extremities of the chain do not approach the boundaries.[22] When the two extremities are very close to a boundary *line*, a new surface scaling behavior is developed[39]

$$\omega_l^S(\mathbf{r}, \mathbf{r}') \sim \omega_{0,l} \, |\mathbf{r} - \mathbf{r}'|^{-2x_1^S} \tag{7.28}$$

where for dense polymers the surface exponent is[22]

$$x_1^S = -1/8 \tag{7.29}$$

again a *negative* value, implying repulsion along the surface. If one extremity is pinched in a *wedge* of angle α, then the corresponding scaling dimension is given by conformal covariance[27,39]

$$x_1^W(\alpha) = \frac{\pi}{\alpha} x_1^S \tag{7.30}$$

such that

$$\omega_l^W(\mathbf{r}, \mathbf{r}') \sim \omega_{0,l} \, |\mathbf{r} - \mathbf{r}'|^{-2x_1^W} \tag{7.31}$$

for two extremities in wedges.

It has been shown analytically in a previous work[25] that Hamiltonian walks on the Manhattan lattice are in the *same universality class* as dense polymers (see also last section). Hence, the exponents x_1^S for HAWs and dense SAWs should be the same.

We obtain here an independent verification of this universality. Here we have found indeed for closed *circuits* on a Manhattan lattice with free boundary conditions (4.24)

$$N_{\mathrm{H},1}^0 = \frac{1}{\mathbf{MN}} N_{\mathrm{H},1}^{\mathrm{f}} \sim e^{G\mathbf{MN}/\pi} (1+\sqrt{2})^{-(\mathbf{M}+\mathbf{N})/2} (\mathbf{MN})^{-1/4} \tag{7.32}$$

and this is just the analog of $\omega_{0,l}$ for a dense Hamiltonian polymer loop of length

$$l = \mathbf{MN}$$

The number of configurations of the open Hamiltonian walks with extremities in the corners of $\mathcal{M}$ (Fig. 18) is

$$N_{\mathrm{H}}^{W} \sim e^{G\mathbf{MN}/\pi}(1+\sqrt{2})^{-(\mathbf{M}+\mathbf{N})/2}(\mathbf{MN})^{0} \tag{7.33}$$

It corresponds exactly to α, $\omega_l^W(\mathbf{r}-\mathbf{r}')$ [(7.30), (7.31)] for $\mathbf{r}$ and $\mathbf{r}'$ in the corners of $\mathcal{M}$, such that $\alpha=\pi/2$, $x_1^W=2x_1^S$, and $|\mathbf{r}-\mathbf{r}'|\sim(\mathbf{MN})^{1/2}$. In this case, we have from (7.31)

$$\omega^W/\omega_0 \sim (\mathbf{MN})^{-x_1^W} = (\mathbf{MN})^{-2x_1^S}$$

while (7.32) and (7.33) give exactly $\omega^W/\omega_0 \sim N_{\mathrm{H}}^W/N_{\mathrm{H}}^0 \sim (\mathbf{MN})^{1/4}$. Hence, from our study of Hamiltonian walks we find

$$x_1^S = -1/8$$

in complete agreement with (7.29) obtained for dense polymers from Coulomb gas methods applied to the $O(n)$ model.[22,25] It is worth noting that here an exact 2D critical exponent $x_1^S=-1/8$ has been computed by *elementary* means, evaluating exactly determinants and numbers of configurations in a critical system.

B. NESTED MULTIPLE WALKS, NONHOMOTOPIC TO ZERO

8. NESTED HAMILTONIAN CIRCUITS AND POTTS MODEL

8.1. General Considerations

Until now, we have always discussed the case where Hamiltonian walks or *rooted* circuits were *adjacent* on the Manhattan lattice and formed a close packing of circuits. On the *torus*, we imposed the further constraint that all circuits were *homotopic to a point*. This gave us the relation to multiconnected spanning *trees*. Then we showed that they were equivalent to a two-dimensional massive free field theory with a critical point at zero fugacity (few walks).

One may wonder now what happens when circuits are allowed to *encircle* other ones and form *nests* on $\mathcal{M}$ (Fig. 21). On a Manhattan *torus* as in Fig. 1, we also release the zero homotopy condition and consider Hamiltonian circuits that can wrap along the torus and become nonhomotopic to a point.

Of course, if we consider nested circuits on $\mathcal{M}$ with *free* edges, all circuits become homotopic to zero (Fig. 21). Then the analysis is slightly simpler, and this nested (unrooted) walk system has been studied in detail

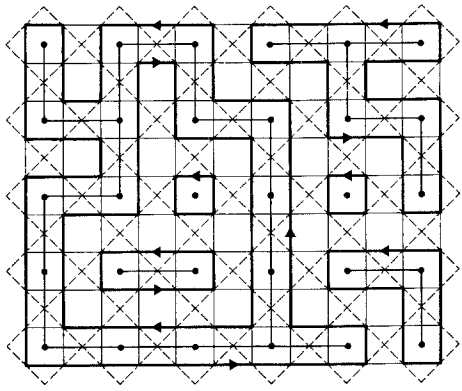

Fig. 21. Depiction of $K=7$ encircling Hamiltonian circuits (heavy lines) on $\mathscr{M}$ with free boundary conditions. In contrast to Fig. 11, the walks can be nested inside one another. One can draw a spanning graph $\mathscr{G}$ on the square lattice $\mathscr{L}_B$ (centers of counterclockwise plaquettes; dots). The perimeters of each connected component of $\mathscr{G}$, including isolated points, give all Hamiltonian circuits.

in ref. 25 and shown to be related to a Q-state Potts model on the square lattice. This also allows us to derive an infinite set of exact critical exponents for Manhattan HAWs,[25] which are those of the Potts model. A relation was then established to the $O(n)$ model and to its critical exponents. This showed the *universality* of the Manhattan Hamiltonian exponents. These successive identities were established for a grand canonical set of nested circuits parametrized by a fugacity z for the fluctuating number of circuits. One has then $z=\sqrt{Q}=n$.[25]

A survey of this theory is given here, which opens a new direction for HAWs on the Manhattan lattice. We shall also consider in detail the torus case, where the nested walks can wrap along the torus generators. The exact continuum limit of the grand canonical partition function for Manhattan Hamiltonian circuits, nested, and with different winding numbers, is given here.

8.2. Equivalence to the Potts Model

We thus consider nested HAWs on $\mathscr{M}$ with *free* boundary conditions. A typical configuration is given in Fig. 21.

Surprisingly, the grand canonical set of nested unrooted Hamiltonian circuits on $\mathscr{M}$ is then in one-to-one correspondence[25] to a Potts model on the unoriented square lattice $\mathscr{L}$, whose number of states Q gives the circuit fugacity $\sqrt{Q}$ of the Hamiltonian system!

Consider indeed a set of K circuits filling the Manhattan lattice $\mathscr{M}$ with $(\mathbf{M}=2M)\times(\mathbf{N}=2N)$ sites and *free* edges (Fig. 21). By drawing their skeletons, one finds a one-to-one correspondence to a *spanning graph* $\mathscr{G}$ on the square lattice $\mathscr{L}$ (here $\mathscr{L}_B$), whose sites are the centers of plaquettes oriented in the same sense as the boundary of $\mathscr{M}$. The spanning graph $\mathscr{G}$ has several connected components, the internal and external perimeters of which are precisely the Hamiltonian circuits.

We introduce a grand canonical partition function for Hamiltonian (encircling) circuits

$$Z_{\mathrm{H}}(z)=\sum_{K\geqslant 1} z^K N'_{\mathrm{H},K} \tag{8.1}$$

with a fugacity z, where $N'_{\mathrm{H},K}$ is the number of configurations of K circuits, the prime denoting the possibility of *nested* configurations.

Note that here, in contrast to the partition function (1.17) for adjacent walks, one *does not count* the position of the origin of each circuit. For $K=1$, we have obviously

$$N'_{\mathrm{H},1}\equiv N^0_{\mathrm{H},1} \tag{8.2}$$

We can write (8.1) as

$$Z_{\mathrm{H}}(z)=\sum_{\mathscr{G}_{\mathrm{H}}\in\mathscr{M}} z^{\mathscr{N}_P} \tag{8.1bis}$$

where the sum is taken over all possible collections $\mathscr{G}_{\mathrm{H}}$ of Hamiltonian circuits on $\mathscr{M}$ with $\mathscr{N}_P$ perimeter loops.

Using the equivalence to spanning graphs $\mathscr{G}$ on $\mathscr{L}$ $(=\mathscr{L}_B)$, we can write identically

$$Z_{\mathrm{H}}(z)=\sum_{\substack{\text{spanning graphs}\\ \mathscr{G}\in\mathscr{L}}} z^{\mathscr{N}_P} \tag{8.3}$$

where $\mathscr{N}_P$ is the number of perimeter lines of $\mathscr{G}$. On the open square lattice $\mathscr{L}$, one has obviously

$$\mathscr{N}_P=\mathscr{N}_L+\mathscr{N}_C \tag{8.4}$$

where $\mathscr{N}_L$ is the number of loops of graph $\mathscr{G}$ and $\mathscr{N}_C$ its number of connected components.

As noted by Kasteleyn, Hamiltonian walks on $\mathscr{M}$ correspond just to Euler walks on the diagonal oriented square lattice $\bar{\mathscr{L}}$ (Fig. 22). So we can transform trivially the HAWs of Fig. 21 into an Euler set on $\bar{\mathscr{L}}$ (Fig. 22).

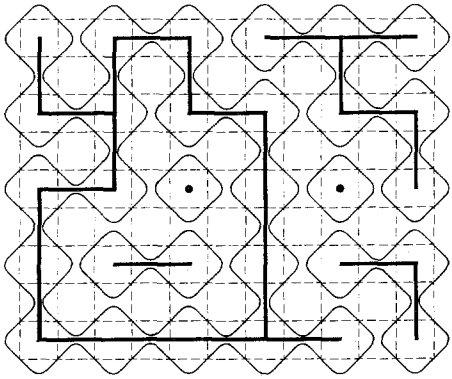

Fig. 22. The polygon decomposition of the surrounding diagonal (unoriented) lattice $\mathscr{Q}$. These polygons form disconnected Eulerian walks on $\mathscr{Q}$. They surround a spanning graph $\mathscr{G}$ (heavy lines) on square lattice $\mathscr{L}$, including isolated points. This graph is typical of the high-temperature expansion of the Potts model.

This Euler set encircles the same former spanning graph on $\mathscr{G}$ (bold lines in Fig. 22). This Euler set just builds a polygon decomposition[40] of the *surrounding lattice* $\mathscr{Q}$ of $\mathscr{L}$, which is just the diagonal square lattice $\bar{\mathscr{Q}}$ *without* its orientation. This is very reminiscent of the usual high-temperature expansion of the Potts model.[26,40] The Potts model Hamiltonian is $\beta H = -\beta \sum_{\langle i,j \rangle} \delta_{\sigma_i \sigma_j}$, where $\langle i, j \rangle$ are nearest neighbors on lattice $\mathscr{L}$ and $\sigma_i = 1,..., Q$. The partition function is given by the Whitney polynomial[26,40]

$$Z_{\text{Potts}} = \sum_{\{\sigma\}} e^{-\beta H} = \sum_{\mathscr{G}} W(\mathscr{G})$$
$$= \sum_{\mathscr{G}} (e^{\beta} - 1)^{\mathscr{N}_B} Q^{\mathscr{N}_C} \tag{8.5}$$

where $W(\mathscr{G})$ is the weight of a spanning graph $\mathscr{G}$ on $\mathscr{L}$ made of $\mathscr{N}_B$ bonds (heavy lines in Fig. 22) and $\mathscr{N}_C$ connected components. In terms of the number of loops $\mathscr{N}_L$ of $\mathscr{G}$ we have (Euler's relation)

$$\mathscr{N}_L = \mathscr{N}_B + \mathscr{N}_C - \mathscr{N}_S \tag{8.6}$$

where the number of sites $\mathscr{N}_S$ of $\mathscr{L}$ is

$$\mathscr{N}_S = M \times N = \tfrac{1}{4}\mathbf{MN}$$

In terms of the $\mathscr{N}_P$ polygons of the decomposition of the surrounding lattice $\mathscr{Q}$, which are drawn inside each loop of $\mathscr{G}$ and around each cluster of

$\mathcal{G}$, one has $\mathcal{N}_P = \mathcal{N}_L + \mathcal{N}_C$, and therefore $\mathcal{N}_C = \frac{1}{2}(\mathcal{N}_P - \mathcal{N}_B + \mathcal{N}_S)$. Hence we can rewrite (8.5) as

$$Z_{\text{Potts}} = Q^{\mathcal{N}_S/2} \sum_{\mathcal{G}} [(e^{\beta} - 1)\, Q^{-1/2}]^{\mathcal{N}_B}\, Q^{\mathcal{N}_P/2} \tag{8.7}$$

The Q-state Potts model is critical[26,40,41] for $Q \in [0, 4]$.

The critical point for $Q \in [0, 4]$ is known by duality to be $(e^{\beta_c} - 1)\, Q^{-1/2} = 1$.[26] Hence from (8.7)

$$Z_{\substack{\text{Potts} \\ \text{critical}}} = Q^{\mathcal{N}_S/2} \sum_{\mathcal{G}} Q^{\mathcal{N}_P/2} \tag{8.8}$$

Comparison to the Hamiltonian grand canonical partition function (8.3) gives the basic identity[25]

$$Z_{\text{H}}(z) = Q^{-\mathcal{N}_S/2} Z_{\substack{\text{Potts} \\ \text{critical}}}(Q) \tag{8.9}$$

for

$$z = \sqrt{Q} \tag{8.10}$$

Hence, *encircling or nested Hamiltonian circuits on the Manhattan lattice are exactly described by a standard critical Potts model on the unoriented square lattice.* In particular, the $Q \to 0$ limit of the Potts model, i.e., $z \to 0$, will enable us to recover the true Hamiltonian limit of a finite number of walks filling the (infinite) Manhattan lattice.

8.3. Application

A first application of this identity concerns the evaluation of the number $N'_{\text{H},K}$ of nested K-circuits. Indeed, the Potts free energy at the critical point on, e.g., the square lattice

$$f(Q, \beta_c) = \lim_{\mathcal{N}_S \to \infty} \frac{1}{\mathcal{N}_S} \ln Z_{\substack{\text{Potts} \\ \text{critical}}}(Q) \tag{8.11}$$

is exactly known[41] as a function of Q. The successive moments $N'_{\text{H},K}$ of (8.1) and (8.9) in the thermodynamic limit have been calculated from it. In particular, at small Q, one finds[25]

$$f(Q, \beta_c) = \frac{1}{2} \ln Q + \frac{4G}{\pi} + \cdots$$

and Eqs. (8.1), (8.9), and (8.11) give

$$\lim_{\mathcal{N}_S \to \infty} \frac{1}{\mathcal{N}_S} \ln N'_{\mathrm{H},1} = \frac{4G}{\pi} \tag{8.12}$$

which is just Kasteleyn's celebrated result (0.3) (since $\mathcal{N}_S = \frac{1}{4}\mathbf{MN}$) obtained here by a completely different method.

8.4. Critical Exponents

8.4.1. Bulk Exponents. Generalizing the above identity between Manhattan Hamiltonian and Potts partition functions, one can also consider correlation functions.[25] We introduce for the Potts model the geometrical correlators[25,42]

$$G_k(X-Y) = \frac{1}{Z_{\mathrm{Potts}}(Q)} \sum_{\mathscr{G}_k} W(\mathscr{G}_k) \tag{8.13}$$

where the sum is taken over all spanning graphs $\mathscr{G}_k$ of $\mathscr{L}$, which involve, among all the polygons of the surrounding lattice $\mathscr{L}$ (at least), k polygons that join a neighborhood of X to one of Y (Fig. 23). At the Potts critical point, we argue as above that[25]

$$G_k(X-Y) = \frac{1}{Z_{\mathrm{H}}(z)} \sum_{\mathscr{G}_k} z^{\mathcal{N}_P(\mathscr{G}_k)} \qquad \text{(critical)} \tag{8.14}$$

i.e., G_k is the correlation function of k Hamiltonian circuits on $\mathscr{M}$, immersed in a grand canonical sea with fugacity $z = \sqrt{Q}$ (Fig. 23). This identification is quite important, since one is able to calculate[22,24,42] the critical behavior of G_k from Coulomb gas methods[23,24] in two dimensions. Indeed, G_k decays at the Potts critical point like

$$G_k(X-Y) \sim |X-Y|^{-2x_k} \qquad \text{(critical)} \tag{8.15}$$

where[24,25,42] x_k is a critical exponent, which depends only on k and Q as

$$x_k = \frac{g}{2}\left(\frac{k}{2}\right)^2 - \frac{(4-g)^2}{8g} \tag{8.16}$$

where g is given by the Coulomb gas parametrization of the Potts model[23,24]

$$z^2 = Q = 2 + 2\cos\tfrac{1}{2}\pi g, \qquad g \in [2,4], \quad Q \in [0,4] \tag{8.17}$$

For the true Hamiltonian problem $z \to 0$, $Q \to 0$, hence $g = 2$, and[25]

$$x_k = \tfrac{1}{4}(k^2 - 1) \tag{8.18}$$

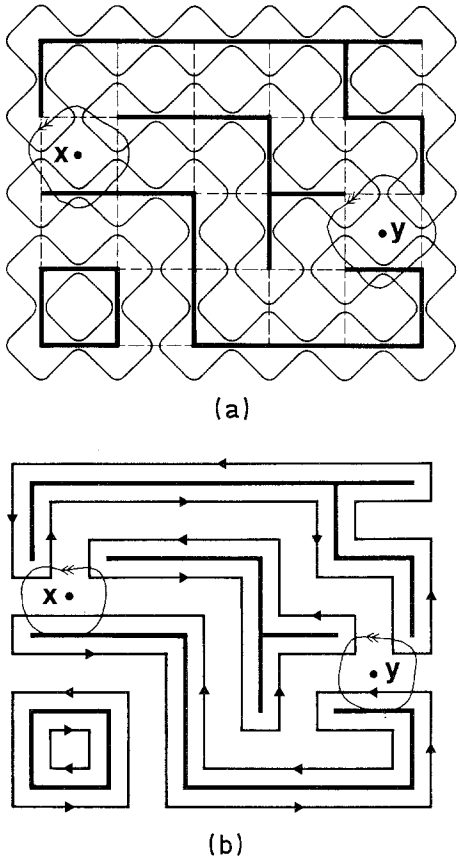

Fig. 23. (a) A graph $\mathcal{G}_3$ contributing to the Potts correlation function $G_3(X-Y)$. (b) The corresponding graph on the Manhattan lattice.

8.4.2. Surface Exponents. When the two points X and Y in (8.15) *approach the boundary* of the Manhattan lattice or of the Potts lattice $\mathcal{L}$, new *surface* scaling dimensions appear. In terms of the Coulomb gas coupling constant g, they read, from the Potts model,[22,25]

$$x_k^S = \tfrac{1}{4} g k^2 + \tfrac{1}{4} k(g-4) \tag{8.19}$$

and for the $Q \to 0$, $z \to 0$ true Hamiltonian limit

$$x_k^S = \tfrac{1}{2} k(k-1) \tag{8.20}$$

The values (8.18) and (8.20) are (universal) critical exponents for Manhattan Hamiltonian walks, characterizing the critical decay of correlations of bunches of k circuits.

8.5. $O(n)$ Model and Universality

The above critical exponents have been derived for the Manhattan lattice; one could wonder if they are universal. First, since they are exponents of the Potts model, one suspects their universality. Indeed, one could consider, e.g., the Kagomé or triangular lattices of Section 6 and generalize straightforwardly the equivalence to a Potts model on a corresponding lattice (actually, this works for any HAW on any covering lattice, as in Kasteleyn's original paper). Second, as discussed in detail in previous work,[20,22,25,42] the exponents (8.16) and (8.19) are also critical exponents of the $O(n)$ model, in its own *low-temperature phase*. Note that this phase is also known to be critical, but with different exponents from those of the critical point.[24]

The $O(n)$ model is defined on the hexagonal lattice $\mathscr{H}$ by the partition function[24]

$$Z_{O(n)} = \int \prod_i d\mathbf{S}_i \prod_{\langle j,l \rangle} (1 + \beta \mathbf{S}_j \cdot \mathbf{S}_l) \tag{8.21}$$

where i, j, l are sites on $\mathscr{H}$, (j, l) being nearest neighbors, and $\mathbf{S}$ is a n-component vector with $|\mathbf{S}|^2 = n$. Then this partition function is that of a loop model,[24]

$$Z_{O(n)} = \sum_{\text{graphs}} \beta^{\mathscr{N}_B} n^{\mathscr{N}_P} \tag{8.22}$$

where the graphs are formed by $\mathscr{N}_P$ *self-* and *mutually avoiding* rings on the honeycomb lattice, of total length $\mathscr{N}_B$. One introduces correlation functions similar to (8.13) for the Potts model

$$G_{O(n),L}(X - Y) = \frac{1}{Z_{O(n)}} \sum_{\mathscr{G}_L} \beta^{\mathscr{N}_B(\mathscr{G}_L)} n^{\mathscr{N}_P(\mathscr{G}_L)} \tag{8.23}$$

where the graphs $\mathscr{G}_L$ on $\mathscr{H}$ are restricted to join by L lines a neighborhood of X to one of Y, possibly with additional loops (Fig. 24). These correlation functions decay at criticality like

$$G_{O(n),L} \sim |X - Y|^{-2x_{O(n),L}} \tag{8.24}$$

where the critical exponent $x_{O(n),L}$ reads, in terms of the standard Coulomb gas parametrization of the $O(n)$ model,[24,43]

$$x_{O(n),L} = \frac{g'}{8} L^2 - \frac{1}{2g'} (1 - g')^2 \tag{8.25}$$

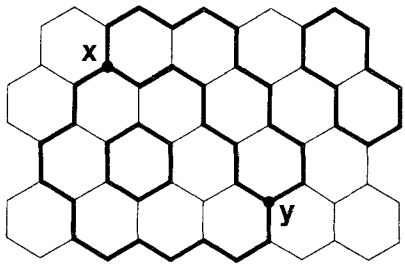

Fig. 24. A graph contributing to the correlation function $G_{O(n),3}(X-Y)$ of the hexagonal $O(n)$ model. In the Potts model it would correspond to $G_{3/2}(X-Y)$, i.e., a "half-integer number" of polygons.

with[24]

$$n = -2\cos \pi g' \tag{8.26}$$

$g' \in [1, 2]$ for $\beta = \beta_c = [2 + (2-n)^{1/2}]^{-1/2}$ (critical point) (8.26a)

$g' \in [0, 1]$ for $\beta > \beta_c$ (low-temperature phase) (8.26b)

The whole low-temperature phase of the $O(n)$ model is indeed critical,[24] with exponents independent of $\beta > \beta_c$. In terms of the high-temperature expansion (8.22) of the $O(n)$ model, this corresponds to a *condensation* of the loops,[22] which densely fill the lattice.

The surface exponents of the $O(n)$ model read similarily[25,39]

$$x^S_{O(n),L} = \tfrac{1}{4} g' L^2 + \tfrac{1}{2} L(g' - 1) \tag{8.25a}$$

Then the critical Potts and low-temperature $O(n)$ models are equivalent for[25]

$$n = \sqrt{Q} = z \tag{8.27}$$

Indeed, comparing (8.8) and (8.22) yields this obvious identification of the loop (or polygon) fugacities. Now (8.27) is satisfied for [see Eqs. (8.17), (8.26b)]

$$\underset{\text{low-}T\, O(n)}{g'} = \underset{\text{Potts critical}}{g/4} \in [1/2, 1] \tag{8.28}$$

Then we check the *identity* of the critical exponents (8.16), (8.19) and (8.25), (8.25a):

$$\begin{aligned} x_{\text{Potts},k} &= x_{O(n),L=2k} \\ x^S_{\text{Potts},k} &= x^S_{O(n),L=2k} \end{aligned} \tag{8.29}$$

i.e., for $\sqrt{Q} = n = z$, the correlations of k polygons in the Q-Potts critical model (Fig. 23) are the same as those of $2k$ lines in the low-temperature $O(n)$ model (Fig. 24). This relation was also observed by Nienhuis for some exponents.[24]

8.6. Hamiltonian Condensation

We thus see that *nested* Hamiltonian circuits on the Manhattan lattice, with a grand canonical fugacity z for the number of circuits, are in the same universality class as the critical $Q=z^2$ Potts model and as the $O(n)$ model for $n=z$ in its low-temperature phase. This holds for $z\in[0,2]$, $Q\in[0,4]$, $n\in[0,2]$, where the models have a second-order phase transition. For $z>2$, the Potts transition becomes first order.[26,41] The Hamiltonian system is still equivalent to the Potts model at its first-order transition point. Hence, the correlation length staying finite, and one is led to conclude[25] that the *critical* nested Hamiltonian system with a walk fugacity z undergoes a phase transition when $z=2$ toward a new phase where the correlations are *screened* and *short range*. This ressembles the case of adjacent Hamiltonian walks. However, as seen in Section 3, the system of *adjacent* walks becomes classical as soon as the fucacity m^2 is nonzero. We thus see an important difference between rooted adjacent and unrooted nested Hamiltonian walks on the Manhattan lattice. The adjacent walks [partition function (1.17)] have only a critical point at zero fugacity, which corresponds to a few infinite walks filling the infinite lattice. Otherwise the correlations inside a thermodynamic melt of adjacent walks are exponentially screened. On the other hand, the allowance of *nested* Hamiltonian circuits makes it possible for the system to describe a *finite continuous line* $z\in[0,2]$ of *critical points*. All correlation functions are algebraically decreasing with critical exponents x_k, (8.16), and x_k^S, (8.19), which vary continuously with the fugacity $z=n=\sqrt{Q}$, as the universality class.

9. WINDING HAMILTONIAN CIRCUITS ON THE TORUS

9.1. General Considerations

We shall now consider the case where multiple Hamiltonian circuits live on the Manhattan torus and can be nested inside each other and be nonhomotopic to zero. An example is given on Fig. 25 for the 4×6 Manhattan torus filled by $K=3$ Hamiltonian circuits, one being homotopic to zero, the other two wrapping once around the torus (compare to Fig. 5). Note that a Manhattan torus is necessarily an even–even lattice (as in Section 3). Then, when one follows one of the geodesics of the torus, one crosses necessarily an *even* number of Hamiltonian lines[4] (Fig. 25). Note then that this shows that a *single* closed HAW filling the lattice (as in

[4] Nonoriented plaquettes of $\mathcal{M}$ have always two antiparallel occupied lines (P. W. Kasteleyn).

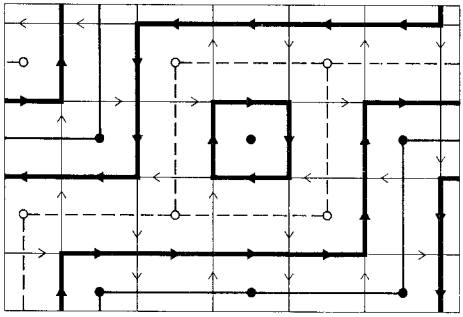

(a)

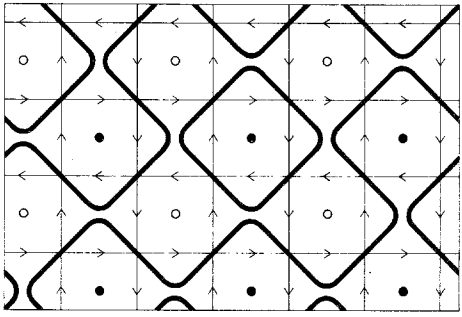

(b)

Fig. 25. (a) $K=3$ HAWs on $\mathscr{M}$, only one being homotopic to zero. Two *nonequivalent* spanning graphs on $\mathscr{L}_A$ and $\mathscr{L}_B$ (thin and dotted lines) correspond to the HAWs. (b) In contrast, a well-defined 3-Euler walk on the diagonal square lattice $\mathscr{2}$ corresponds to the 3-HAW.

Fig. 1) is necessarily homotopic to zero. Indeed, a single loop *non*-homotopic to zero on a torus crosses necessarily one of the geodesics an odd number of times. For this reason the topology of the torus becomes relevant when there are at least two Hamiltonian circuits filling the lattice.

Let us call $N_{\mathrm{H},K}(\mathbf{T})$ the total number of configurations of K Hamiltonian circuits filling the Manhattan torus, with no restriction on the topology. The grand canonical generating function on the torus T is then defined as in Section 8 [Eq. (8.1)]

$$Z_{\mathrm{H}}^{\mathrm{T}}(z)=\sum_{K\geqslant 1} z^K N_{\mathrm{H},K}(\mathbf{T}) \tag{9.1}$$

One must note that this toroidal grand canonical partition function is no longer exactly that of a Potts model on the torus. Each HAW

configuration on the torus is now related to two nonequivalent spanning graphs on $\mathscr{L}_A$ or $\mathscr{L}_B$ (Fig. 25a). In contrast, there is still one polygon decomposition of the surrounding lattice $\mathscr{2}$ (Fig. 25b) corresponding to the HAWs. As before, this polygon decomposition is just the Eulerian set of circuits on diagonal square lattice $\bar{\mathscr{2}}$, to which the Hamiltonian circuits are equivalent.

Hence, we see that counting K-circuits on the Manhattan torus is equivalent to counting polygon decompositions of the torus $\mathscr{2}$. Thus, as in Eq. (8.3),

$$Z_{\mathrm{H}}^{\mathbf{T}}(z) = \mathscr{Z}(Q) \equiv \sum_{\substack{\text{polygon} \\ \text{decompositions of } \mathscr{2}}} Q^{\mathscr{N}_P/2} \tag{9.2}$$

with

$$Q^{1/2} = z \tag{9.2bis}$$

But the transformation to spanning graphs[44] on $\mathscr{L}_A$ or $\mathscr{L}_B$ is ambiguous on the torus. For instance, in the case of Figs. 25a and 25b one has, respectively, the numbers of clusters, loops, and polygons

$$\mathscr{N}_C^A = 2, \qquad \mathscr{N}_L^A = 0, \qquad \mathscr{N}_P = K = 3$$
$$\mathscr{N}_C^B = 1, \qquad \mathscr{N}_L^B = 1, \qquad \mathscr{N}_P = K = 3$$

None of these sets of numbers satisfies relation (8.4), which is necessary for identifying the Potts partition function (8.5) with the polygon representation (8.7). The relation (8.4) was characteristic of the *free* square lattice, where all Potts clusters and all Hamiltonian circuits were homotopic to zero.

This only means that the identity of (9.1) with the Potts partition function is not entirely exact on the torus. These partition functions are actually related to each other, as we shall see below. Naturally, the critical properties of the model and its universality class do not depend on the torus topology. The critical exponents x_k, x_k^S [(8.16), (8.19)] in Section 8 remain valid and are those of a critical Potts model with $\sqrt{Q} = z$ and of an $O(n)$ model in the critical ordered phase. Furthermore, it happens that the continuum limit of the partition function (9.1) can be found exactly, and is even simpler than that of the Potts model on the torus,[45] to which it is intimately related. Let us now evaluate it.

We first remark that our Manhattan partition function (9.1) or polygon partition function (9.2) is in the continuum limit the partition function of (dense) self- and mutually avoiding loops on the torus (Fig. 26), with the particular condition that an *even* number of lines is crossed when following a geodesic on the torus. Hence, the Hamiltonian lines or

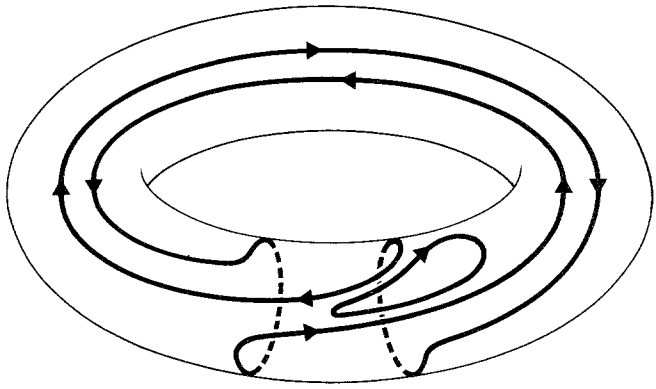

Fig. 26. The topology of the 3-walk of Fig. 25 in the continuum limit.

polygons can be considered as lines of change of height in an SOS model on T. The SOS model is then always amenable[23,24] to a free field theory with discontinuities along the geodesics.[45]

The SOS model is defined on the diagonal square lattice $\mathscr{L}$ (Fig. 25b) by orienting arbitrarily each closed line or polygon, which is then considered as a wall between regions of constant height differing by a constant $\pm\varphi_0$.[23,24] In the SOS model a factor e^{iu} (e^{-iu}) is associated with each left (right) turn along a polygon. Along a polygon homotopic to zero, the total algebraic number of turns is always ± 4. For a polygon wrapping along the torus the algebraic sum is zero, since it makes a equal number of left and right turns on the surrounding lattice $\mathscr{L}$. Hence, summing over the orientations gives a factor $2\cos 4u$ for zero homotopy and 2 for nonzero homotopy. The SOS partition function then reads

$$\mathscr{Z}_{\mathrm{SOS}} \equiv \sum_{\text{polygons}} (2\cos 4u)^{\mathscr{N}_P} 2^{\tilde{\mathscr{N}}_P} \tag{9.3}$$

where $\mathscr{N}_P$ (resp. $\tilde{\mathscr{N}}_P$) is the number of polygons homotopic to 0 (resp. nonhomotopic to 0).

This SOS sum is similar to the polygon partition function (9.2) for

$$z = Q^{1/2} = 2\cos 4u \tag{9.4}$$

However, the polygons nonhomotopic to a point have a factor 2 instead of $Q^{1/2}$. It will thus be convenient to introduce a double sum, which weights differently zero and nonzero homotopic curves

$$\mathscr{Z}(Q, \tilde{Q}) = \sum_{\text{polygons}} Q^{\mathscr{N}_P/2} \tilde{Q}^{\tilde{\mathscr{N}}_P/2} \tag{9.5}$$

The simple SOS value (9.3) corresponds to the end of the Potts critical line $\tilde{Q}=4$ for the nonzero homotopic circuits and to $Q(\in[0,4])$ for the zero homotopic ones. Note also that by using the same correspondence between Eulerian polygons in the SOS model and Hamiltonian walks on the Manhattan lattice (Fig. 25), we have

$$\mathscr{Z}(Q,\tilde{Q})\equiv Z_{\mathrm{H}}^{\mathrm{T}}(z,\tilde{z}) \tag{9.6}$$

where

$$Z_{\mathrm{H}}^{\mathrm{T}}(z,\tilde{z})=\sum_{\substack{K\geqslant 0\\ \tilde{K}\geqslant 0}} z^{K}\tilde{z}^{\tilde{K}}N_{\mathrm{H},K,\tilde{K}}(\mathbf{T}) \tag{9.7}$$

is the grand canonical partition function of $K+\tilde{K}$ Hamiltonian circuits on the Manhattan torus, K being homotopic to a point, and $\tilde{K}$ being not. It is worth noting that $N_{\mathrm{H},0,0}=0$ and $N_{\mathrm{H},0,1}=0$.

9.2. Exact Continuum Partition Functions

We use the formalism established in refs. 45, where critical partition functions on the 2D torus were expressed in terms of a free field with defect lines in the Coulomb gas formalism.[23,24] We start with $\mathscr{Z}_{\mathrm{SOS}}$ in (9.3), which is simpler. The torus polygon partition function (9.3) in the continuum limit can be represented as the continuum partition function of a system of double SOS wall lines (Fig. 26). In the continuum limit the standard Coulomb gas parametrization of the critical Potts model or the SOS model (for $\varphi_0=\pi/2$) is then, as in Section 8,[23,24]

$$Q=2+2\cos \pi g/2, \qquad g\in[2,4] \tag{9.8}$$

$$8u/\pi=\pm(2-g/2) \bmod 4 \tag{9.9}$$

Then the SOS partition functions can be written in the continuum in terms of a two-dimensional free field with some defect lines on the torus.[45] In the continuum, each wall line corresponds to a line where the two-dimensional free field has discontinuities multiple of 2π. One considers the free field action

$$\mathscr{A}=\frac{g}{4\pi}\int (\nabla\varphi)^2\, d^2x \tag{9.10}$$

where g is given by (9.8), and whose periodic partition function is, on the torus,

$$Z_1(g)=\int_{\varphi \text{ periodic}} [D\varphi]\, e^{-\mathscr{A}} \tag{9.11}$$

and after a proper renormalization (setting $\tau = \tau_R + i\tau_I$)

$$Z_1(g) = \frac{g^{1/2}}{\tau_I^{1/2}\eta(q)\,\eta(\bar{q})} \tag{9.12}$$

Then one needs the free field with discontinuities along the geodesics[45]

$$Z_{m',m}(g) = \int_{\substack{\delta\varphi|_1 = 2\pi m' \\ \delta\varphi|_2 = 2\pi m}} [D\varphi]\, e^{-\mathscr{A}}$$

where one imposes a discontinuity of $2\pi m'$ ($2\pi m$) on φ along the geodesic ω_1 (ω_2). We evaluate $Z_{m',m}(g)$ as

$$Z_{m',m}(g) = Z_1(g) \exp\left(-\pi g \frac{m'^2 + m^2(\tau_R^2 + \tau_I^2) - 2\tau_R m m'}{\tau_I} \right) \tag{9.13}$$

While Z_1 in (9.12) is modular invariant, $Z_{m',m}$ is not. A simple modular invariant is obtained by summing over m', m and defining a Coulombic partition function

$$Z_c[g, \mathbf{f}] = \mathbf{f} \sum_{m', m \in \mathbf{fZ}} Z_{m',m}(g) \tag{9.14}$$

with the following properties[45]:

$$Z_c[g, \mathbf{f}] = Z_c\left[\frac{1}{g}, \frac{1}{\mathbf{f}}\right] = Z_c[g\mathbf{f}^2, 1] \tag{9.15}$$

After a Poisson transformation on variable m' one finds the Coulomb gas representation[45]

$$Z_c[g, 1] = \frac{1}{\eta\bar{\eta}} \sum_{e,m \in \mathbf{Z}} q^{(e/\sqrt{g} + m\sqrt{g})^2/4} \bar{q}^{(e/\sqrt{g} - m\sqrt{g})^2/4} \tag{9.16}$$

which will be useful later.

In the continuum limit, the SOS partition function (9.3), (9.4) is then given very simply in term of this free field with frustrations by the double sum over possible discontinuities[45]

$$\mathscr{Z}_{\mathrm{SOS}} \to Z_c[g/4, 1] \tag{9.16bis}$$

This also gives the continuum limit of the polygon or Hamiltonian partition functions (9.5) and (9.7) for $Q = z^2$ parametrized by (9.8), and for the nonzero homotopy parameter *fixed* at $\tilde{Q} = 4$, $\tilde{z} = 2$.

It remains to find the continuum limit of the general partition functions (9.6), (9.7), and (9.2). The correct weight is given to the polygons of HAWs not homotopic to a point by introducing in the Coulomb gas representation a supplementary electric charge e_0,[45,46] which plays the same role as the electric charge $\pm e_0$ introduced at infinity in the cylinder limit.[36] It parametrizes $\tilde{Q}$ as

$$\tilde{Q}^{1/2} = 2 \cos \tfrac{1}{2}\pi e_0 \tag{9.17}$$

In particular, the preceding case $\tilde{Q}=4$ corresponds to $e_0=0$, while the symmetric model $[Q=\tilde{Q}$; (9.2)] is recovered for

$$e_0 = \pm(2 - g/2) \bmod 4 \tag{9.18}$$

Then, a study of the topological properties of parallel frustration lines on the torus yields[45] the following continuum limit of $\mathscr{Z}(Q, \tilde{Q})$ of (9.5) (this can be extracted from the discussion of the Potts model in ref. 45)

$$\mathscr{Z}(Q, \tilde{Q}) \to \hat{Z}[g, e_0] \tag{9.19}$$

with

$$\hat{Z}[g, e_0] = \sum_{m', m \in \mathbf{Z}} Z_{m',m}\left(\frac{g}{4}\right) \cos(\pi e_0 m' \wedge m) \tag{9.20}$$

where $m' \wedge m$ denotes the greatest common divisor of integers m' and m. For $e_0=0$, one recovers (9.14) and (9.16bis).

This continuum limit thus also gives the explicit answer to the Hamiltonian walk partition function on the Manhattan torus (9.7). We have the limit

$$Z_{\mathrm{H}}^{\mathbf{T}}(z, \tilde{z}) \to \hat{Z}[g, e_0] \tag{9.21}$$

with the parametrization

$$\begin{aligned} &z = 2 \cos \tfrac{1}{2}\pi(2 - \tfrac{1}{2}g), && z \in [-2, 2], \quad g \in [0, 4] \\ &\tilde{z} = 2 \cos \tfrac{1}{2}\pi e_0, && \tilde{z} \in [-2, 2] \end{aligned} \tag{9.22}$$

One can finally note that this partition function is related to that of the critical Q-state Potts model on the torus with $Q^{1/2}=z$. The complete expression of the latter is indeed[45]

$$\mathscr{Z}_{\mathrm{Potts}}^{\mathbf{T}}(Q) \to \hat{Z}[g, e_0] + \tfrac{1}{2}(Q-1)(Z_c[g, 1] - Z_c[g/4, 1]) \tag{9.23}$$

where the two last terms involving the Coulombic partition function (9.14) reestablish the correct weights for Potts clusters on a torus, which are slightly different from those of the polygon decomposition.

9.3. $O(n)$ Model

As we have seen, the critical Q-state Potts model is related to the $O(n)$ model (8.21), (8.22) in its critical low-temperature phase for $n=\sqrt{Q}$. It is then instructive to compare their partition functions on the torus. On the periodic hexagonal lattice $\mathscr{H}$ we generalize the partition function (8.22) into[22,45]

$$\mathscr{Z}_{O(n),\tilde{n}} = \sum_{\text{graphs}} \beta^{\mathscr{N}_B} n^{\mathscr{N}_P} \tilde{n}^{\tilde{\mathscr{N}}_P} \tag{9.24}$$

where the graphs are made of nonintersecting polygons on toroidal $\mathscr{H}$. Here $\mathscr{N}_B$ is the total number of bonds, and $\mathscr{N}_P$ (resp. $\tilde{\mathscr{N}}_P$) is the total number of polygons homotopic to zero (resp. nonhomotopic to zero).

The critical point is[24] $\beta_c=[2+(2-n)^{1/2}]^{-1/2}$, and the model is critical for $n\in[-2, 2]$, $\tilde{n}\in[-2, 2]$. The difference from the Potts-like polygon model (9.5) lies in the fact that now the closed lines on the torus can cross the geodesics an *odd* number of times. For instance, single loops nonhomotopic to zero exist. The continuum limit of (9.22) is the modular invariant partition function[22,45]

$$\mathscr{Z}_{O(n),\tilde{n}} \to \hat{Z}[g', e_0'] \tag{9.25}$$

with the parametrization

$$\begin{aligned} n &= -2\cos \pi g', \qquad g' \in [1, 2] \quad \text{for } \beta=\beta_c \\ &\qquad\qquad\quad g' \in [0, 1] \quad \text{for } \beta>\beta_c \\ \tilde{n} &= 2\cos \pi e_0', \qquad \tilde{n}\in[-2, 2] \end{aligned} \tag{9.26}$$

The pure $O(n)$ model (8.22) where all loops on the torus are weighted equivalently is then obtained for

$$e_0' = \pm(g'-1) \bmod 2$$

The $O(n)$, $\tilde{n}$ model in the low-temperature phase is related to the Potts-like model (9.5) or the Hamiltonian model (9.7) by the equations

$$n=Q^{1/2}=z, \qquad \tilde{n}=\tilde{Q}^{1/2}=\tilde{z} \tag{9.27}$$

which are satisfied for

$$g'_{O(n)} = \tfrac{1}{4} g_{\text{Potts}}, \qquad e'_{0,O(n)} = \tfrac{1}{2} e_{0,\text{Potts}}$$

Consider then the $O(n)$, $\tilde{n}$ partition function (9.25):

$$\mathscr{Z}_{O(n),\tilde{n}} \to \hat{Z}[g', e'_0] = \hat{Z}\left[\frac{g}{4}, \frac{e_0}{2}\right]$$

$$= \sum_{m',m \in \mathbf{Z}} Z_{m',m}\left(\frac{g}{16}\right) \cos\left[\frac{\pi}{2} e_0 (m \wedge m')\right] \quad (9.28)$$

Isolating the even–even terms and using the obvious relation [see (9.12), (9.13)]

$$Z_{2m',2m}(g/16) = \tfrac{1}{2} Z_{m',m}(g/4)$$

we find from (9.20)

$$\mathscr{Z}_{O(n),\tilde{n}} \to \tfrac{1}{2}\hat{Z}[g, e_0] - \hat{Z}_{\text{odd}}[g, e_0]$$

where

$$\hat{Z}_{\text{odd}}[g, e_0] = \sum_{\substack{(m,m') \in \mathbf{Z}^2 \\ m' \text{ or } m \notin 2\mathbf{Z}}} Z_{m',m}\left(\frac{g}{16}\right) \cos\left[\frac{\pi}{2} e_0 (m' \wedge m)\right] \quad (9.29)$$

is the partition function of lines crossing one geodesic an odd number of times, while $\hat{Z}[g, e_0]$ is precisely the continuum limit of the Potts-like $\mathscr{Z}(Q, \tilde{Q})$ in (9.19) or of the Manhattan $Z_{\text{H}}^{\text{T}}(z, \tilde{z})$ in (9.21), made of double lines.

9.4. The $Q, \tilde{Q} \to 0$ Limit

Let us consider what happens when we consider the true Hamiltonian limit where only a finite number of circuits fill the lattice: $z = 0$, $\tilde{z} = 0$, $Q = 0$, $\tilde{Q} = 0$. The corresponding values of the Coulomb gas coupling constant g and floating electric charge e_0 are, from (9.22),

$$g = 2, \qquad e_0 = \pm 1 \bmod 4 \quad (9.30)$$

The partition function (9.7) should be trivial, since by definition a set of Hamiltonian walks cannot be empty. For $e_0 = \pm 1$, the continuum limit (9.20) reads, by separating the congruence classes $m \wedge m' = 0 \bmod 2$, $m \wedge m' = 1 \bmod 2$,

$$\hat{Z}[g, 1] = 2 \sum_{m', m \in 2\mathbf{Z}} Z_{m', m}\left(\frac{g}{4}\right) - \sum_{m', m \in \mathbf{Z}} Z_{m', m}\left(\frac{g}{4}\right)$$
$$= Z_c\left[\frac{g}{4}, 2\right] - Z_c\left[\frac{g}{4}, 1\right]$$
$$= Z_c[g, 1] - Z_c\left[\frac{g}{4}, 1\right] \tag{9.31}$$

where we have used the definition (9.14) and the second duality identity in (9.15). We thus have, for $g = 2$,

$$\hat{Z}[2, 1] = Z_c[2, 1] - Z_c[1/2, 1] = 0 \tag{9.32}$$

with use of the first duality property (9.15). QED. The same result was obtained in ref. 22 when considering the $n = \tilde{n} = 0$ dense polymer limit of (9.25) for $g' = 1/2$, $e_0' = 1/2$:

$$\hat{Z}[1/2, 1/2] = 0 \tag{9.33}$$

Hence, as expected, these partition functions are trivial. Their derivatives are not trivial, however. They count the number of configurations of closed Hamiltonian loops. In (9.19) and (9.21) the derivative $\partial/\partial z \sim \partial/\partial g$ counts the number of circuits homotopic to zero, while $\partial/\partial \tilde{z} \sim \partial/\partial e_0$ selects the circuits nonhomotopic to zero. It is then very interesting to evaluate the first moments of the Hamiltonian generating function (9.21).

9.4.1 Moments. We use the definition (9.7)

$$N_{\mathrm{H}, 1, 0} = \frac{\partial}{\partial z} Z_{\mathrm{H}}^{\mathrm{T}}(z, \tilde{z})|_{z = \tilde{z} = 0} \tag{9.34}$$

$$N_{\mathrm{H}, 0, 1} = \frac{\partial}{\partial \tilde{z}} Z_{\mathrm{H}}^{\mathrm{T}}(z, \tilde{z})|_{z = \tilde{z} = 0} \tag{9.35}$$

which are, respectively, the numbers of single Hamiltonian circuits homotopic to zero or not homotopic to zero on the Manhattan torus. We calculate their continuum limits from (9.21) and (9.22),

$$X_{\mathrm{H}} = \frac{dg}{dz} \frac{\partial}{\partial g} \hat{Z}[g, e_0] \tag{9.34bis}$$

$$\tilde{X}_{\mathrm{H}} = \frac{de_0}{d\tilde{z}} \frac{\partial}{\partial e_0} \hat{Z}[g, e_0] \tag{9.35bis}$$

From (9.22) we have

$$X_{\mathrm{H}} = \frac{2}{\pi \sin \frac{1}{2}\pi(2-g/2)} \frac{\partial}{\partial g} \hat{Z}[g, 1] \Big|_{g=2} \tag{9.36}$$

$$\tilde{X}_{\mathrm{H}} = -\frac{1}{\pi \sin \frac{1}{2}\pi e_0} \frac{\partial}{\partial e_0} \hat{Z}[2, e_0] \Big|_{e_0=1} \tag{9.37}$$

9.4.2. Paths Homotopic to Zero. Let us evaluate X_{H} first. Using the identity (9.31), we have

$$\frac{\partial}{\partial g} \hat{Z}[g, 1] = Z_c'[g, 1] - \frac{1}{4} Z_c'\left[\frac{g}{4}, 1\right]$$

where $Z_c'[g, 1] \equiv (\partial/\partial g) Z_c[g, 1]$, which, according to (9.15), obeys $Z_c'[g, 1] = -g^{-2} Z_c'[1/g, 1]$. Hence we find for Hamiltonian walks ($g = 2$)

$$X_{\mathrm{H}} = -\frac{1}{\pi} Z_c'\left[\frac{1}{2}, 1\right] \tag{9.38}$$

The derivative of the Coulombic partition function (9.14) for $g = \frac{1}{2}$ can be calculated exactly.[22] Due to (9.16), we have in general

$$Z_c[g, 1] = \frac{1}{\eta\bar{\eta}} \sum_{e,m \in \mathbf{Z}} (q\bar{q})^{(e^2/g + m^2 g)/4} \left(\frac{q}{\bar{q}}\right)^{em/2}$$

and

$$Z_c'[g, 1] = \frac{\ln q\bar{q}}{\eta\bar{\eta}} \sum_{e,m \in \mathbf{Z}} \left(\frac{m^2}{4} - \frac{e^2}{4g^2}\right) (q\bar{q})^{(e^2/g + m^2 g)/4} \left(\frac{q}{\bar{q}}\right)^{em/2}$$

For $g = \frac{1}{2}$, it involves the double sum

$$S = \sum_{e,m \in \mathbf{Z}} \left(\frac{m^2}{4} - e^2\right) q^{(m/2+e)^2/2} \bar{q}^{(m/2-e)^2/2}$$

By use of the Jacobi identity[29]

$$\tfrac{1}{2} \sum_{n \in \mathbf{Z}} (-1)^n (2n+1)\, q^{(n^2+n)/2} = P^3(q)$$

we find

$$S = \tfrac{1}{2}(q\bar{q})^{1/8} P^3(q)\, P^3(\bar{q}) = \tfrac{1}{2}\eta^3(q)\, \eta^3(\bar{q})$$

Hence

$$Z_c'[\tfrac{1}{2}, 1] = \tfrac{1}{2} \ln q\bar{q}\, \eta^2(q)\, \eta^2(\bar{q})$$

We therefore find the "continuum number" of single Hamiltonian circuits homotopic to zero:

$$X_{\mathrm{H}} = 2 \operatorname{Im} \tau\, \eta^2(q)\, \eta^2(\bar{q}) \tag{9.39}$$

where we used $q = e^{2\pi i\tau}$. This is just the continuum version of the famous number $N_{\mathrm{H},1}^0$, (0.1), of Hamiltonian circuits on the Manhattan lattice. We have, according to Eq. (3.21),

$$N_{\mathrm{H},1,0} \equiv N_{\mathrm{H},1}^0 = e^{G\mathbf{MN}/\pi} X_{\mathrm{H}} \tag{9.40}$$

We note that the exact enumeration result (3.21) and the continuum value (9.39) obtained from conformal invariance theory are related by the ultraviolet lattice-dependent part $e^{G\mathbf{MN}/\pi}$, which is characteristic of the Manhattan lattice. This is in agreement with the discussion of Section 3.5. The *modular invariant factor* (9.39) *is entirely universal* and does not depend on the lattice. It does not even depend on the density of the walks, and has been obtained also for dense polymers[22] (see next section).

9.4.3. Paths Nonhomotopic to Zero. We evaluate $\tilde{X}$ in (9.37). By use of the definition (9.20) at values $e_0 \pm 1$ of the floating electric charge

$$\frac{\partial}{\partial e_0} \hat{Z}[g, e_0]\Big|_{e_0 = 1} = \sum_{m', m \in \mathbf{Z}} Z_{m',m} \left(\frac{g}{4}\right) \sin \pi(m \wedge m') \equiv 0 \tag{9.41}$$

since $m \wedge m' \in \mathbf{Z}$. Hence for a single path not homotopic to zero

$$\tilde{X}_{\mathrm{H}} = 0 \tag{9.42}$$

This gives another proof of the already noted fact that there are *no single Hamiltonian circuits nonhomotopic to zero on the Manhattan torus.* Note that (9.41) holds for any g, hence any z, Q. This implies that one cannot fill the Manhattan torus better with a single Hamiltonian circuit nonhomotopic to zero and a set of other circuits homotopic to zero, whatever the number of circuits:

$$N_{\mathrm{H},K,1} \equiv 0 \qquad \text{for any } K \tag{9.43}$$

10. COMPARISON TO DENSE POLYMERS

10.1. True Hamiltonian Limit $z \to 0$

On the Manhattan lattice, true Hamiltonian walks in finite number are obtained in the zero-fugacity limit $z \to 0$. According to Section 8, this limit corresponds to the $Q \to 0$ critical Potts model or the $O(n=0)$ model for $\beta > \beta_c = (2+\sqrt{2})^{-1/2}$ on the hexagonal lattice. Hence the statistical systems made up of true Manhattan HAWs $z=0$, Potts critical $Q=0$, and $O(n=0)$ model, $\beta > \beta_c$, have *identical critical properties.*

As seen in (8.29), the critical exponents x_k, x_k^S governing the decay of the correlation (8.14) of k true Hamiltonian circuits on $\mathscr{M}$, or the correlation (8.13) of the trees on $\mathscr{L}$, or k Potts polygons on $\mathscr{Q}$, or finally the correlation (8.23) of $L=2k$ SAW lines of the $n=0$ model all have the same exact values [Eqs. (8.18), (8.20)]

$$x_k = (k^2-1)/4, \qquad x_k^S = k(k-1)/2$$

This is not surprising. First, the Potts $Q=0$ limit is known[26,44] to describe generally spanning trees, and HAWs on Manhattan are directly related to such trees. Second, the low-temperature phase of the $n=0$ model is known[20–22] to describe *dense polymers*, i.e., dense SAWs.

10.2. Dense Polymers

Dense polymers are polymers that are in finite number and fill a finite fraction of the available space.[20–22] In a lattice box of Λ sites, the total length of the polymers l defines an occupied fraction of sites[22]

$$f = l/\Lambda \tag{10.1}$$

and in the infinite-lattice limit, dense polymers are such that $l \to \infty$, $\Lambda \to \infty$, $0 < f \leqslant 1$, $f=0$ corresponds to usual dilute SAWs, while $f=1$ corresponds to Hamiltonian walks. The critical exponents do not depend[22,24] on the inverse temperature $\beta > \beta_c = (2+\sqrt{2})^{-1/2}$ of the $O(n=0)$ model in its low-temperature phase. Now, the actual value of the occupied fraction f is determined[22] by the value of the inverse temperature β, with $f=0$ for $\beta = \beta_c$ (dilute SAWs) and $f \to 1$ for $\beta \to \infty$ (Hamiltonian limit). Hence the critical exponents for dense polymers, usually written as[20–22,25] ($L=2k$)

$$x'_L = x_{\substack{O(n=0),L \\ \beta > \beta_c}} = (L^2-4)/16 \tag{10.2}$$

$$x'^S_L \equiv x^S_{\substack{O(n=0),L \\ \beta > \beta_c}} = L(L-2)/8 \tag{10.3}$$

are independent of β and thus of the density f of (10.1) for $f > 0$.

It was not entirely obvious, even if the limit $\beta \to \infty$ should yield the Hamiltonian limit, that the critical exponents of Hamiltonian walks on a Manhattan oriented lattice are the same as those of dense polymers.

This study[25] reported here shows that both the Hamiltonian constraint and the Manhattan orientation are irrelevant for the infrared critical properties of (dense) walks.

Quite remarkably, we have also obtained, besides the general equivalent of nested HAWs to Potts or $O(n)$ models, a direct check in Section 7 of the validity of (10.2) and (10.3). Indeed, the surface exponent $x_1^S = -1/8$ [Eq. (7.29)], obtained directly from the exact calculation of corner–corner walks (Fig. 18), is in perfect agreement with the first value for $L = 1$ of the surface exponents (10.3).

Note also that on $\mathscr{M}$ we had to consider the correlation of k circuits, which led to an even number of polymer lines $L = 2k$ in (8.29). However, the odd values of L that actually occur for genuine dense polymers also may have a physical realization for Manhattan HAWs. The corner-to-corner walk of Section 7 illustrates $L = 1$. This can be generalized to any L odd on the odd–odd $\mathscr{M}$ lattice by introducing $(L-1)/2$ circuits joining two corners. Their critical exponent will be $x_L^W = 2x_L^S$ [Eq. (7.30)]. However, in the *bulk* on lattice $\mathscr{M}$, due to the Hamiltonian constraint and the Manhattan orientation, it is not geometrically possible to accommodate an odd number of lines, but this is a pure artifact of the constraints. The universal exponents (10.2), (10.3) are those of Hamiltonian walks on a wide class of (nonpathological) lattices and of dense polymers.

10.3. Networks of Fixed Topology

In Section 6 we found the configuration exponent $\bar{\gamma}_0$ of a single closed HAW in any Manhattan-like domain $\mathscr{D}$. This result is used here to conjecture new exact critical exponents for two-dimensional dense polymers. We shall deduce from it the unsuspected fact that the configuration γ exponents[47] of dense polymers should depend, not only on the boundary conditions, as shown in ref. 22, but, in the case of free boundary conditions, also on the *shape* of the domain that the dense polymers fill.

Let us consider a *branched* polymer[47] $\mathscr{G}$ made up of various polymer chains of the same size chemically tied together at some vertices (Fig. 27). When L chains are chemically bound together at a vertex, we call it an L-vertex,[47] $L = 1$ corresponding to free ends. The total length of the polymer is l. The topology of $\mathscr{G}$ is fixed and described (partially) by the set $\{n_L\}$ of numbers of L-leg vertices in $\mathscr{G}$. Then the asymptotic number of *dense*

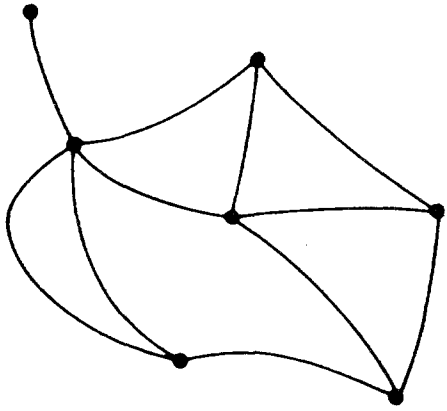

Fig. 27. A polymer network of fixed topology.

configurations of the polymer $\mathscr{G}$ inside a given box $\mathscr{D}$ is expected to scale like

$$\omega_{\mathscr{G}} \sim [\mu^D(f)]^l \{\exp[-\mathscr{B}(f) l^{1/2}]\}\, l^{\bar{\gamma}_{\mathscr{G}}-1}, \qquad l \to \infty \tag{10.4}$$

where $\mu^D(f)$ and $e^{-\mathscr{B}(f)}$ are nonuniversal bulk and perimeter "connectivity constants," which can be numerically shown[22] to depend on the occupied fraction (10.1). For periodic boundary conditions (torus), $\mathscr{B} \equiv 0$. The value of $\mathscr{B}$ can also depend on the box shape. $\bar{\gamma}_{\mathscr{G}}$ is a *critical exponent*, which is supposed to depend only on the topology of $\mathscr{G}$,[20,47] on the boundary conditions[22] imposed on box $\mathscr{D}$ (periodic or free), and also on the geometrical *shape* of $\mathscr{D}$ (for free boundary conditions). In ref. 22 it is argued that, whereas $\bar{\gamma}_{\mathscr{G}}$ governing the absolute number of configurations $\omega_{\mathscr{G}}$ depends on the boundaries, a *universal* critical behavior is expected for the relative number $\omega_{\mathscr{G}}/\omega_0$, where ω_0 is the configuration number of a *single, dense closed walk* of length l.

Then[20,22]

$$\omega_{\mathscr{G}}/\omega_0 \sim l^{\gamma_{\mathscr{G}}^D} \qquad (l \to \infty) \tag{10.5}$$

with a universal dense critical exponent[20]

$$\gamma_{\mathscr{G}}^D = \sum_{L \geqslant 1} n_L (2-L)(L+18)/32 \tag{10.6}$$

$\gamma_{\mathscr{G}}^D$ is thus believed to be independent of boundary conditions and, *a fortiori*, of the box shape. It depends only on the topology[47] $\{n_L\}$ of the network $\mathscr{G}$.

Now, the number of configurations ω_0 of a dense single loop itself scales like, as in (10.4),

$$\omega_0 \sim [\mu^D(f)]^l \{\exp[-\mathscr{B}(f) l^{1/2}]\}\, l^{\bar{\gamma}_0 - 1}, \qquad l \to \infty \tag{10.7}$$

where $\bar{\gamma}_0$ depends a priori on boundary conditions and on shape. The results (3.21) and (4.24) found for a single Hamiltonian circuit on the *rectangular* Manhattan lattice are in agreement with this asymptotic form. We deduce the respective value of the exponent $\bar{\gamma}_0$:

$$\begin{aligned} &\bar{\gamma}_{0,\mathrm{P}} = 1 \qquad &&\text{(periodic Manhattan torus)} \\ &\bar{\gamma}_{0,\mathrm{F}} = 3/4 \qquad &&\text{(free Manhattan rectangle)} \end{aligned} \tag{10.8}$$

For a free Manhattan domain $\mathscr{D}$ of arbitrary shape, we found in Section 6.5

$$\bar{\gamma}_{0,\mathrm{F}} - 1 = -\zeta(0) \tag{10.9}$$

where $\zeta(0)$ is given by (6.13). It is then very tempting to conjecture that these values of $\bar{\gamma}_0$ derived for Manhattan HAWs are actually universal within the class of dense polymers.[22] This conjecture is appealing since we have seen that $\zeta(0)$ is a purely geometrical object, independent of the regularization of the continuum limit. If we thus assume that the values (10.8) and (10.9) also apply to a dense polymer loop, then, from (10.5) and (10.7), the number of configurations $\omega_{\mathscr{G}}$ itself of the dense branched network $\mathscr{G}$ scales like

$$\omega_{\mathscr{G}} \sim [\mu_D(f)]^l \{\exp[-\mathscr{B}(f) l^{1/2}]\}\, l^{\bar{\gamma}_{\mathscr{G}} - 1}$$

with

$$\begin{aligned} &\bar{\gamma}_{\mathscr{G},\mathrm{P}} = \gamma_{\mathscr{G}}^D + 1 \qquad &&\text{(torus)} \\ &\bar{\gamma}_{\mathscr{G},\mathrm{F}} = \gamma_{\mathscr{G}}^D - \zeta(0) \qquad &&\text{(free BC)} \end{aligned} \tag{10.10}$$

where [Eq. (6.13)]

$$\zeta(0) = \sum_j \frac{1}{24}\left(\frac{\pi}{\alpha_j} - \frac{\alpha_j}{\pi}\right) + \sum_i \frac{1}{12\pi}\int_{\gamma_i} \frac{dl}{\rho} \tag{10.11}$$

This conjecture, obtained from the Dirichlet spectral theory (Section 6.5), completes the study of ref. 22 on dense polymers. The "universal" critical exponent $\bar{\gamma}_{\mathscr{G},\mathrm{F}}$ should therefore depend both on the network topology through the exact expression (10.6) of $\gamma_{\mathscr{G}}^D$ and on the boundary's shape through $\zeta(0)$ above. Numerical checks would be most welcome to test this rather intricate conjecture!

11. CONCLUSION

In summary, we have shown how the Hamiltonian problem on the special Manhattan lattice $\mathcal{M}$ is in fact deeply related to known statistical models in two dimensions. First, if one considers only multiply connected and *rooted adjacent* walks or circuits on $\mathcal{M}$ with a fugacity m^2, then the system is completely equivalent to multiply connected spanning trees and the correlation functions are those of a massive free field theory. The Hamiltonian system is then only critical in the zero-mass limit $m=0$, corresponding to a vanishing concentration of walks. Second, when one allows the multiple (unrooted) closed walks to encircle one another, the fugacity being $\sqrt{Q}$, one obtains a complete equivalence to a Q-state Potts model at its critical point. So the system remains *critical* when unrooted walks can encircle one another, for any fugacity ($\sqrt{Q} \leqslant 2$), in contrast to the massive free field theory of rooted walks constrained to be adjacent. The limit $Q \to 0$ is known to describe spanning trees with vanishing concentrations, and recovers the $m \to 0$ limit of the field theory. However, the two theories have allowed us to calculate different geometrical correlation functions in both (rooted walks in the free field, bunches of circuits in the Potts model).

These two rather orthogonal directions suggest that it should be possible to combine them into a unified description by allowing the temperature of the Potts model to vary from its critical value, which introduces the required mass scale in the theory.

It is also to be noted that this mapping of Hamiltonian Manhattan walks onto quite classic statistical systems shows that they are much more universal than originally thought. They also furnish an interesting laboratory to test some general results of critical phenomena and conformal invariance theories. As we have shown in detail here, many properties can be determined exactly, essentially by combinatorial or determinant methods, such as rooted walk correlation functions and a nontrivial surface exponent of the $O(n)$ model, $n \to 0$. This suggests that this model could be exactly solvable.

APPENDIX A. ASYMPTOTIC NUMBERS OF WALKS

We want to evaluate the basic expressions in (3.12)–(3.14),

$$D = \prod_{\mathbf{k} \neq \mathbf{0}} \lambda_{\mathbf{k}}, \qquad S_{-1} = \sum_{\mathbf{k} \neq \mathbf{0}} (\lambda_{\mathbf{k}})^{-1}, \qquad S_{-2} = \sum_{\mathbf{k} \neq \mathbf{0}} (\lambda_{\mathbf{k}})^{-2} \tag{A.1}$$

where $\lambda_{\mathbf{k}}$ is the free field eigenvalue on the torus

$$\lambda_{\mathbf{k}} = 4 - 2\cos 2\pi \frac{m}{N} - 2\cos 2\pi \frac{n}{N}, \qquad 0 \leqslant m \leqslant M-1, \quad 0 \leqslant n \leqslant N-1$$

1. The product D is evaluated via its logarithm

$$\ln D = \sum_{\substack{0 \leqslant m \leqslant M-1 \\ 0 \leqslant n \leqslant N-1 \\ (m,n) \neq (0,0)}} \ln\left(4 - 2\cos 2\pi \frac{m}{M} - 2\cos 2\pi \frac{n}{N}\right) \tag{A.2}$$

The zero mode can be reinserted by the regularization

$$\begin{aligned} \ln D &= \lim_{\varepsilon \to 0} [\Delta(\varepsilon) - \ln \varepsilon] \\ \Delta(\varepsilon) &= \sum_{\substack{0 \leqslant m \leqslant M-1 \\ 0 \leqslant n \leqslant N-1}} \ln(4 + \varepsilon - 2c_m - 2c_n) \end{aligned} \tag{A.3}$$

where the sum is now as in (A.2), but with $m=0$, $n=0$ included; and where $c_m = \cos(2\pi m/M)$, $c_n = \cos(2\pi n/N)$.

We set

$$2 \operatorname{ch} t_n = 4 + \varepsilon - 2c_n \qquad (t_n > 0) \tag{A.4}$$

and use the Fourier transform

$$\ln[2(\operatorname{ch} t - \cos\theta)] = t - \sum_{k \in \mathbf{Z}^*} \frac{e^{-|k|t}}{|k|} e^{ik\theta} \tag{A.5}$$

for

$$\theta = \theta_m = 2\pi m/M \tag{A.6}$$

Hence we have

$$\begin{aligned} \Delta(\varepsilon) &= \sum_{\substack{0 \leqslant m \leqslant M-1 \\ 0 \leqslant n \leqslant N-1}} \left(t_n - \sum_{k \in \mathbf{Z}^*} \frac{e^{-|k|t_n}}{|k|} e^{2\pi i k m/M}\right) \\ &= \sum_{0 \leqslant n \leqslant N-1} \left(M t_n - 2 \sum_{k \in \mathbf{N}^*} \frac{e^{-kMt_n}}{k}\right) \\ &= \sum_{0 \leqslant n \leqslant N-1} [M t_n + 2\ln(1 - e^{-Mt_n})] \end{aligned} \tag{A.7}$$

When $\varepsilon \to 0$, the value of t_0 reads, from (A.4),

$$t_0 = \varepsilon^{1/2}[1 + O(\varepsilon)] \tag{A.8}$$

Hence (A.3) and (A.7) give

$$\ln D = 2\ln M + \sum_{1 \leqslant n \leqslant N-1} [M t_n + 2\ln(1 - e^{-Mt_n})] \tag{A.9}$$

where now t_n corresponds to $\varepsilon = 0$ in (A.4). Note that this value is exact and includes no asymptotic evaluation. The latter is performed by using Euler–MacLaurin formula

$$\sum_{1 \leqslant n \leqslant N-1} f(n) = \int_0^N f(n)\, dn - \frac{1}{2}[f(0) + f(N)] + \sum_{p \geqslant 1} (-1)^{p-1} \frac{B_{2p}}{(2p)!} [f^{(2p-1)}(N) - f^{(2p-1)}(0)] \quad \text{(A.10)}$$

where the B_{2p} are Bernouilli numbers

$$B_2 = 1/6, \qquad B_4 = -1/30, \ldots$$

We set in the continuum limit

$$\theta = 2\pi n/N \in [0, 2\pi] \quad \text{(A.11)}$$

and

$$\operatorname{ch} t(\theta) + \cos\theta = 2, \qquad t = \theta - \theta^3/12 + O(\theta^5), \qquad \theta \to 0 \quad \text{(A.12)}$$

The period is π. One has also

$$\operatorname{sh}(t/2) = \sin(\theta/2) \quad \text{(A.13)}$$

$$\sum_{1 \leqslant n \leqslant N-1} t_n = N \int_0^\pi t(\theta) \frac{d\theta}{\pi} + \frac{1}{12} \frac{2\pi}{N} [t'(2\pi^-) - t'(0^+)] + O\left(\frac{1}{N^2}\right) \quad \text{(A.14)}$$

The derivative reads

$$t'(\theta) = (\sin\theta)/(\operatorname{sh} t) \quad \text{(A.15)}$$

Hence $t'(0^+) = -t'(2\pi^-) = 1$, and

$$M \sum_{1 \leqslant n \leqslant N-1} t_n = MNI - \frac{1}{6} 2\pi \frac{M}{N} + O\left(\frac{M}{N^2}\right) \quad \text{(A.16)}$$

where

$$I = \int_0^\pi t(\theta) \frac{d\theta}{\pi} = \frac{4}{\pi} \int_0^{\pi/2} dx \ln[\sin x + (1 + \sin^2 x)^{1/2}] = \frac{4G}{\pi} = 1.166243616\ldots \quad \text{(A.17)}$$

where G is Catalan's constant

$$G = 1 - \frac{1}{3^2} + \frac{1}{5^2} + \cdots = 8 \sum_{n \geqslant 0} \frac{2n+1}{(4n+1)^2 (4n+3)^2}$$

The continuum limit of the last sum in (A.9) is obtained simply by replacing t_n by its equivalent near the origin

$$t_n = 2\pi \frac{n}{N} + O\left[\left(\frac{n}{N}\right)^3\right] \tag{A.18}$$

and this gives, near the two ends of the Brillouin zone,

$$\sum_{1 \leqslant n \leqslant N-1} \ln(1 - e^{-Mt_n}) \to 2 \ln \prod_{n=1}^{\infty} (1 - q^n) \tag{A.19}$$

where

$$q = e^{-2\pi M/N} \tag{A.20}$$

Collecting the results (A.16) and (A.19) into (A.9) gives finally (3.18),

$$\ln D = \frac{4G}{\pi} MN + \ln MN + 4 \ln[P(q)\, q^{1/24} \xi^{1/4}] + O\left(\frac{1}{(MN)^{1/2}}\right) \tag{A.21}$$

where $P(q) = \prod_{n \geqslant 1} (1 - q^n)$, $\xi = M/N$. QED

2. The second sum S_{-1} in (A.1) is evaluated is a similar way. We write

$$S_{-1} = \lim_{\varepsilon \to 0} \left[\sigma_{-1}(\varepsilon) - \frac{1}{\varepsilon} \right] \tag{A.22a}$$

where

$$\sigma_{-1}(\varepsilon) = \sum_{\substack{0 \leqslant m \leqslant M-1 \\ 0 \leqslant n \leqslant N-1}} (4 + \varepsilon - 2c_m - 2c_n)^{-1} \tag{A.22b}$$

We use the same parametrization as in (A.4) and

$$\frac{1}{2(\operatorname{ch} t - \cos\theta)} = \sum_{k \in \mathbf{Z}} e^{ik\theta} \frac{e^{-|k|t}}{2 \operatorname{sh} t} \tag{A.23}$$

Hence

$$\begin{aligned} \sigma_{-1}(\varepsilon) &= \sum_{0 \leqslant n \leqslant N-1} \sum_{0 \leqslant m \leqslant M-1} e^{2\pi i k m/M} \frac{e^{-|k| t_n}}{2 \operatorname{sh} t_n} \\ &= M \sum_{n=0}^{N-1} \sum_{k \in \mathbf{Z}} \frac{e^{-|k| M t_n}}{2 \operatorname{sh} t_n} = M \sum_{n=0}^{N-1} f(t_n) \end{aligned} \tag{A.24}$$

with

$$f(t_n)=\frac{1}{2\,\mathrm{sh}\,t_n}\frac{1+e^{-Mt_n}}{1-e^{-Mt_n}} \tag{A.25}$$

The diverging contribution coming from $n=0$ for $\varepsilon\to 0$ is obtained after a careful series expansion

$$f(t_0)=\frac{1}{\varepsilon}+\frac{M^2-1}{12}+\cdots$$

Hence, from (A.22),

$$S_{-1}=\frac{M^2-1}{12}+2M\sum_{1\leqslant n\leqslant (N-1)/2} f(t_n) \tag{A.26}$$

where now t_n is obtained from (A.4) for $\varepsilon=0$. Since t_n is symmetric with respect to $N/2$, the Brillouin zone has been brought back to the origin, assuming, e.g., N to be odd. The converging rates suggest the splitting

$$f(t_n)=\frac{1}{2\,\mathrm{sh}\,t_n}+\frac{1}{\mathrm{sh}\,t_n}\frac{e^{-Mt_n}}{1-e^{-Mt_n}} \tag{A.27}$$

The first sum in (A.26) is then evaluated by the Euler–MacLaurin equation, the second converges very rapidly, and the expansion (A.18) of t_n around the origin suffices. We set asymptotically

$$2\sum_{1\leqslant n\leqslant (N-1)/2} f(t_n)\approx \sigma_1+\sigma_2+\sigma_3$$

$$\sigma_1=\sum_{1\leqslant n\leqslant (N-1)/2}\left(\frac{1}{\mathrm{sh}\,t_n}-\frac{N}{2\pi n}\right)\approx -\frac{N}{2\pi}\ln\frac{\pi}{2\sqrt{2}}$$

$$\sigma_2=\sum_{1\leqslant n\leqslant (N-1)/2}\frac{N}{2\pi n}=\frac{N}{2\pi}\left(\ln\frac{N}{2}+\gamma+\cdots\right)$$

$$\sigma_3=\sum_{1\leqslant n\leqslant (N-1)/2}\frac{N}{2\pi n}\frac{2e^{-2\pi\xi n}}{1-e^{-2\pi\xi n}}$$

$$\approx\frac{N}{2\pi}2\sum_{n=1}^{\infty}\frac{1}{n}\frac{q^n}{1-q^n}=\frac{N}{2\pi}[-2\ln P(q)]$$

Collecting all these value, we find for S_{-1} of (A.26)

$$S_{-1}=\frac{MN}{4\pi}\left\{\ln MN+2\ln\frac{\sqrt{2}\,e^{\gamma}}{\pi}-4\ln[P(q)q^{1/24}\xi^{1/4}]+O\left[\frac{1}{(MN)^{1/2}}\right]\right\} \tag{A.28}$$

which is Eq. (3.22). QED

3. The last sum S_{-2} in (A.1) is evaluated in the same way:

$$S_{-2} = \lim_{\varepsilon \to 0} \left[\sigma_{-2}(\varepsilon) - \frac{1}{\varepsilon^2} \right] \tag{A.29}$$

where now

$$\sigma_{-2}(\varepsilon) = \sum_{\substack{0 \leqslant m \leqslant M-1 \\ 0 \leqslant n \leqslant N-1}} (4 + \varepsilon - 2c_m - 2c_n)^{-2} \tag{A.30}$$

We use the Fourier transform

$$(\operatorname{ch} t - \cos\theta)^{-2} = \sum_{k \in \mathbf{Z}} e^{ik\theta} \frac{e^{-|k|t}}{(\operatorname{sh} t)^2} (\coth t + |k|) \tag{A.31}$$

which can be obtained by differentiating (A.23) with respect to t. Then σ_{-2} is reduced to the single sum, after some calculations,

$$\begin{aligned} \sigma_{-2}(\varepsilon) &= \sum_{0 \leqslant n \leqslant N-1} \frac{M}{4(\operatorname{sh} t_n)^2} \left[\coth \frac{Mt_n}{2} \coth t_n + 2M \frac{e^{-Mt_n}}{(1-e^{-Mt_n})^2} \right] \\ &\equiv \sum_{0 \leqslant n \leqslant N-1} g(t_n) \end{aligned} \tag{A.32}$$

The divergence in the $n=0$ term for $\varepsilon \to 0$ is extracted after some calculations:

$$\lim_{\varepsilon \to 0} \left[g(t_0) - \frac{1}{\varepsilon^2} \right] = \frac{M^4}{2^4 \cdot 45} + \frac{M^2}{72} - \frac{11}{6!} \tag{A.33}$$

Hence we find the *exact* sum

$$S_{-2} = \frac{M^4}{2^4 \cdot 45} + \frac{M^2}{72} - \frac{11}{6!} + \sum_{1 \leqslant n \leqslant N-1} g(t_n) \tag{A.34}$$

where now $t_n > 0$ is the solution of

$$\operatorname{ch} t_n + \cos(2\pi n/N) = 2 \tag{A.35}$$

Until now there has been no approximation.

To take the $N \to \infty$ limit, we split the sum in (A.34) into (using the symmetry of t_n, and assuming N to be odd)

$$\begin{aligned} \sum_n g(t_n) &= \sum_{1 \leqslant n \leqslant (N-1)/2} \frac{M}{\operatorname{sh}^2 t_n} \left[\frac{1}{2} \coth t_n + \coth t_n \frac{e^{-Mt_n}}{1-e^{-Mt_n}} + M \frac{e^{-Mt_n}}{(1-e^{-Mt_n})^2} \right] \\ &\equiv \sigma_1 + \sigma_2 + \sigma_3 \end{aligned} \tag{A.36}$$

The first sum is evaluated by the Euler–MacLaurin formula, after subtraction of the diverging terms near the origin:

$$\sigma_1 = \sigma_1' + \sigma_1''$$

$$\begin{aligned}\sigma_1' &\equiv \sum_{1 \leqslant n \leqslant (N-1)/2} \frac{M}{2}\left[\frac{\coth t_n}{\mathrm{sh}^2 t_n} - \left(\frac{N}{2\pi n}\right)^3 - \frac{1}{4}\frac{N}{2\pi n}\right] \\ &\approx \frac{MN}{4\pi}\int_0^\pi d\theta \left[\frac{\coth t(\theta)}{\mathrm{sh}^2 t(\theta)} - \frac{1}{\theta^3} - \frac{1}{4\theta}\right] \\ &\equiv \frac{MN}{4\pi} I'\end{aligned} \tag{A.37}$$

$$\begin{aligned}\sigma_1'' &= \sum_{1 \leqslant n \leqslant (N-1)/2} \frac{M}{2}\left[\left(\frac{N}{2\pi n}\right)^3 + \frac{1}{4}\frac{N}{2\pi n}\right] \\ &\approx \frac{MN^3}{2(2\pi)^3}\left[\zeta(3) - \frac{2}{N^2}\right] + \frac{MN}{16\pi}\left(\ln\frac{N}{2} + \gamma\right)\end{aligned} \tag{A.38}$$

The other two sums in (A.36) converge very rapidly. So the expansion (A.18) of t_n near $n=0$ is sufficient, and the continuum limit reads immediately

$$\begin{aligned}\sigma_2 &\to \frac{MN^3}{(2\pi)^3}\sum_{n=1}^{\infty}\frac{1}{n^3}\frac{q^n}{1-q^n} + \frac{MN}{8\pi}\sum_{n=1}^{\infty}\frac{1}{n}\frac{q^n}{1-q^n} + \frac{M^2}{12}\sum_{n=1}^{\infty}\frac{q^n}{(1-q^n)^2} \\ \sigma_3 &\to \left(\frac{MN}{2\pi}\right)^2\sum_{n=1}^{\infty}\frac{1}{n^2}\frac{q^n}{(1-q^n)^2} - \frac{1}{6}M^2\sum_{n=1}^{\infty}\frac{q^n}{(1-q^n)^2} \\ &\quad + \frac{1}{12}2\pi\frac{M^3}{N}\sum_{n=1}^{\infty}\frac{q^n(1+q^n)}{(1-q^n)^3}\end{aligned} \tag{A.39}$$

Collecting Eqs. (A.34)–(A.39) gives finally

$$\begin{aligned}S_{-2} = {} & \frac{M^4}{2^4\cdot 45} + \frac{MN^3}{2(2\pi)^3}\left[\zeta(3) - \frac{2}{N^2}\right] \\ & + \frac{MN^3}{(2\pi)^3}\sum_{n\geqslant 1}\frac{1}{n^3}\frac{q^n}{1-q^n} \\ & + \left(\frac{MN}{2\pi}\right)^2\sum_{n\geqslant 1}\frac{1}{n^2}\frac{q^n}{(1-q^n)^2} + \frac{MN}{4\pi}I' \\ & + \frac{MN}{16\pi}\left(\ln\frac{N}{2} + \gamma\right) + \frac{M^2}{72} + \frac{MN}{8\pi}\sum_{n=1}^{\infty}\frac{1}{n}\frac{q^n}{1-q^n} - \frac{1}{12}M^2\sum_{n=1}^{\infty}\frac{q^n}{(1-q^n)^2} \\ & + \frac{1}{12}2\pi\frac{M^3}{N}\sum_{n=1}^{\infty}\frac{q^n(1+q^n)}{(1-q^n)^3}\end{aligned} \tag{A.40}$$

Terms are reordered for getting a modular invariant form

$$S_{-2}=\left(\frac{MN}{2\pi}\right)^2\left\{\frac{(2\pi\xi)^2}{2^4\cdot 45}+\frac{1}{2\pi\xi}\left[\frac{1}{2}\zeta(3)+\sum_{n=1}^{\infty}\frac{1}{n^3}\frac{q^n}{1-q^n}\right]+\sum_{n=1}^{\infty}\frac{1}{n^2}\frac{q^n}{(1-q^n)^2}\right\}$$
$$+\frac{MN}{16\pi}\ln\left[(MN)^{1/2}\xi^{-1/2}\frac{e^{\gamma}}{2}\right]-\frac{MN}{(2\pi)^3}+\frac{MN}{72}\xi+\frac{MN}{4\pi}I'$$
$$+\frac{MN}{8\pi}\sum_{n=1}^{\infty}\frac{1}{n}\frac{q^n}{1-q^n}-\frac{1}{12}MN\xi\sum_{n=1}^{\infty}\frac{q^n}{(1-q^n)^2}+\frac{MN}{12}2\pi\xi^2\sum_{n=1}^{\infty}n\frac{q^n(1+q^n)}{(1-q^n)^3} \tag{A.41}$$

We can use the identities

$$\sum_{n\geqslant 1}\frac{1}{n}\frac{q^n}{1-q^n}=-\ln P(q)$$
$$\sum_{n\geqslant 1}\frac{q^n}{(1-q^n)^2}=-\frac{qP'(q)}{P(q)} \tag{A.42}$$

and $\eta(q)=q^{1/24}P(q)$ to finally write the asymptotic evaluation of S_{-2} at orders $\mathscr{A}^2$ and $\mathscr{A}$ (with $\mathscr{A}=MN$) as

$$S_{-2}=\left(\frac{\mathscr{A}}{2\pi}\right)^2\left\{\frac{(2\pi\xi)^2}{2^4\cdot 45}+\frac{1}{2\pi\xi}\left[\frac{1}{2}\xi(3)+\sum_{n\geqslant 1}\frac{1}{n^3}\frac{q^n}{1-q^n}\right]+\sum_{n\geqslant 1}\frac{1}{n^2}\frac{q^n}{(1-q^n)^2}\right\}$$
$$+\frac{\mathscr{A}}{16\pi}\ln\left[\mathscr{A}^{1/2}\eta^{-2}(q)\xi^{-1/2}\frac{e^{\gamma}}{2}\right]+\frac{1}{36}\frac{\mathscr{A}}{16\pi}(2\pi\xi)-\frac{\mathscr{A}}{(2\pi)^3}+\frac{\mathscr{A}}{4\pi}I'$$
$$+\frac{\mathscr{A}}{12}\xi q\frac{P'(q)}{P(q)}+\frac{\mathscr{A}}{12}2\pi\xi^2\sum_{n\geqslant 1}n\frac{q^n(1+q^n)}{(1-q^n)^3} \tag{A.43}$$

The continuum limit is given by the dominant term $\sim(\text{area})^2$, which is modular invariant and recovers (3.24). QED

Note that the continuum limits obtained in this Appendix, namely $\ln D$ [Eq. (A.21)], S_{-1} [Eq. (A.28)], and S_{-2} [Eq. (A.41)], have also been obtained independently in this paper as moments of the FSS continuum massive free-field partition function on the torus [Eq. (3.70)] in the zero-mass limit [see Eqs. (3.72) and (3.73)]. Hence the two limits (FSS continuum, zero mass) commute, as expected.

APPENDIX B. DIRICHLET–NEUMANN DUALITY

To prove the duality equation (5.14), we evaluate first the Neumann Gaussian integral $\mathcal{I}$ (5.3), (5.4) on graph G. We consider the normalized eigenmodes of $\mathbf{C}$

$$\mathbf{C}X_n = \lambda_n X_n, \qquad n = 0,..., N_0(G) - 1$$

the zero mode being

$$\lambda_0 = 0, \qquad X_0(i) = \frac{1}{[N_0(G)]^{1/2}} \qquad \forall i \in G$$

Any φ can be expanded onto the X_n,

$$\varphi = \sum_{n=0}^{N_0 - 1} a_n X_n = \frac{a_0}{\sqrt{N_0}} + \sum_{n \neq 0} a_n X_n \tag{B.1}$$

and we rewrite $\mathcal{I}$ as

$$\mathcal{I} = \int_{-\infty}^{+\infty} \prod_{n=1}^{N_0(G)-1} da_n \, da_0 \exp\left(-\frac{1}{2} \sum_{n \neq 0} a_n^2 \lambda_n \right) \delta(\varphi(0))$$

$$= (2\pi)^{[N_0(G)-1]/2} \left(\prod_{n \neq 0} \lambda_n \right)^{-1/2} N_0^{1/2}(G)$$

where the last factor comes from the projection (B.1) of φ onto the zero mode.

Hence

$$\mathcal{I} = (2\pi)^{[N_0(G)-1]/2} \left(\frac{\det' \mathbf{C}}{N_0(G)} \right)^{-1/2} \tag{B.2}$$

To transform the integral $\mathcal{I}$ in (5.3) into that of a Dirichlet problem, we introduce the $N_1(G)$ variables [$N_1(G)$ is the number of bonds or links of G]

$$\varphi_{ij} = \varphi(i) - \varphi(j)$$

associated with links of the dual lattice G^* of G (see Fig. 12). Around each elementary plaquette P of G we have obviously $\sum_{\langle i,j \rangle \in P} \varphi_{ij} = 0$ and this is enforced by introducing plaquette Lagrange multipliers $\tilde{\varphi}_P$ in (5.3), which we rewrite as

$$\mathcal{I} = \int \prod_{\langle i,j \rangle \in G^*} d\varphi_{ij} \prod_P \frac{d\tilde{\varphi}_P}{2\pi} \exp\left(-\frac{1}{2} \sum_{G^*} \varphi_{ij}^2 + i \sum_P \tilde{\varphi}_P \sum_{\langle i,j \rangle \in P} \varphi_{ij} \right) \tag{B.3}$$

Each link $\langle i, j \rangle$ belongs to two plaquettes with alternate directions, so we have by integrating on the φ_{ij}

$$\mathscr{I} = (2\pi)^{[N_1(G)-1]/2} \int \prod_P \frac{d\tilde{\varphi}_P}{2\pi} \exp\left[-\frac{1}{2} \sum_{\langle P, P' \rangle}^{(0)} (\tilde{\varphi}_P - \tilde{\varphi}_{P'})^2 \right] \tag{B.4}$$

where the sum runs onto adjacent plaquetes $\langle P, P' \rangle$, i.e., nearest neighbor variables $\tilde{\varphi}_P$, $\tilde{\varphi}_{P'}$ on the dual lattice, and where the superscript (0) means that the sum must be extended to external sites of the dual lattice G^* that are not centers of plaquettes, with a zero value of $\tilde{\varphi}_P$ there (Fig. 12). So (B.4) is just associated with the combinatoric Laplacian with *Dirichlet* boundary conditions on the dual lattice G^* [see (5.7)]. Hence, by integration,

$$\mathscr{I} = (2\pi)^{[N_1(G)-1]/2} (2\pi)^{-N_2(G)/2} \det{}^{-1/2}(-\Delta)|_{G^*, \text{Dirichlet}} \tag{B.5}$$

where $N_2(G)$ is the number of plaquettes or loops of G, i.e., the number of internal sites of G^*. Using the Euler relation (2.1) and comparing (B.2) and (B.5) gives the expected result

$$\det' \mathbf{C}_G \equiv \det(-\Delta)|_{G, \text{Neumann}} = N_0(G) \det(-\Delta)|_{G^*, \text{Dirichlet}}$$

of which (5.13) is a particular case on the quasi-self-dual rectangular lattice.

ACKNOWLEDGMENTS

It is a pleasure to thank C. Itzykson for a discussion which initiated this work, J. M. Luck for his help in Sections 7.2 and 7.3, J. L. Cardy for discussions, and I. Kostov for reading the manuscript. We are also grateful to P. W. Kasteleyn for a careful reading of this work and his interesting comments.

REFERENCES

1. W. Hamilton, Tour around the world: Twenty towns on the earth are figured by the 20 vertices of a regular dodecahedron (a polyhedron with 12 pentagonal faces and 20 vertices).
2. C. Berge, *Graphes et hypergraphes* (Dunod, Paris, 1970).
3. L. Euler, *Commentationes Arithmeticae Collectae* (St. Peterburg, 1766), p. 337.
4. P. W. Kasteleyn, *Physica* **29**:1329 (1963).
5. F. Harary, ed., *Graph Theory and Theoretical Physics* (Academic Press, London, 1967).
6. T. van Aardenne-Ehrenfest and N. G. de Bruijn, *Simon Stevin* **28**:203 (1951).
7. W. T. Tutte, *Proc. Camb. Phil. Soc.* **44**:463 (1948).
8. G. Kirchhoff, *Ann. Phys. Chem.* **72**:497 (1847).

9. M. N. Barber, *Physica* **48**:237 (1970).
10. A. Malakis, *Physica* **84A**:256 (1976).
11. W. J. C. Orr, *Trans. Faraday Soc.* **43**:12 (1947).
12. C. Domb, *Polymer* **15**:259 (1974).
13. J. F. Nagle, *Proc. R. Soc. Lond. A* **337**:569 (1974).
14. M. Gordon, P. Kapadia, and A. Malakis, *J. Phys. A* **5**:751 (1976).
15. P. D. Gujrati and M. Goldstein, *J. Chem. Phys.* **74**:2596 (1981).
16. T. G. Schmaltz, G. E. Hite, and D. J. Klein, *J. Phys. A* **17**:445 (1984).
17. H. Orland, C. Itzykson, and C. De Dominicis, *J. Phys. Lett. (Paris)* **46**:L353 (1985).
18. J. F. Nagle, P. D. Gujrati, and M. Goldstein, *J. Phys. Chem.* **88**:4599 (1984); J. F. Nagle, *J. Stat. Phys.* **38**:531 (1985).
19. M. G. Bawendi and K. F. Freed, *J. Chem. Phys.* **84**:7036 (1986).
20. B. Duplantier, *J. Phys. A* **19**:L1009 (1986).
21. H. Saleur, *Phys. Rev. B* **35**:3657 (1987).
22. B. Duplantier and H. Saleur, *Nucl. Phys. B* **290**[FS20]:**291** (1987).
23. M. den Nijs, *Phys. Rev. B* **27**:1674 (1983), and references therein.
24. B. Nienhuis, *Phys. Rev. Lett.* **49**:1062 (1982); *J. Stat. Phys.* **34**:781 (1984); in *Phase Transitions and Critical Phenomena*, Vol. 11, C. Domb and J. L. Lebowitz, eds. (Academic Press, London, 1987).
25. B. Duplantier, *J. Stat. Phys.* **49**:411 (1987).
26. F. Y. Wu, *Rev. Mod. Phys.* **54**:239 (1982).
27. J. L. Cardy, in *Phase Transitions and Critical Phenomena*, Vol. 11, C. Domb and J. L. Lebowitz, eds. (Academic Press, London, 1987).
28. J. L. Cardy, *Nucl. Phys. B* **275**[FS17]:580 (1986).
29. A. Weil, *Elliptic Functions According to Eisenstein and Kronecker* (Springer-Verlag, 1976).
30. C. Itzykson and J. B. Zuber, *Nucl. Phys. B* **275**:561 (1986).
31. N. L. Balazs, C. Schmit, and A. Voros, *J. Stat. Phys.* **46**:1067 (1987), and references therein.
32. A. E. Ferdinand and M. E. Fisher, *Phys. Rev. B* **185**:832 (1969).
33. H. Saleur and C. Itzykson, *J. Stat. Phys.* **48**:449 (1987).
34. C. Itzykson, Marseille Lecture Notes, SPhT/86 (1986).
35. R. G. Petschek and P. Pfeuty, *Phys. Rev. Lett.* **58**:1096 (1987).
36. H. Blöte, M. P. Nightingale, and J. L. Cardy, *Phys. Rev. Lett.* **56**:742 (1986); I. Affleck, *Phys. Rev. Lett.* **56**:746 (1986).
37. M. Gaudin, *J. Phys. (Paris)* **48**:1633 (1987).
38. M. Kac, *Am. Math. Monthly* **73**:1 (1966); H. P. McKean and I. M. Singer, *J. Diff. Geom.* 1:43 (1967); H. P. Baltes and E. R. Hilf, *Spectra of Finite Systems* (Bibliographisches Institut, Mannheim, 1976), Chapter VI.
39. B. Duplantier and H. Saleur, *Phys. Rev. Lett.* **57**:3179 (1986).
40. R. J. Baxter, S. B. Kelland, and F. Y. Wu, *J. Phys. A* **9**:397 (1976).
41. R. J. Baxter, *J. Phys. C* **6**:L445 (1973).
42. H. Saleur and B. Duplantier, *Phys. Rev. Lett.* **58**:2325 (1987).
43. H. Saleur, *J. Phys. A* **19**:L807 (1986).
44. C. M. Fortuin and P. W. Kasteleyn, *Physica* **57**:536 (1972).
45. P. Di Francesco, H. Saleur, and J. B. Zuber, *Nucl. Phys. B* **285**[FS19]:**454** (1987); *J. Stat. Phys.* **49**:57 (1987).
46. V. L. S. Dotsenko and V. A. Fateev, *Nucl. Phys. B* **240**:312 (1984).
47. B. Duplantier, *Phys. Rev. Lett.* **57**:941 (1986).